# CHARACTERIZATION OF STRUCTURAL AND REPLICATION GENES IN *MICROPLITIS DEMOLITOR* BRACOVIRUS

by

Michael James Arvin

(Under the Direction of Michael R Strand)

ABSTRACT

Microgastroid wasps (Hymenoptera: Braconidae) are endoparasitoids that primarily parasitize larval stage Lepidoptera. Bracoviruses (BVs) are endogenized nudiviruses that wasps have coopted for functions in successfully parasitizing hosts. Viral genes are expressed in wasp ovaries during BV replication resulting in formation of virions which wasps deliver to hosts during parasitism. BVs are descended from nudiviruses (Family: *Nudiviridae*), an understudied group of insect pathogens. BVs retain viral replication genes that were first identified and characterized in baculoviruses (Family: *Baculoviridae*), sister group to nudiviruses. *Microplitis demolitor* is a microgastroid wasp that carries *Microplitis demolitor* bracovirus (MdBV) and parasitizes larval stages of the moth *Chrysodeixis includens*. Some genes shared with baculoviruses retain conserved roles in MdBV, however not all conserved genes have been studied. There remain many uncharacterized viral genes for which there are no functional predictions. This study had four objectives: 1) Conduct a proteomic analysis of MdBV virions, 2)

functionally analyze a gene named *HzNVorf64-like*, 3) characterize MdBV genes that are homologs of oral infectivity factors that are present both in baculoviruses and nudiviruses and 4) characterize MdBV genes that are predicted integrases. In this research I separated MdBV viral nucleocapsids from envelopes and performed proteomics on both fractions and found that most baculovirus-like gene products were localized to the same fraction in MdBV as they are in baculoviruses. Gene products from unknown viral genes were assigned to nucleocapsid, envelope, or both fractions based on my data. I focused on *HzNVorf64-like* (*MdBVe46*), a betanudivirus gene homolog that produces a 46kDa product assigned to the viral envelope. I found that MdBVe46 is required for viral envelope formation and infection of *C. includens*. I next focused on baculovirus oral infectivity factors (PIFs), envelope proteins that are conserved in MdBV (*p74/pif-0*, *pif-1*, *pif-2*, *pif-3*, *pif-4*, *pif-5-1*, *pif-5-2*, *pif-5-3*, *pif-6* and *vp91/pif-8*). Functional assays indicated that select PIFs play important roles in MdBV infection and morphogenesis. I looked at viral tyrosine recombinases conserved in MdBV (*vlf-1a*, *vlf-1b-1*, *vlf-1b-2*, *int-1*, *int-2*), including 4 uncharacterized nudivirus-like genes (*k425_451*, *k425_468*, *k425_475*, *HzNVorf93-like*). I found that all integrases and two unknowns (*k425_475*, *HzNVorf93-like*) are involved in processing MdBV proviral DNA.

INDEX WORDS: Endogenized nudivirus, *Microplitis demolitor* bracovirus (MdBV), Bracovirus, Oral infectivity factor, Tyrosine recombinase, Integrase

# CHARACTERIZATION OF STRUCTURAL AND REPLICATION GENES IN *MICROPLITIS DEMOLITOR* BRACOVIRUS

by

Michael James Arvin

B.S., The University of Florida, 2014

A Dissertation Submitted to the Graduate Faculty of The University of Georgia in Partial Fulfillment of the Requirements for the Degree

DOCTOR OF PHILOSOPHY

ATHENS, GEORGIA

2020

# CHARACTERIZATION OF STRUCTURAL AND REPLICATION GENES IN *MICROPLITIS DEMOLITOR* BRACOVIRUS

by

Michael James Arvin

Major Professor: Michael R Strand

Committee: Gaelen R Burke
Mark R Brown
Kerry M Oliver

Electronic Version Approved:

Ron Walcott
Dean of the Graduate School
The University of Georgia
December 2020

## DEDICATION

I dedicate this dissertation to my parents and to my little sister, Annika. Thank you for your love and support.

## ACKNOWLEDGEMENTS

My sincerest thanks to all the great people who supported me on my journey to earning my degree.

I would like to thank Rene, Coen, Caterina, and Dawn for their love and support, as well as my little sister for her continued belief in me.

Special thanks to Robin, Janneke, and Rachel.

I am deeply grateful to my advisor, Dr. Michael Strand, for his support, insights, and direction throughout the stages of my PhD. I am particularly thankful for the freedom he afforded me to explore bracovirus biology, as well as his creative analogies and persistence in teaching me about science.

I would like to thank my committee members, who each offered me their support and wisdom that allowed me to overcome challenges. I thank Dr. Gaelen Burke for the knowledge she shared of MdBV biology and her expertise in helping me plan my experiments. I thank Dr. Mark Brown for his assistance in proteomics and for his vegetables. I am grateful to Dr. Kerry Oliver for his perspective on symbionts and for his support.

I owe much to members of the Strand lab and thank them for their knowledge and patience in teaching me the skills I needed to succeed. I would like to thank Dr. Jai Eum and Dr. Kavita Bitra for their lessons in molecular biology and genetics. I thank Dr. Bret Boyd for teaching me about phylogenetics, bioinformatics and parasitic lice.

A special thanks to Mrs. Jena Johnson and her elite team of assistants for their ceaseless organizational and material support of my research. My work would not have been possible but for the efforts of Mr. JB Singco, Ms. Allison Johnson, Ms. Lilith South, Mr. Bradley Mackett and Mr. Severen Brown. Special mention to Mrs. Jena Johnson and her excellent photography skills.

Special thanks to Ms. Taylor Harrell for her efforts in supporting my work.

I would like to thank the people working at UGA support facilities who made my work possible. I would like to thank Mrs. Mary Ard, Dr. John Shields, and Mrs. Beth Richardson for their expertise and their efforts spent training me in the art of electron microscopy.

I am grateful to Mrs. Sherry Wrona, Mr. Sam Waychoff, Mrs. Nancy Jordan, and Mrs. Michelle Hatcher for their administrative efforts to make my life at UGA easier.

I thank Dr. Kevin Vogel for his encouragement of my personal growth and for his academic wisdom.

I thank Ruby Harrison, Jayce Brandt, Kerri Coon, Benjamin Phipps, Ange Lorenzi for their moral support and material contribution to my research.

Special thanks to my friends Ben Gochnour, Brent Phelan, Little Dog and Sweet Dee, with whom I have shared many good times here in Athens, GA.

I would like to thank the men in the Athens Developing Community and the Athens iGroup for their love and support.

Special thanks to Tiffany, Pinky, Angel, and Snoopy.

Met dank aan mijn vrienden van het Sancta en al mijn leraren.

## TABLE OF CONTENTS

# 1. INTRODUCTION AND LITERATURE REVIEW

## 1.1 Polydnaviruses

Polydnaviruses (PDVs) are double stranded (ds) DNA viruses that have been coopted by parasitoid wasps (order Hymenoptera) for functions in wasp reproduction. PDVs persist in wasp species as proviruses, integrated into the genome of every cell, including germ cells. As such PDVs are transmitted vertically from parent to offspring. Viral particles, also known as virions, are produced solely in specialized calyx cells in the ovaries of female wasps and consist of circular dsDNAs packaged into enveloped nucleocapsids. They are stored in the lumen of the ovaries until they are used by the wasp [1]. Parasitoid wasps are insects that reproduce by laying eggs in or on the bodies of other arthropods, referred to as hosts. Parasitoids are important natural enemies of many agricultural pests and make up over 80% of all known wasp species. Wasps carrying PDVs generally parasitize the larval stages of lepidopterans (moths and butterflies) by injecting eggs and virions into the body cavity using their ovipositor [2]. PDV virions infect host cells and the expression of virulence genes cause changes to immunity and development that benefit wasp offspring [3]. In contrast to typical, non-mutualistic viruses, PDVs are not capable of replicating in the hosts of wasps but are considered indispensable to the survival of wasp offspring. Thus there is an obligate mutualistic relationship where wasp reproduction is fully dependent upon PDV virions, and PDVs rely on the survival of wasp progeny for transmission [4, 5]. PDVs have received limited attention because their life cycle and

unusual biology make it difficult to work on them. However, recent studies have advanced the understanding of PDVs and shed light on these symbiotic relationships.

Two genera of PDVs are currently recognized, the *Bracovirus* (BV), which are associated with the wasp family Braconidae, and the *Ichnovirus* (IV), which are associated with the Ichneumonidae [1]. Recent work in PDV biology has primarily focused on BVs, where several advances have been made. These include the evolutionary origins of BVs [6-8], the organization and content of BV genomes [8, 9], and the function of some BV genes [10]. Features of BVs that are poorly understood include how their genomes are amplified during replication, what regulates this amplification, and what signals are needed to initiate transcription of replication genes [11, 12]. The function of many BV genes also remains unknown.

### 1.2 Origins of Bracoviruses (BVs)

Phylogenetic study of all known BV-carrying braconid wasps has shown that they form a monophyletic clade called the microgastroid complex, containing roughly 50,000 species, each of which carries a unique BV [6, 13]. This clade, and therefore also the wasp-BV association, is ~100 million years old [8, 14, 15]. Recent sequencing has identified BV genes expressed, in the ovaries of *Microplitis demolitor* and other microgastroid species during virion replication, that are homologous to genes found in betanudiviruses (family *Nudiviridae*) [7, 8, 10]. Nudiviruses, and their sister group the baculoviruses, are large enveloped DNA viruses that infect insects and they are the closest known relatives of BVs [16, 17].

Today, BV genomes are integrated into wasp genomes as two functional components. The first are the nudivirus-like genes, which are necessary for replication of BV virions. Some of these genes are grouped together in the wasp genome while others are dispersed [10]. All are expressed in calyx cells during pupal and adult stages of the female wasp in association with virus replication [7, 10]. The second component consists of DNA domains, called proviral segments which reside within loci in the wasp genome and contain virulence genes. Proviral segments are amplified, processed, and packaged into virions as circular dsDNAs during replication, but none of the genes on proviral segments are transcribed in the wasp [18]. Virions are injected into the wasp host along with the egg, after which the dsDNA segments integrate into the host genome [19]. Many virulence genes are then transcribed in host cells [20, 21]. Many of these genes are homologs of known insect genes, while a few are homologs of virus genes [22].

### 1.3 Bracoviruses encode a number of genes that are nudivirus and/or baculovirus homologs

Most of the BV nudivirus-like genes are members of a conserved set of genes associated with replication of all known nudiviruses and baculoviruses. Together these genes are often referred to as core genes [10, 23]. Baculoviruses are a diverse group of dsDNA viruses that infect a wide range of insects, primarily through midgut epithelial cells (i.e. orally) [24]. Baculovirus particles consist of enveloped capsids that contain the circular viral genome. During infection, the whole viral genome persists episomally in the nuclei of infected cells, where viral genes are expressed. A set of important baculovirus genes are those involved in the amplification of proviral DNAs, which are packaged into virions

[24]. It is still unclear how these circular genomes are amplified. Evidence points to baculovirus replication resulting in DNA concatemers consisting of many multiples of the full genome length. This has been taken to suggest that baculovirus DNA amplification happens by way of rolling circle replication combined with recombination of viral DNA [25, 26]. After this concatemerization, the amplified viral DNA is then processed into circular genomes. Baculoviruses encode six essential genes required for DNA replication, a DNA polymerase (*dnapol*), *helicase*, three late expression factors (*lef-1* – *lef-3*) and an origin binding protein (*ie1*). Sequencing data indicate that only *helicase* is conserved in MdBV, while the others are absent [10].

Late gene expression in baculoviruses plays a major role in the formation of virions. Under the influence of the viral RNA polymerase many genes coding for capsid and envelope components are expressed. One major capsid component is *vp39*, one of the most abundant viral proteins found during infection. It is the main structural virion component and might play a role in nucleocapsid transport [27, 28]. Certain late genes coding for virion membrane components in baculoviruses, such as the PIF genes, are responsible for *per os* infectivity, whose loss disables oral infection of host insects. MdBV encodes homologs of many of these baculovirus-like genes, despite the fact that BVs do not infect orally. Some of these genes have expanded into multimember families in MdBV and other BVs [7, 10]. Another well-studied baculovirus structural gene is *vlf-1*, a single copy gene important for the structural integrity of capsids [29]. It is also a member of the lambda integrase protein family, recognizable by a conserved motif and catalytic tyrosine residue. Integrase family members are found in a wide variety of organisms, including viruses where they are involved in excision and integration of viral DNA, as well as

decatenation of replicated viral genomes [24, 30, 31]. Members of this integrase family usually form tetramers upon association with DNA, and mediate strand exchange via a cruciform Holliday Junction Intermediate [32]. In baculoviruses *vlf-1* is a single copy gene and has been implicated in genome processing and packaging, as well as the final maturation of virions [24]. It has also been found to bind strongly to cruciform DNA, and might form complexes as a homotetramer or a heterotetramer that binds to other currently unknown proteins, as is true for some lambda integrase family members [33, 34]. In nudiviruses, *vlf-1* has duplicated into two genes, *vlf-1* and *int-1*.

### 1.4 Bracovirus structural genes

BV virions, including MdBV, consist of barrel-shaped nucleocapsids that contain circular, double stranded DNAs and are surrounded by a single envelope [35, 36]. Genomic and proteomic data from three braconid wasps, *Cotesia congregata*, *Chelonus inanitus*, and *Microplitis demolitor*, show that BVs share many conserved baculovirus structural genes, including the previously mentioned PIF genes and capsid components *vp39* and *vlf-1* [7, 37]. For most of the structural genes, proteomic analysis shows that they are part of BV virions [8, 10, 38]. Both *vp39* and *vlf-1* homologs were investigated for their role in capsid formation. Knockdown of *vp39* in *M. demolitor* by RNA interference had a strong negative effect on infectivity in the wasp host, although it did not cause a noticeable lack of capsids, as seen from TEM. Knockdown of MdBV *vlf-1* caused aberrant or absent nucleocapsids. A knockdown of *pif-1* or *p74*, two baculovirus infectivity factor homologs (PIFs), drastically reduced viral gene expression by cells infected with MdBV virions. The apparent function of these genes is unclear but could still mirror that of their baculovirus homologs [10].

Most BV structural genes with baculovirus homologs remain uncharacterized, some of which have expanded into gene families within BVs. Still other BV genes, like *HzNVorf64*, lack baculovirus or nudivirus homologs and have entirely unknown functions but are detected in MdBV virions.

### 1.5 Bracovirus DNA amplification and processing

In contrast to baculoviruses, BV genomic DNAs are integrated into the genomes of wasps as linear DNA. However, BV virions package circular DNA segments. For this to happen, segments must first be amplified and circularized (processed) before they can be packaged. The exact mechanism for segment amplification is unknown, but recent work has revealed more about the intermediate stages of BV proviral DNA [11, 24]. It was initially thought that proviral segments are first excised from the genome in calyx cells, circularized, and then amplified by rolling circle amplification similar to baculoviruses [39]. However, recent evidence shows that segments are not excised before amplification, that proviral loci are amplified to form concatemers, and that the nudivirus-like cluster is also amplified, although the reason for the latter is unclear [11, 40]. In BVs, proviral segments are delineated by short, direct repeat junctions named wasp integration motifs (WIMs). Circularized segments contain only one WIM [10, 19]. These proviral segments are amplified as part of a replication unit (RU). An RU consists of one or more proviral segments and its WIMs, as well as some flanking wasp DNA. The flanking wasp DNAs encode RU boundaries, which are identified by specific single nucleotide positions [11]. During DNA amplification RUs form concatemers, which are long strands of dsDNA consisting of many RUs strung together. There are two types of concatemer, one joined

in a head-to-head and tail-to-tail fashion, and one in a head-to-tail fashion. The way in which each RU is amplified is consistent every time, and RU boundary motif differences correlate with the concatemeric intermediates they form [11]. Ultimately, the segments are excised from these concatemeric intermediates at the WIMs and circularized, and leftover flanking DNA in the RU is rejoined and left unpackaged. The nudivirus-like gene cluster is also amplified, although it does not form any concatemers, and no elements from this cluster are packaged into virions [10, 11].

It is unclear what genes regulate DNA amplification or processing in BVs. As noted above, of the six essential baculovirus DNA amplification genes, most are missing in BVs, including *dnapol*. This suggests that wasp machinery now amplifies proviral DNA. However, many nudivirus-like genes have not been characterized, and may yet play a significant role in DNA amplification. As stated previously, *vlf-1* and *int-1* are members of the *integrase* protein family of tyrosine recombinases that are conserved in BVs and are implicated in viral genome processing in baculoviruses. In MdBV, these genes consist of *vlf-1, vlf-1b-1*, *vlf-1b-2*, *int-1*, and *int-2*. Knockdowns of *vlf-1* and *int-1* have been shown to drastically reduce concatemer processing [7, 10].

### 1.6 The rationale and goals of the dissertation

Although many features of BV biology are understood, a number of significant gaps also exist. This dissertation aims to fill in some of these gaps by expanding on recent work as well as by addressing unexplored avenues in BV biology. By investigating BV gene homologs known from baculoviruses I am refining the current understanding of both groups of viruses and the core molecular mechanics by which they function. Decades of

thorough investigation into baculoviruses has led to the development of valuable tools with biotechnological applications [24, 41]. Similarly, by expanding on previous work characterizing BV genes we gain more insight into a unique and complex biological system that could offer future researchers novel molecular tools. Packaging of specific DNAs into replication-defective virus particles, a unique feature of PDVs, is interesting from a medical technology perspective. Gene therapy is currently a frontier of medical science and it relies heavily on replication-defective viral particles to deliver genetic material to patients [42, 43]. Additionally, deeper understanding of PDVs sheds more light on the complex interaction between parasitoid wasps and their arthropod hosts, a dynamic important to those with interests in insect physiology or agriculture.

The aim of this research project is to address some of the gaps in the BV literature by studying the wasp *Microplitis demolitor* and its BV named *M. demolitor* bracovirus (MdBV). In this study I pursue 3 general aims: 1) Characterize unknown nudivirus-like BV genes 2) Characterize the function of genes with hypothesized roles in MdBV infection; 3) Investigate candidate genes with functions in viral DNA amplification and processing. The following chapters describe the results of my investigations following from the previously stated research aims. In chapter 2 I describe the characterization of a highly expressed nudivirus-like gene, *HzNVorf64-like*, involved in structural virion formation of MdBV. In addition, I report on a proteomics experiment separating BV gene products into viral envelope or nucleocapsid fractions. Chapter 3 reports on my investigation of MdBV PIFs and their involvement in BV infection of host cells. In chapter 4 I investigate the MdBV λ integrase gene family as well as other genes with a hypothesized role in DNA

amplification or processing. In chapter 5 I summarize the main results and draw general conclusions.

## 1.7 References


1. Strand, M.R. and G.R. Burke, *Polydnaviruses: from discovery to current insights.* Virology, 2015. **0**: p. 393-402.

2. Pennacchio, F. and M.R. Strand, *Evolution of developmental strategies in parasitic hymenoptera.* Annu Rev Entomol, 2006. **51**: p. 233-58.

3. Strand, M.R. and E.A. Wong, *The growth and role of Microplitis demolitor teratocytes in parasitism of Pseudoplusia includens.* J Insect Physiol, 1991. **37**(7): p. 503-515.

4. Fleming, J.A.G.W., *Polydnaviruses: Mutualists and Pathogens.* Ann Rev Entomology, 1992. **37**(1): p. 401-425.

5. Strand, M.R. and G.R. Burke, *Polydnaviruses as symbionts and gene delivery systems.* PLoS Pathog, 2012. **8**(7): p. e1002757.

6. Murphy, N., et al., *Phylogeny of the parasitic microgastroid subfamilies (Hymenoptera: Braconidae) based on sequence data from seven genes, with an improved time estimate of the origin of the lineage.* Mol Phylogenet Evol, 2008. **47**(1): p. 378-95.

7. Burke, G.R. and M.R. Strand, *Deep sequencing identifies viral and wasp genes with potential roles in replication of Microplitis demolitor Bracovirus.* J Virol, 2012. **86**(6): p. 3293-306.

8. Bezier, A., et al., *Polydnaviruses of braconid wasps derive from an ancestral nudivirus.* Science, 2009. **323**(5916): p. 926-30.

9. Burke, G.R., et al., *Widespread genome reorganization of an obligate virus mutualist.* PLoS Genet, 2014. **10**(9): p. e1004660.

10. Burke, G.R., et al., *Mutualistic polydnaviruses share essential replication gene functions with pathogenic ancestors.* PLoS Pathog, 2013. **9**(5): p. e1003348.

11. Burke, G.R., et al., *Microplitis demolitor Bracovirus Proviral Loci and Clustered Replication Genes Exhibit Distinct DNA Amplification Patterns during Replication.* J Virol, 2015. **89**(18): p. 9511-23.

12. Strand, M.R. and G.R. Burke, *Polydnavirus-wasp associations: evolution, genome organization, and function.* Curr Opin Virol, 2013. **3**(5): p. 587-94.

13. Rodriguez, J.J., et al., *Extrapolations from field studies and known faunas converge on dramatically increased estimates of global microgastrine parasitoid wasp species richness (Hymenoptera: Braconidae).* Insect Conserv Divers, 2013. **6**(4): p. 530-536.

14. Whitfield, J.B., *Estimating the age of the polydnavirus/braconid wasp symbiosis.* Proc Natl Acad Sci U S A, 2002. **99**(11): p. 7508-13.

15. Bezier, A., et al., *The genome of the nucleopolyhedrosis-causing virus from Tipula oleracea sheds new light on the Nudiviridae family.* J Virol, 2015. **89**(6): p. 3008-25.

16. Wang, Y. and J.A. Jehle, *Nudiviruses and other large, double-stranded circular DNA viruses of invertebrates: new insights on an old topic.* J Invertebr Pathol, 2009. **101**(3): p. 187-93.

17. Theze, J., et al., *Paleozoic origin of insect large dsDNA viruses.* Proc Natl Acad Sci U S A, 2011. **108**(38): p. 15931-5.

18. Strand, M.R. and G.R. Burke, *Polydnaviruses: Nature's Genetic Engineers.* Annual Review of Virology, 2014. **1**(1): p. 333-354.

19. Beck, M.H., et al., *The encapsidated genome of Microplitis demolitor bracovirus integrates into the host Pseudoplusia includens.* J Virol, 2011. **85**(22): p. 11685-96.

20. Beck, M. and M.R. Strand, *Glc1.8 from Microplitis demolitor Bracovirus Induces a Loss of Adhesion and Phagocytosis in Insect High Five and S2 Cells.* J of Virol, 2005. **79**(3): p. 1861-1870.

21. Beck, M.H. and M.R. Strand, *A novel polydnavirus protein inhibits the insect prophenoloxidase activation pathway.* Proc Natl Acad Sci U S A, 2007. **104**(49): p. 19267-72.

22. Desjardins, C.A., et al., *Comparative genomics of mutualistic viruses of Glyptapanteles parasitic wasps.* Genome Biol, 2008. **9**(12): p. R183.

23. Bezier, A., et al., *Functional endogenous viral elements in the genome of the parasitoid wasp Cotesia congregata: insights into the evolutionary dynamics of bracoviruses.* Philos Trans R Soc Lond B Biol Sci, 2013. **368**(1626): p. 20130047.

24. Rohrmann, G.F., *Baculovirus Molecular Biology*. 4th ed. 2019, Bethesda (MD): National Center for Biotechnology Information (US).

25. Wu, Y., G. Liu, and E.B. Carstens, *Replication, Integration, and Packaging of Plasmid DNA following Cotransfection with Baculovirus Viral DNA.* J Virol, 1999. **73**(7): p. 5473-5480.

26. Chen, T., D. Sahri, and E.B. Carstens, *Characterization of the Interaction between P143 and LEF-3 from Two Different Baculovirus Species: Choristoneura fumiferana Nucleopolyhedrovirus LEF-3 Can Complement Autographa californica Nucleopolyhedrovirus LEF-3 in Supporting DNA Replication.* J Virol, 2004. **78**(1): p. 329-339.

27. Wang, R., et al., *Proteomics of the Autographa californica Nucleopolyhedrovirus Budded Virions.* J Virol, 2010. **84**(14): p. 7233-7242.

28. Danquah, J.O., et al., *Direct Interaction of Baculovirus Capsid Proteins VP39 and EXON0 with Kinesin-1 in Insect Cells Determined by Fluorescence Resonance Energy Transfer-Fluorescence Lifetime Imaging Microscopy.* J Virol, 2012. **86**(2): p. 844-853.

29. McLachlin, J.R. and L.K. Miller, *Identification and characterization of vlf-1, a baculovirus gene involved in very late gene expression.* J Virol, 1994. **68**(12): p. 7746-7756.

30. Gopaul, D.N. and G.D. Van Duyne, *Structure and mechanism in site-specific recombination.* Current Opinion in Structural Biology, 1999. **9**(1): p. 14-20.

31. Esposito, D. and J.J. Scocca, *The integrase family of tyrosine recombinases: evolution of a conserved active site domain.* Nucleic Acids Res, 1997. **25**(18): p. 3605-3614.

32. Grindley, N.D., K.L. Whiteson, and P.A. Rice, *Mechanisms of site-specific recombination.* Annu Rev Biochem, 2006. **75**: p. 567-605.

33. Yang, S. and L.K. Miller, *Activation of Baculovirus Very Late Promoters by Interaction with Very Late Factor 1.* J Virol, 1999. **73**(4): p. 3404-3409.

34. Mikhailov, V.S. and G.F. Rohrmann, *Binding of the baculovirus very late expression factor 1 (VLF-1) to different DNA structures.* BMC Mol Biol, 2002. **3**: p. 14-14.

35. Albrecht, U., et al., *Polydnavirus of the parasitic wasp Chelonus inanitus (Braconidae): characterization, genome organization and time point of replication.* J Gen Virol, 1994. **75 ( Pt 12)**: p. 3353-63.

36. Strand, M.R., et al., *Persistence and expression of Microplitis demolitor polydnavirus in Pseudoplusia includens.* J Gen Virol, 1992. **73 ( Pt 7)**: p. 1627-35.

37. Bezier, A., et al., *Polydnavirus hidden face: the genes producing virus particles of parasitic wasps.* J Invertebr Pathol, 2009. **101**(3): p. 194-203.

38. Wetterwald, C., et al., *Identification of bracovirus particle proteins and analysis of their transcript levels at the stage of virion formation.* J Gen Virol, 2010. **91**(Pt 10): p. 2610-9.

39. Savary, S., et al., *Excision of the polydnavirus chromosomal integrated EP1 sequence of the parasitoid wasp Cotesia congregata (Braconidae, Microgastinae) at potential recombinase binding sites.* J Gen Virol, 1997. **78 ( Pt 12)**: p. 3125-34.

40. Louis, F., et al., *The bracovirus genome of the parasitoid wasp Cotesia congregata is amplified within 13 replication units, including sequences not packaged in the particles.* J Virol, 2013. **87**(17): p. 9649-60.

41. Tsai, C.H., et al., *Baculovirus as Versatile Vectors for Protein Display and Biotechnological Applications.* Curr Issues Mol Biol, 2020. **34**: p. 231-256.

42. Kohn, D.B. and C.Y. Kuo, *New frontiers in the therapy of primary immunodeficiency: From gene addition to gene editing.* J Allergy Clin Immunol, 2017. **139**(3): p. 726-732.

43. Singh, S.P., et al., Gene therapy: recent development in the treatment of various diseases*.* Int J of Pharm Chem Biol Sci, 2016. **6**(2): p. 205.

# 2. *MDBVE46* IS A VIRION ENVELOPE GENE THAT *MICROPLITIS DEMOLITOR* BRACOVIRUS REQUIRES FOR VIRION ENVELOPE FORMATION AND SUCCESSFUL PARASITISM OF HOSTS BY THE WASP *MICROPLITIS DEMOLITOR*

## 2.1 INTRODUCTION

As mentioned in chapter one, strong evidence supports that all BVs evolved from a betanudivirus (family *Nudiviridae*) that integrated into the germline of the common microgastroid ancestor ~100 million years ago [1-3]. The *Nudiviridae* is currently subdivided into two genera, the *Alpha-* and *Betanudivirus,* and is sister to the *Baculoviridae* [4, 5]. Viruses in both families are distinguished by their large (~80-230 kb), circular, double-stranded DNA genomes, enveloped virions, and host ranges that are restricted to insects or other arthropods [4, 5]. Most baculoviruses and nudiviruses are horizontally transmitted between hosts by oral ingestion and usually establish systemic infections that are fatal to permissive hosts. Their large genomes persist as episomes in the nuclei of infected host cells and consist of conserved core genes that primarily have functions in replication and variable inventories of virulence genes with roles in infecting permissive hosts. Baculoviruses encode 39 core genes of which all have been experimentally studied in model species [5]. Nudiviruses encode 32 core genes of which none have been studied experimentally but the 21 shared with baculoviruses provide inferences about function [5].

BVs also produce enveloped virions that package circular, dsDNAs but differ from baculoviruses and nudiviruses in that: 1) replication only occurs in ovary calyx cells of female wasps, 2) resulting virions are replication-defective, 3) no disease occurs in wasps but females co-inject virions when laying eggs that cause disease in hosts, and 4) integration into the germline results in BV genome components always being vertically transmitted to offspring [6-9]. BV genome components consist of 34 genes with known or hypothesized functions in producing virions plus multiple virulence genes [3, 10, 11]. Approximately half of the genes with known or hypothesized functions in virion formation are baculovirus homologs, which include four RNA polymerase subunits plus predicted structural genes, while the remainder are either homologs of nudivirus genes or are unknown outside of BV carrying wasps [3, 10, 11]. These genes are widely dispersed in the genomes of wasps and while expressed in calyx cells are largely not amplified [11]. In addition, none are present in the DNAs that are packaged into nucleocapsids, which results in BV virions not being able to replicate [12]. Reciprocally, most virulence genes are not expressed in wasps but all reside in dispersed domains of the wasp genome called proviral segments that are amplified and processed during replication to produce multiple, circular dsDNAs that are packaged into nucleocapsids [13-16]. Most of these virulence genes are then expressed after virions infect host cells, which causes several of the disease symptoms BV-infected hosts exhibit. Thus, BVs are endogenized nudiviruses that wasps use as transducing agents to deliver virulence genes to hosts [6-9, 17, 18].

*Microplitis demolitor* produces *Microplitis demolitor* bracovirus (MdBV) and parasitizes the larval stage of the moth *Chrysodeixis includens* [19]. Sequencing of the

*M. demolitor* genome indicates most MdBV core genes are single copy but some have diversified into multimember families (*ac92-like, vlf-1, int, pif-5, HzNVorf9-like, odv-e66, 35a*) [12, 20]. MdBV proviral segments are named alphabetically (A-X) and reside in 8 loci [11, 16]. We previously conducted a proteomic analysis of purified MdBV virions and developed RNA interference (RNAi) methods to ask if select baculovirus-like core genes retain conserved functions. Results detected all baculovirus-like structural core genes in MdBV virions [21]. RNAi knockdown of two MdBV RNA polymerase genes (*lef-4, lef-9*) disabled the expression of baculovirus-like structural core genes, while knockdown of certain baculovirus-like structural core genes resulted in virion phenotypes that are consistent with known functions of baculovirus homologs [21]. Yet as previously noted, approximately half of the predicted MdBV core genes share no homology with baculoviruses to guide functional predictions. In this study, I separated MdBV virions into envelope and nucleocapsid fractions before proteomic analysis to generate additional insights about structural gene products. I then selected for further study an MdBV gene unknown from baculoviruses that was originally named *HzNVorf64-like* (14, 15). My results indicate that nearly all baculovirus-like structural gene products localize to the envelope and nucleocapsid of MdBV virions as found for homologs in the occlusion-derived form of baculoviruses. I rename *HzNVorf64-like* as *MdBVe46* and show that this gene encodes an envelope protein that is required for virion formation and successful parasitism of *C. includens* larvae by *M. demolitor.*

## 2.2 Results

### 2.2.1 Several MdBV core gene products are preferentially detected in envelope or nucleocapsid fractions

Two samples of MdBV virions were independently collected and separated into envelope (E) and nucleocapsid (N) fractions. After SDS-PAGE and in-gel digestion with trypsin, each sample was analyzed by liquid chromatography-tandem mass spectrometry using an Orbitrap Elite mass spectrometer with resulting mass spectra compared to an MdBV gene database. Table 2.1 presents all MdBV gene products for which 3 or more peptides were identified. For each product I also indicate which are homologs of genes present in all sequenced baculoviruses, alphanudiviruses, betanudiviruses and/or other BVs. For each product, I compared summed peptide counts by Chi-square or Fisher's Exact Test to an expected distribution of 0.5 if equally distributed between the two fractions [22]. Results indicated that 30 gene products significantly differed from the expected distribution by being preferentially detected in the E-fraction, 16 differed by being preferentially detected in the N-fraction, and 15 did not differ from the expected distribution and were thus assigned as E- and N-associated (Table 2.1). Nearly all MdBV gene products that were homologs of baculovirus structural genes were similarly assigned by the results to either the envelope or nucleocapsid fraction as in a previous proteomic analysis of corresponding homologs in baculovirus virions [23]. The only exceptions were: 1) the products of the two *ac92*-like genes in *M. demolitor* that my analysis classified as E- and N-associated in MdBV virions, while *ac92* is a single copy gene that was classified as E-associated in occlusion-derived baculovirus virions, and 2) the product of the *38K* gene in *M. demolitor* that my results also classified as E- and N-

associated but was identified as N-associated in baculoviruses [23]. For MdBV gene products that are unknown from baculoviruses, two nudivirus-like proteins I previously identified in MdBV virions were preferentially detected in the envelope fraction (*HzNVorf64-like*, *HzNVorf94-like*) while five others (*Int-1*, *HzNVorf93-like*, *HzNVorf9-like*, *HzNVorf106-like*, *HzNVorf118-like*, *HzNVorf128-like*) were assigned as nucleocapsid-associated (Table 2.1). In contrast, other gene products currently known only from other BVs were either preferentially detected in the envelope fraction (*K425_450*), nucleocapsid fraction (*27B-like-1*, some *35a* family members, *K425_459*), or both fractions (some *35a* family members, *K425_461* (Table 2.1). Lastly, three products not detected in the previous proteomic analysis of whole virions [21] were detected in the current study (*27b-like-1*, *Cc50C22.5-like*, *Cc50C22.6-like-1*) (Table 2.1).

### 2.2.2 *HzNVorf64-like* is a late structural envelope gene that I rename as *MdBVe46*

I selected *HzNVorf64-like* for further study because the preceding results classified it as an envelope component while earlier data identified it as among the most strongly expressed of the MdBV core genes that are unknown from baculoviruses [10]. I thus reasoned this intronless, single copy gene could potentially be important in virion morphogenesis and/or host infection. *HzNVorf64-like* codes for a 390 amino acid protein with a predicted molecular mass of 45.5 kDa that PSI-BLAST indicated is ~80% identical to single copy orthologs in all other BV-producing braconids that sequence data are available for including *Cotesia congregata*, *Cotesia chilonis* and *Toxoneuron nigriceps*. As previously noted, the *Nudiviridae* is currently subdivided into two genera [24]. *Heliothis zea* nudivirus 1 (HzNV1) is assigned to the *Betanudivirus* and is the species in which

*HzNVorf64* was first identified as a gene of unknown function [25, 26]. Two other species, *Tipula oleracea* nudivirus (ToNV) and *Penaeus monodon* nudivirus (PmNV) were assigned to the same clade as HzNV1 and also encode *HzNVorf64-like* genes [2]. However, similar to most BV genes shared with baculoviruses and/or nudiviruses, overall sequence identity of these genes to MdBV *HzNVorf64-like* was relatively low (~30%). In contrast, no recognizable *HzNVorf64-like* genes were identified by PSI-BLAST in *Gryllus bimaculatus* nudivirus, *Oryctes rhinoceros* nudivirus, and *Drosophila innubia* nudivirus that are assigned to the *Alphanudivirus* [24]. A conserved domain search further detected no regions of homology between MdBV *HzNVorf64-like* and other proteins in public databases.

A single mature *M. demolitor* larva usually emerges 7 days after an adult female lays an egg into the body of a *C. includens* larva. The wasp larva then spins a cocoon and pupates on day 1 post-emergence (stage 1), matures on day 2 and 3 (stage 2, 3), and emerges from the cocoon as an adult on day 4 (stage 4) [10]. I previously determined that the MdBV baculovirus-like RNA polymerase subunit genes (*lef4, lef8, lef9, p47*) are expressed in newly formed stage 1 pupae, while expression of baculovirus-like structural genes such as *p74* and *vp39* are first detected in stage 2 pupae [10, 21]. I thus categorized the former as early and the latter as late genes while documenting by transmission electron microscopy (TEM) that MdBV virions first appear in the nuclei of stage 3 pupal calyx cells [21]. In this study, I first detected expression of *HzNVorf64-like* in the ovaries of stage 2 pupae, which was followed by an increase in transcript abundance in stage 3 pupae and declines in transcript abundance in stage 4 pupae and newly emerged (Day 1) adults (Fig. 2.1A). I generated a polyclonal antibody to

*HzNVorf64-like* that detected a single protein of predicted mass on immunoblots of whole virions (Fig. 2.1B). Consistent with my proteomic data, this antibody also strongly detected *HzNVorf64-like* in the E-fraction but only very weakly detected it in the N-fraction (Fig. 2.1B). I therefore renamed *HzNVorf64-like* as *MdBVe46* and classified it as a late structural envelope gene (Table 2.1; Fig. 2.1).

### 2.2.3 *MdBVe46* knockdown disrupts virion formation

I injected a double-stranded (ds) RNA specific for *MdBVe46* (treatment) or a control gene (enhanced green fluorescent protein: *e*GFP) absent in *M. demolitor* into stage 1 larvae that had spun cocoons followed by the isolation of total RNA and DNA from the ovaries of newly emerged adult females. qPCR assays indicated that transcript abundance of *MdBVe46* was reduced ~90% in treatment wasps when compared to controls (Fig. 2.2A), whereas no differences in transcript abundance were detected for three other MdBV structural genes that code for proteins classified as envelope (*p74, pif-8*) or nucleocapsid components (*vp39*) (Fig. 2.2B-D). *MdBVe46* was likewise readily detected by on immunoblots of ovary extracts of control wasps but was nearly undetectable in treatment wasps (Fig. 2.2E), which supported that *MdBVe46* was strongly and selectively knocked down at both the transcript and protein level.

Given evidence that *MdBVe46* is a late structural envelope gene, I examined ovaries from pupae and adults by TEM to determine if knockdown affected virion morphogenesis. Control wasps showed no alterations relative to previous studies [27, 28] with cylindrical nucleocapsids and envelope profiles appearing *de novo* in calyx cell nuclei in early stage 3 pupae and parallel arrays of virions being present in virogenic

stroma by late stage 3 (Fig. 2.3A, B). Lysis of calyx cells in stage 4 control pupae and adults thereafter resulted in virions accumulating to high density in the calyx lumen and forming 'calyx fluid' that adult females inject into hosts (Fig. 2.3C). Fully consistent with prior studies, virions in the calyx fluid of control wasps were characterized by the presence of a single, proximately-located nucleocapsid that was surrounded by an envelope of uniform width but variable length (Fig. 2.3C). In treatment wasps, nucleocapsids but no envelope profiles appeared de novo in early stage 3 calyx cell nuclei (Fig. 2.3D). In late stage 3 nuclei, some envelope profiles were observed but only disorganized assemblages of nucleocapsids with and without envelopes were observed (Fig. 2.3E, F). Calyx cells lysed in stage 4 treatment pupae and adults, but the particles that accumulated in the calyx lumen were morphologically highly variable (Fig. 2.3G). This variation included the envelopment of multiple or single nucleocapsids by an envelope that maintained a rounded profile (Fig. 2.3G). Rounded envelope profiles with no nucleocapsids as well as nucleocapsids with no envelope were also observed (Fig. 2.3G).

Counting particles in the calyx lumen of newly emerged treatment adults further suggested the density of nucleocapsids with and without envelopes was lower than in control wasps (Fig. 2.4A). As previously noted, *M. demolitor* encodes 25 proviral segments (A-X), which are differentially amplified during replication and are processed into the circular dsDNA segments that are packaged into virions [11, 16]. However, prior results also indicate only one circularized segment is packaged per virion which results in all 25 segments being distributed across the population of virions that accumulate in the calyx lumen [14]. I thus selected three MdBV DNA segments (segments O, R, S) as markers and used quantitative PCR (qPCR) to estimate their abundance in calyx fluid.

Consistent with observing lower particle densities in the calyx lumen by TEM (Fig. 2.4A), qPCR assays indicated that segments O, R, and S were less abundant in calyx fluid from treatment versus control wasps (Fig. 2.4B). I then further assessed this outcome by pretreating calyx fluid from treatment wasps with DNase before isolation of DNA since prior studies had shown that nucleocapsids normally protect packaged DNAs from DNase [21]. This assay showed that O, R and S copy number did not differ between samples that were pretreated with DNase and those that were not (Fig. 2.4C), which indicated that *MdBVe46* knockdown reduces the number of DNA segment-containing nucleocapsids in calyx fluid rather than increasing the abundance of unpackaged viral DNAs or compromising nucleocapsid integrity.

### 2.2.4 *MdBVe46* knockdown greatly reduces infection of *C. includens* hemocytes and fat body

When *M. demolitor* oviposits into a *C. includens* larva, MdBV primarily infects hemocytes and fat body cells via entry into the cytoplasm followed by migration of nucleocapsids to the nucleus where encapsidated DNAs are discharged [14, 27]. Virulence genes are then transcribed beginning 2-4 h post-infection which thereafter continues until wasp offspring complete their development [14, 29]. Since *MdBVe46* knockdown reduced but did not prevent MdBV from accumulating in calyx fluid, I assessed whether these particles were infectious by allowing treatment and control wasps to singly oviposit into *C. includens* larvae followed by isolation of DNA from hemocytes and fat body 24 h later. Measuring absolute copy number of segments O, R and S relative to a single copy *C. includens* gene (*psp*) indicated each was readily detected in hosts attacked by control wasps but were

almost undetectable in hosts attacked by treatment wasps (Fig. 2.5A). Segment O encodes three virulence genes with known functions in suppressing host immune defenses that kill wasp offspring with *glc1.8* normally being abundantly expressed in infected host hemocytes and fat body [30-32]. Consistent with the near absence of segment O in these cell types, transcript abundance of *glc1.8* was also almost undetectable in hosts attacked by treatment wasps (Fig. 2.5B).

### 2.2.5 *MdBVe46* knockdown also greatly reduces the proportion of *C. includens* larvae that are successfully parasitized by *M. demolitor*

BV infection and the associated expression of virulence genes is thought to promote the successful parasitism of hosts by disabling immune defenses and altering the growth of hosts in ways that enable wasp offspring to develop [summarized in [6, 7, 33]. However, *M. demolitor* and other BV-carrying microgastrine braconids also introduce three other factors that have known or hypothesized functions in parasitism: 1) venom produced in a venom gland that wasps inject into hosts with eggs and BVs, 2) teratocytes, which are specialized cells that develop during embryogenesis and are released into hosts when wasp eggs hatch, and 3) products that developing wasp larvae secrete [33-36]. In the case of *M. demolitor,* parasitized *C. includens* exhibit a severe reduction in weight gain and never pupate [19, 37], while injection of wasp eggs into non-parasitized hosts usually results in encapsulation of newly hatched first instars by hemocytes [38]. In the current study, I examined the reproductive tract of treatment wasps, which showed that all possessed a venom gland that morphologically looked no different from venom glands in control wasps. I further observed that the ovaries of treatment and control wasps both

contained mature eggs. Dissection of *C. includens* larvae immediately after oviposition indicated that treatment and control females laid eggs while dissections 48 h later showed that most eggs hatched. *MdBVe46* knockdown thus reduced MdBV infection to near undetectable levels in *C. includens* but did not appear to prevent females from introducing venom or viable eggs.

I therefore asked if *MdBVe46* knockdown affected the fate of *C. includens* larvae that *M. demolitor* oviposited into by allowing individual treatment and control females to attack 10-15 *C. includens* larvae. Each host larva was oviposited into once and then reared until one of three outcomes occurred: 1) the host exhibited reduced growth and a mature wasp larva developed which usually emerged, pupated and eclosed as an adult (=parasitized), 2) hosts exhibited reduced growth and/or failed to pupate but no mature wasp larva developed (=symptomatic), or 3) the host pupated and usually emerged as an adult moth (=non-parasitized). No significant differences were detected between individual treatment (Fisher's Exact Test; df=6; p=0.10) or control wasps (Chi-square Test; df=7; p=0.76) in the proportion of hosts that were parasitized. I thus pooled all hosts attacked by individual treatment and control females for data analysis, which revealed an overall strong difference in the fate of hosts that were oviposited into by treatment or control females (Fisher's Exact Test; df=2; $p<0.0001$). Most strikingly, only 12% of hosts that treatment females oviposited into were successfully parasitized and produced a mature wasp offspring, whereas 72% of hosts that control wasps oviposited into did so (Fig. 2.6). In contrast, 63% of hosts treatment females oviposited into were symptomatic while 24% were non-parasitized, whereas 28% of hosts that control wasps oviposited into were symptomatic and none were non-parasitized (Fig. 2.6). I dissected all symptomatic hosts

attacked by treatment wasps on the day they died. Forty-two contained teratocytes, which indicated that most eggs laid by treatment wasps hatched, but I only recovered wasp larvae from 8 of these symptomatic hosts. All were dead first instars of which 2 were encapsulated by *C. includens* hemocytes.

### 2.3 Discussion

While BVs produce only one virion type, baculoviruses produce two: 1) occlusion-derived virus that is embedded in a protein matrix and orally infects hosts, and 2) budded virus that disseminates infections within hosts [5]. Proteomic and immunoblotting studies identify the same structural core gene products in occlusion-derived and budded nucleocapsids, whereas envelope formation and composition markedly differ [23, 39]. Occlusion-derived virus envelopes form de novo in the nuclei of infected cells and contain 11 core gene products while budded viruses acquire an envelope when exiting cells that contains 3 viral gene products plus several host proteins [23, 40, 41]. Some nudiviruses also produce occluded virions [42, 43], whereas BVs are never occluded [23, 40, 41]. However, the *de novo* assembly of nudivirus and BV virions during replication much more strongly resembles morphogenesis of occlusion-derived than budded baculoviruses [42, 43]. Nudiviruses and BVs also both encode several baculovirus-like genes that in baculoviruses generate products detected in occlusion-derived but not budded envelope components [3, 11, 43, 44]. These include multiple *per os* infectivity factor (PIF) genes (*p74, pif1-6, 8, odv-e66*) that baculoviruses require for oral infection of hosts but are dispensable for infection of host-derived cell lines or when injected into the hemocoel of host insects [45, 46].

Previous proteomic analysis of intact MdBV virions detected all baculovirus-like PIF gene products, several other baculovirus-like core gene products and several core gene products that are unknown from baculoviruses [21]. In the first part of this study, I built upon these previous results by separating MdBV virions into envelope and nucleocapsid fractions to: 1) assess whether the baculovirus-like structural core gene products localize to the same fractions reported for occlusion-derived baculoviruses, and 2) classify core gene products that are unknown from baculoviruses as envelope and/or nucleocapsid components. For the MdBV core genes that have diversified into large families (*odv-e66, 35a*), I was also interested in whether products for most or all of these genes are detected since several family members were unknown in the previous proteomic analysis of MdBV virions [21] but were identified when the *M. demolitor* genome was sequenced and annotated [11, 12]. Several isotopic methods have been developed to measure absolute protein abundances by mass spectrometry [47] but I selected a label-free approach because my interest was in the relative abundance of individual core gene products between two fractions. I further selected spectral (=peptide) counts for each product as the unit of measure because they linearly increase with molar abundance and their distributions can be compared between samples [22].

Results assigned most MdBV baculovirus-like core gene products to the same fractions that homologs were assigned to for occlusion-derived baculovirus virions [23]. This finding supports previous results indicating that several baculovirus-like core genes in MdBV retain conserved functions [21], while also indirectly supporting that proteomic assignments for core gene products unknown from baculoviruses are likely correct. Interestingly, the results identified most ODV-E66 and 35A family members in MdBV

virions with the former primarily being assigned as envelope-associated and the latter being primarily assigned as envelope and nucleocapsid associated. However, these results cannot distinguish between whether each ODV-E66 and 35A product is present in all MdBV virions or vary among the virions in calyx fluid. ODV-E66 derives from a single copy gene in baculoviruses and is both a potential PIF complex component and a chondroitinase that may promote midgut infection by facilitating virus entry through the peritrophic matrix that lines the midgut [48, 49]. BVs never *per os* infect hosts since wasps always inject them into the body when laying eggs. However, chondroitinase activity could still play a role in infection since sulfated glycosaminoglycans have been detected in several insect tissues [50]. Diversification of ODV-E66 into a multimember family could further be of interest if correlated with the viral DNA a given virion packages as this could influence the suite of virulence genes that are expressed in particular host cell types. Producing family member-specific antibodies is one future direction for determining how ODV-E66 and 35A gene products are distributed among MdBV virions, while similar to the MDBVE46 antibody I produced would also have utility in determining whether the proteomics-based assignments are correct or require revision.

Since BV genome components are integrated into the genomes of wasps and produce non-replicating particles, I previously developed RNAi methods that can be used for functional studies by selectively knocking down the expression of MdBV genes [21]. I further reported that several baculovirus-like core genes retain conserved functions [21] but in the case of envelope-associated PIF genes I was uncertain what role(s) they might have when BVs do not orally infect hosts. Yet similar to baculoviruses, knockdown of two MdBV PIF genes, *p74* and *pif*-1, had no effects on infection of *C. includens* cells although

reduced virulence gene expression suggested a potential effect on translocation of nucleocapsids to host cell nuclei [21]. I thus used the proteomic data generated in the current study to identify other MdBV core gene products that are envelope components that could have potential functions in infecting host cells. This led us to focus the second part of this study on MdBV *HzNVorf64-like* that I renamed as *MdBVe46.* Sequence analysis indicates that *HzNVorf64-like* genes are present in other BVs and nudiviruses assigned to the same clade as HzNV1 [8] but are absent in nudiviruses currently assigned to the *Alphanudivirus* and baculoviruses. A very recent study reported the sequence for a new nudivirus that infects a crustacean while also suggesting further division of the *Nudiviridae* into five genera but an *HzNVorf64-like* gene appears to be absent in this virus [51].

Expression of *MdBVe46* in *M. demolitor* coincides with when other MdBV structural core genes are transcribed [21] while the MDBVE46 antibody I generated fully supports assignment of this protein as an envelope component that can be knocked down to near undetectable levels by RNAi. *MdBVe46* knockdown further alters virion morphogenesis and results in almost undetectable infection of *C. includens* hemocytes and fat body. Studies of occlusion-derived baculoviruses indicate that nucleocapsids acquire their envelopes from intranuclear microvesicles [39], while the core gene *ac93* is implicated in envelope formation despite not being identified in envelope fractions prepared from occlusion-derived virions [23, 40, 52]. Two other core genes, *ac51* and *ac142,* have also been implicated in directing envelopes to correctly enclose baculovirus nucleocapsids [53, 54]. No *ac93, ac51* or *ac142* homologs have been identified in BVs or nudiviruses

[5], but the RNAi and TEM studies suggest a role for *MdBVe46* in both envelope formation and correctly enclosing MdBV nucleocapsids.

The primary immune defense against parasitoids is encapsulation, which in *C. includens* and other Lepidoptera is characterized by binding of two hemocyte types, granular cells and plasmatocytes, to the surface of eggs and/or larvae [55-57]. Most evidence implicating BVs in successful parasitism of hosts derive from studies showing that permissive hosts encapsulate wasp progeny in the absence of BV co-infection but do not when present [summarized in [58]. Several virulence gene products encoded by MdBV and other BVs have also been identified that kill or prevent immune cells from binding to foreign surfaces while also inhibiting the production of several immune effector molecules that exhibit anti-parasitoid activity [14, 32, 59, 60]. A few BV virulence genes have also been implicated in altering host growth and molting, which is thought to be important for development of wasp offspring [61, 62].

Yet as previously noted, all BV-carrying braconids introduce other factors into hosts via venom, teratocytes or wasp larval secretions whose functions largely remain unknown [35, 36]. In the case of *M. demolitor,* coupled transcriptome and proteomic data indicate that venom, teratocyte and larval secretory products exhibit almost no overlap with MdBV virulence gene products or one another which suggests functionally partitioned rather than redundant roles in parasitism of *C. includens* [21]. However, the inability to prevent BVs from infecting hosts that wasps naturally oviposit into has made it impossible to assess whether BV loss actually compromises offspring survival when the other factors wasps introduce into hosts are still present. Thus, finding that *MdBVe46* knockdown near fully prevents MdBV from infecting *C. includens* but does not eliminate

venom, teratocytes or wasp larvae enabled us to conduct such an experiment. The finding that *MdBVe46* knockdown greatly reduces wasp offspring survival strongly supports a key role for MdBV in successful parasitism of *C. includens*. However, since most hosts attacked by treatment wasps exhibit alterations in growth that are similar to parasitized hosts yet largely fail to produce mature wasps suggests other factors besides MdBV are primarily responsible for preventing *C. includens* from pupating. This finding is also consistent with an earlier study showing that injection of a physiological dose of MdBV into *C. includens* also does not fully prevent hosts from growing, whereas co-injection of MdBV and teratocytes reduces growth and pupation rates to similar levels as naturally parasitized hosts [63]. On the other hand, my finding that most progeny fail to survive in hosts attacked by treatment wasps supports earlier findings that MdBV encodes multiple virulence genes with immunosuppressive functions and prevents the *C. includens* immune system from killing wasp offspring [63].

## 2.4 Methods

### 2.4.1 Insects and cell lines

*M. demolitor* and *C. includens* were reared as previously described at 27°C under a 16 h light: 8 h dark photoperiod a [38]. After mating, male and female wasps were maintained at 18°C under a 16 h light: 8 h dark photoperiod. Wasp progeny were staged after emerging from *C. includens* and spinning a cocoon by the criteria in [10].

### 2.4.2 Proteomic analysis of virion envelope and nucleocapsid fractions

MdBV virions were isolated from 200 *M. demolitor* ovary pairs and purified as previously described [21]. Virions were resuspended in PBS containing 0.1% nonidet P40 for 30 min with gentle agitation to solubilize virion envelopes [64] and centrifuged at 20,000 x *g* for 5 min. The supernatant containing envelope proteins was then collected while the pellet containing nucleocapsids was washed three additional times by resuspension in PBS and centrifugation. Envelope and nucleocapsid fractions were then lyophilized overnight, resuspended in deionized water and proteins in each sample acetone precipitated. After centrifugation and decanting of the supernatants, the protein pellets were solubilized in SDS-PAGE sample buffer, electrophoresed on 4-20% Tris-Glycine gels (Bio-Rad), and in-gel digested with trypsin (20 µg/ml) overnight in 20 mM ammonium bicarbonate. Tryptic fragments were extracted using 50% acetonitrile and 0.1% trifluoroacetic acid and vacuum dried. Samples (4 µl) were then analyzed using an Orbitrap Elite mass spectrometer, coupled to an Easy-nLC II Liquid Chromatography (LC) instrument (Thermo Fisher Scientific). Samples were desalted and pre-concentrated on a C18 Easy LC pre-column (100um internal diameter (ID) x 2 cm, 5 µm particle packing (PP)). Peptides were eluted from a reverse-phase column (75 um ID x 10 cm, 3 µm PP) with a gradient of 10-35% B for 70 min, 35-95% B for 10 min, 95% B for 5 min (A =0.1% formic acid in water, B = 0.1% formic acid in acetonitrile) at 300 nl/min. Nanospray ionization was performed with a spray voltage of 2kV, with a capillary temperature of 200°C. The Orbitrap mass analyzer was used to provide resolutions of 120,000 and 30,000 for MS and MS/MS analyses, respectively. Briefly, a cycle of one full-scan mass spectrum (300-2000 m/z) was performed, followed by continuous cycles of CID and HCD

MS/MS spectra acquisitions of the 2 or 5 most abundant peptide ions throughout the LC separation until the candidate ions were exhausted. Data were acquired using Xcalibur software (Thermo Fisher Scientific). MdBV proteins were identified by searching against a custom database using Mascot 2.6 (Matrix Science Inc.). The database was made by merging the gff3 files containing manual annotation of nudivirus-like genes in the *M. demolitor* genome (available at the Ag Data Commons http://dx.doi.org/10.15482/USDA.ADC/1432667) with the annotation of all other wasp genes available on NCBI (GCF_000572035.2, https://www.ncbi.nlm.nih.gov/genome/annotation_euk/Microplitis_demolitor/101) using the GFF3Toolkit (https://github.com/NAL-i5K/GFF3toolkit) [23]. Protein sequences were then extracted from the merged gff3 file using GenomeTools extractfeat [22]. Data were visualized with ProteomeDiscoverer1.4 (Thermo Fisher Scientific). Peptides with scores greater than the identity score ($p$<0.05) were considered significant matches. Only ORFs that were matched by at least three peptide spectra were considered positive identifications. To assess the relative abundance of identified proteins between fractions, spectral (=peptide) counts for each identified gene product were pooled across replicates and compared to a hypothesized probability of 0.5 if equally distributed between the two fractions by G-test or Fisher's Exact test if peptide counts in one of the fractions was less than 5 [22].

### 2.4.3 Quantitative PCR (qPCR) measurement of *HzNVorf64* transcript abundance

*MdBVe46* transcript abundance was analyzed by qPCR in time course studies by isolating total RNA from the ovaries of individual stage 4 pupae and day 1 adults. Total

RNA was extracted from ovaries using the QIAGEN RNeasy kit following the standard kit protocol with a 15 min on-column DNase treatment and elution in 30µl of RNase-free $H_2O$. RNA concentration was measured using a Nanodrop Spectrophotometer and cDNA was synthesized using Invitrogen reagents including the Superscript III enzyme and oligo(dT) primers (Invitrogen) from total RNA normalized across samples. Quantitative PCR (qPCR) was then used to estimate transcript abundance across stages. An absolute standard curve was first generated by PCR amplifying *MdBVe46* using specific primers (Table 2.2). The product was cloned into pCR4-TOPO and after transforming and propagating in *Escherichia coli,* plasmid was isolated by miniprepping (Qiagen) and Sanger sequenced to confirm the identity of the cloned product (Eurofins). The threshold cycle ($C_T$) values for serial dilutions of $10^2$-$10^7$ plasmid copies were then used to generate a standard curve followed by experimental qPCR assays using ovary cDNA as template with results from each biological replicate fit to the standard curve [21]. This generated an estimate for copy number of *MdBVe46* per ng of total RNA that was isolated from each ovary pair. Standard curves, experimental qPCR assays, and melting curve analyses were performed using a Rotor-Gene Q and Rotor-Gene SYBR green PCR kit (Qiagen) with 1 uM primers and 1 ul of DNA or cDNA per 10 ul reaction. After 5 minutes of denaturation at 95°C, a two-step amplification cycle with 95° C for 5 sec denaturation and 60°C for 20 sec of annealing and extension was used for 45 cycles. Melting curve analyses were performed to ensure that amplified products were specific for the gene of interest. At least three independently acquired biological replicates were analyzed per stage with each sample internally replicated 4 times.

### 2.4.4 RNAi assays

RNAi assays were performed as detailed in [21]. In brief, *MdBVe46*-specific forward and reverse primers with added T7 promoter adaptors were designed for double-stranded (ds) RNA (dsRNA) synthesis (Table 2.2) using cDNA prepared from day 1 adult wasp ovaries as template and the MegaScript RNAi Kit (Ambion). Stage 1 *M. demolitor* were injected in the abdomen with 0.5-1 µl of 400-500 ng/µl *MdBVe46* dsRNA while control wasps were injected with a non-specific dsRNA to the bacterial *eGFP* gene [21]. qPCR was then used to detect differences in expression of *MdBVe46* and select other transcripts (*p74, pif-8, vp39*) in ovaries between treatment and control wasps. Total RNA was extracted from ovaries, its concentration determined, and first-strand cDNA synthesized as described above. The corresponding cDNA for each gene of interest was PCR amplified using specific primers (Table 2.2), cloned into pCR4-TOPO, and after propagating and miniprepping its identity confirmed by Sanger sequencing. Standard curves were then generated followed by determination of copy numbers for each transcript in ovary samples with values standardized per ng of total RNA. A minimum of three independently acquired biological replicates were analyzed per stage for each gene with each sample internally replicated 4 times. Values generated from treatment and control wasps were then statistically compared by t-test.

### 2.4.5 Antibody production and immunoblotting assays

Polyclonal antibodies to MdBVe46 were commercially produced (Pacific Immunology) by immunizing two rabbits with equal amounts of two synthesized peptides corresponding to amino acids 2-22 (DIKNFELVLGEDKPKGIIVKDC) and 330-355

(DNFRLKDKNKIDIQPKEVIELVEQIC) of the deduced sequence for MDBVE46. Both rabbits produced antisera that recognized MDBVE46 but antiserum from rabbit 1 was used in all immunoblotting experiments which consisted of isolating MdBV virions from control and *MdBVe46* knockdown wasps and preparing envelope and nucleocapsid fractions as described above. Samples were electrophoresed on 5-20% SDS-PAGE gradient gels and transferred to PVDF (Immobilon). Blots were then probed with anti-HzNVorf64 (1:2500) or an anti-actin antibody (1:1000, A2103; Sigma). Samples were visualized by adding a peroxidase-conjugated goat anti-rabbit secondary antibody (Jackson; 1:10000) followed by a chemiluminescent substrate (Clarity ECL, Biorad).

### 2.4.6 Electron microscopy

Electron microscopy was performed as in [29] with slight modification. Half-ovaries from dsRNA-injected wasps were fixed in 3% glutaraldehyde in phosphate buffer (pH7.0) at 4°C. Fixed ovaries were rinsed with buffer and post-fixed using 1% osmium tetroxide. Ovaries were then block stained using 0.5% uranyl acetate before being dehydrated in graded ethanol solutions, 100% acetone, and 100% propylene oxide. Ovaries were embedded in Spurr's resin, thin sectioned, and after staining examined using a Hitachi transmission electron microscope.

### 2.4.7 PCR-based estimates of MdBV virions containing segments O, R and S

The titer of MdBV virions with DNase-protected episomes of MdBV segments O, R and S were quantified by qPCR using established methods [14, 21]. Ovaries were dissected from individual treatment or control wasps in PBS followed by piercing the calyx with

forceps and gently extruding calyx fluid from the lumen. Calyx fluid was then either kept untreated or 1 µl of TURBO DNase from the Ambion DNA free kit was added at incubated at 37°C for 40 min to digest all free wasp and episomal viral DNAs. After the addition of EDTA (10 mM) to inactivate the DNase, 250 µg of proteinase K (Roche) and 2% sarcosyl were added to samples, followed by incubation at 62°C for 1 h and by phenol:chloroform extraction and ethanol precipitation in the presence of 0.3 M sodium acetate, pH 5.2. DNA pellets were resuspended in 30 µl of 10 mM Tris-Cl pH 8.5 and diluted to 1 ng per µl for use as template. I then estimated the copy number of MdBV segment O, R and S in a given sample by generating absolute standard curves by first PCR amplifying a domain in each circularized segment using specific primers (Table 2.2) followed by cloning of the product into pCR4-TOPO (Invitrogen), miniprepping and Sanger sequencing of cloned products to confirm identity. The threshold cycle ($C_T$) values for serial dilutions of $10^2$-$10^7$ plasmid copies were used to produce a standard curve followed by experimental qPCR assays using DNA isolated from calyx fluid to which data were fit to each standard curve as described above. A minimum of three independently acquired biological replicates were analyzed for each viral segment with each sample internally replicated 4 times. Samples from treatment and control wasps for each segment were then statistically compared by *t*-test.

### 2.4.8 Infection assays

Stage 1 wasps were injected with ds-*MdBVe46* or ds-*e*GFP followed by allowing newly emerged adult females to parasitize *C. includens* larvae for 3 days. Treatment and control females were then allowed to individually oviposit into three hosts (fourth instar), which

were held at 27°C for 24 h. The ovaries of each treatment and control wasp were analyzed to assess transcript abundance of *MbBVe46* as described above. Only hosts in which the treatment females exhibited >90% knockdown relative to the control females were then used for subsequent analysis which consisted of collecting hemocytes and fat body from the three hosts each female oviposited into as previously described [14]. Hemocytes or fat body from each host where then pooled and lysis buffer (4 M guanidine hydrochloride, 2% Sarkosyl, 50 mM Tris-Cl (pH 7.6), and 10 mM EDTA) [65] added to a volume of 200 µl. Samples were then phenol: chloroform extracted followed by precipitation of nucleic acids using 0.3 M sodium acetate, 25 µg of glycogen, and 100% isopropanol. Samples were rinsed with 70% ethanol, recentrifuged and solubilized in 100 µl water. Each sample was then split in half to obtain both DNA and RNA fractions. For DNA isolation, RNase A (6.6 µg/µl) was added to the DNA fraction followed by phenol-chloroform extraction and reprecipitation while for total RNA isolation DNase was added to the RNA fraction using the Turbo DNA-free kit (Ambion) followed by elution in water.

An absolute standard curve for the single copy *C. includens psp* gene [66] was generated by PCR amplifying a portion of this gene using specific primers (Table 2.2), cloning of the PCR product and generating threshold cycle ($C_T$) values as described above. I then estimated the copy number of MdBV segment O, R and S and the *psp* gene through experimental qPCR reactions using 1 µM primers and 1 µl of DNA from hemocyte or fat body samples per 10 µl reaction. Reaction conditions and sample replication were as described above with resulting data reported as copy number of segment O, R or S per copy of the *psp* gene. I assessed transcript abundance of the MdBV *glc1.8* gene that resides on DNA segment O by synthesizing first-strand cDNA from hemocyte and fat body

total RNA as described above. These cDNA pools were then used as templates to PCR amplify a region of *glc1.8* using specific primers (Table 2.2), followed by cloning into pCR4-TOPO, and Sanger sequencing. After propagating and miniprepping this plasmid, a standard curve was generated as described above followed by determination of *glc1.8* copy number in hemocyte and fat body samples with values standardized per 1 ng of total RNA.

### 2.4.9 Oviposition Assays

The effects of *MdBVe46* knockdown on the outcome of parasitism was assessed by allowing newly emerged treatment and control wasps to oviposit into cohorts of *C. includens* larvae on three consecutive days. On day 4, treatment and control females were then allowed to individually oviposit into 10-15 hosts (fourth instar), which were individually placed in rearing cups containing artificial diet and held at 27°C. After ovipositing in these hosts, the ovaries of each treatment and control wasp were analyzed to assess transcript abundance of *MdBVe46* as described above. Only hosts in which the treatment females exhibited >90% knockdown relative to the control females were then used for subsequent analysis which consisted of maintaining each host a female oviposited into until a mature wasp larva developed (classified as parasitized), the host pupated (classified as non-parasitized), or the host died but produced no mature wasp offspring (classified as symptomatic). I first assessed whether the proportion of hosts that were classified as parasitized differed among the 7 treatment or 8 control female wasps that were used in the experiment using a Fisher's Exact Test or a Chi-square goodness of fit test respectively. I then assessed whether the proportion of hosts that were classified

as parasitized, symptomatic and non-parasitized differed between treatment and control wasps by conducting a second Fisher's Exact Test.

## 2.5 References


1. Whitfield, J.B., *Estimating the age of the polydnavirus/braconid wasp symbiosis.* Proc Natl Acad Sci U S A, 2002. **99**(11): p. 7508-13.

2. Bezier, A., et al., *The genome of the nucleopolyhedrosis-causing virus from Tipula oleracea sheds new light on the Nudiviridae family.* J Virol, 2015. **89**(6): p. 3008-25.

3. Bezier, A., et al., *Polydnaviruses of braconid wasps derive from an ancestral nudivirus.* Science, 2009. **323**(5916): p. 926-30.

4. Wang, Y. and J.A. Jehle, *Nudiviruses and other large, double-stranded circular DNA viruses of invertebrates: new insights on an old topic.* J Invertebr Pathol, 2009. **101**(3): p. 187-93.

5. Rohrmann, G.F., *Baculovirus Molecular Biology*. 4th ed. 2019, Bethesda (MD): National Center for Biotechnology Information (US).

6. Gundersen-Rindal, D., et al., *Parasitoid polydnaviruses: evolution, pathology and applications.* Biocontrol Sci Technol, 2013. **23**(1): p. 1-61.

7. Strand, M.R. and G.R. Burke, *Polydnaviruses: Nature's Genetic Engineers.* Ann Rev Virol, 2014. **1**(1): p. 333-354.

8. Gauthier, J., J.M. Drezen, and E.A. Herniou, *The recurrent domestication of viruses: major evolutionary transitions in parasitic wasps.* Parasitology, 2018. **145**(6): p. 713-723.

9. Strand, M.R. and G.R. Burke, *Polydnaviruses: Evolution and Function.* Curr Issues Mol Biol, 2019. **34**: p. 163-182.

10. Burke, G.R. and M.R. Strand, *Deep sequencing identifies viral and wasp genes with potential roles in replication of Microplitis demolitor Bracovirus.* J Virol, 2012. **86**(6): p. 3293-306.

11. Burke, G.R., et al., *Widespread genome reorganization of an obligate virus mutualist.* PLoS Genet, 2014. **10**(9): p. e1004660.

12. Burke, G.R., *Common themes in three independently derived endogenous nudivirus elements in parasitoid wasps.* Curr Opin Insect Sci, 2019. **32**: p. 28-35.

13. Annaheim, M. and B. Lanzrein, *Genome organization of the Chelonus inanitus polydnavirus: excision sites, spacers and abundance of proviral and excised segments.* J Gen Virol, 2007. **88**(Pt 2): p. 450-7.

14. Beck, M.H., R.B. Inman, and M.R. Strand, *Microplitis demolitor bracovirus genome segments vary in abundance and are individually packaged in virions.* Virology, 2007. **359**(1): p. 179-89.

15. Louis, F., et al., *The bracovirus genome of the parasitoid wasp Cotesia congregata is amplified within 13 replication units, including sequences not packaged in the particles.* J Virol, 2013. **87**(17): p. 9649-60.

16. Burke, G.R., et al., *Microplitis demolitor Bracovirus Proviral Loci and Clustered Replication Genes Exhibit Distinct DNA Amplification Patterns during Replication.* J Virol, 2015. **89**(18): p. 9511-23.

17. Herniou, E.A., et al., *When parasitic wasps hijacked viruses: genomic and functional evolution of polydnaviruses.* Philos Trans R Soc Lond B Biol Sci, 2013. **368**(1626): p. 20130051.

18. Strand, M.R. and G.R. Burke, *Polydnavirus-wasp associations: evolution, genome organization, and function.* Curr Opin Virol, 2013. **3**(5): p. 587-94.

19. Strand, M.R., J.A. Johnson, and J.D. Culin, *Developmental interactions between the parasitoid Microplitis demolitor (Hymenoptera: Braconidae) and its host Heliothis virescens (Lepidoptera: Noctuidae).* Ann Entomol Soc Am, 1988. **81**(5): p. 822-830.

20. Burke, G.R., et al., *Whole Genome Sequence of the Parasitoid Wasp Microplitis demolitor That Harbors an Endogenous Virus Mutualist.* G3: Genes|Genomes|Genetics, 2018. **8**(9): p. 2875-2880.

21. Burke, G.R., et al., *Mutualistic polydnaviruses share essential replication gene functions with pathogenic ancestors.* PLoS Pathog, 2013. **9**(5): p. e1003348.

22. Cooper, B., J. Feng, and W.M. Garrett, *Relative, label-free protein quantitation: spectral counting error statistics from nine replicate MudPIT samples.* J Am Soc Mass Spectrom, 2010. **21**(9): p. 1534-46.

23. Hou, D., et al., *Comparative Proteomics Reveal Fundamental Structural and Functional Differences between the Two Progeny Phenotypes of a Baculovirus.* J Virol, 2013. **87**(2): p. 829-839.

24. Harrison, R.L., et al., *ICTV Virus Taxonomy Profile: Nudiviridae.* J Gen Virol, 2020. **101**(1): p. 3-4.

25. Guttieri, M.C. and J.P. Burand, *Location, Nucleotide Sequence, and Regulation of the P51 Late Gene of the Hz-1 Insect Virus: Identification of a Putative Late Regulatory Element.* Virus Genes, 2001. **23**(1): p. 17-25.

26. Cheng, C.-H., et al., *Analysis of the Complete Genome Sequence of the Hz-1 Virus Suggests that It Is Related to Members of the Baculoviridae.* J Virol, 2002. **76**(18): p. 9024-9034.

27. Strand, M.R., *Microplitis Demolitor Polydnavirus Infects and Expresses in Specific Morphotypes of Pseudoplusia Includens Haemocytes.* J Gen Virol, 1994. **75**(11): p. 3007-3020.

28. Burke, G.R. and M.R. Strand, *Polydnaviruses of Parasitic Wasps: Domestication of Viruses To Act as Gene Delivery Vectors.* Insects, 2012. **3**(1): p. 91-119.

29. Strand, M.R., et al., *Persistence and expression of Microplitis demolitor polydnavirus in Pseudoplusia includens.* J Gen Virol, 1992. **73 ( Pt 7)**: p. 1627-35.

30. Lu, Z., et al., *The viral protein Egf1.0 is a dual activity inhibitor of prophenoloxidase-activating proteinases 1 and 3 from Manduca sexta.* J Biol Chem, 2008. **283**(31): p. 21325-33.

31. Beck, M.H. and M.R. Strand, *A novel polydnavirus protein inhibits the insect prophenoloxidase activation pathway.* Proc Natl Acad Sci U S A, 2007. **104**(49): p. 19267-72.

32. Beck, M. and M.R. Strand, *Glc1.8 from Microplitis demolitor Bracovirus Induces a Loss of Adhesion and Phagocytosis in Insect High Five and S2 Cells.* J Virol, 2005. **79**(3): p. 1861-1870.

33. Pennacchio, F. and M.R. Strand, *Evolution of developmental strategies in parasitic hymenoptera.* Annu Rev Entomol, 2006. **51**: p. 233-58.

34. Vinson, S.B. and G.F. Iwantsch, *Host Suitability for Insect Parasitoids.* Ann Rev Entomol, 1980. **25**(1): p. 397-419.

35. Asgari, S. and D.B. Rivers, *Venom proteins from endoparasitoid wasps and their role in host-parasite interactions.* Annu Rev Entomol, 2011. **56**: p. 313-35.

36. Strand, M.R., *Teratocytes and their functions in parasitoids.* Curr Opin Insect Sci, 2014. **6**: p. 68-73.

37. Pruijssers, A.J., et al., *Infection by a symbiotic polydnavirus induces wasting and inhibits metamorphosis of the mothPseudoplusia includens.* J Exp Biology, 2009. **212**(18): p. 2998-3006.

38. Strand, M.R. and T. Noda, *Alterations in the hemocytes of Pseudoplusia includens after parasitism by Microplitis demolitor.* J Insect Physiol., 1991. **37**(11): p. 839-850.

39. Braunagel, S.C. and M.D. Summers, *Molecular biology of the baculovirus occlusion-derived virus envelope.* Curr Drug Targets, 2007. **8**(10): p. 1084-95.

40. Braunagel, S.C., et al., *Determination of the protein composition of the occlusion-derived virus of Autographa californica nucleopolyhedrovirus.* Proc Natl Acad Sci U S A, 2003. **100**(17): p. 9797-9802.

41. Fang, M., X. Dai, and D.A. Theilmann, *Autographa californica multiple nucleopolyhedrovirus EXON0 (ORF141) is required for efficient egress of nucleocapsids from the nucleus.* J Virol, 2007. **81**(18): p. 9859-9869.

42. Stoltz, D.B. and S.B. Vinson, *Viruses and Parasitism in Insects*, in *Advances in Virus Research*, F.B.B.K.M. Max A. Lauffer and M.S. Kenneth, Editors. 1979, Academic Press. p. 125-171.

43. Jehle, J.A., *Nudiviruses*, in *Insect Virology*, K.J. S Asgari, Editor. 2010: Norwich, UK: Caister Acad. p. 153-70.

44. Wang, Y., et al., *The genome of Gryllus bimaculatus nudivirus indicates an ancient diversification of baculovirus-related nonoccluded nudiviruses of insects.* J Virol, 2007. **81**(10): p. 5395-406.

45. Zheng, Q., et al., *Protein–protein interactions of the baculovirus per os infectivity factors (PIFs) in the PIF complex.* J Gen Virol, 2017. **98**(4): p. 853-861.

46. Boogaard, B., M.M. van Oers, and J.W.M. van Lent, *An Advanced View on Baculovirus per Os Infectivity Factors.* Insects, 2018. **9**(3).

47. Krey, J.F., et al., *Accurate label-free protein quantitation with high- and low-resolution mass spectrometers.* J Proteome Res, 2014. **13**(2): p. 1034-1044.

48. Sugiura, N., et al., *Baculovirus Envelope Protein ODV-E66 Is a Novel Chondroitinase with Distinct Substrate Specificity.* Journal Biol Chem, 2011. **286**(33): p. 29026-29034.

49. Xiang, X., et al., *Autographa californica multiple nucleopolyhedrovirus odv-e66 is an essential gene required for oral infectivity.* Virus Res, 2011. **158**(1): p. 72-78.

50. Dietrich, C.P., et al., *A relationship between the inhibition of heparan sulfate and chondroitin sulfate synthesis and the inhibition of molting by selenate in the hemipteran Rhodnius prolixus.* Biochem Biophys Res Commun, 1987. **146**(2): p. 652-658.

51. Allain, T.W., et al., *A novel nudivirus infecting the invasive demon shrimp Dikerogammarus haemobaphes (Amphipoda).* Sci Rep, 2020. **10**(1): p. 14816.

52. Yuan, M., et al., *Identification of Autographa californica nucleopolyhedrovirus ac93 as a core gene and its requirement for intranuclear microvesicle formation and nuclear egress of nucleocapsids.* J Virol, 2011. **85**(22): p. 11664-74.

53. McCarthy, C.B., et al., *Autographa californica multiple nucleopolyhedrovirus ac142, a core gene that is essential for BV production and ODV envelopment.* Virology, 2008. **372**(2): p. 325-39.

54. Shen, Y., M. Feng, and X. Wu, *Bombyx mori nucleopolyhedrovirus ORF40 is essential for budded virus production and occlusion-derived virus envelopment.* J Gen Virol, 2018. **99**(6): p. 837-850.

55. Gillespie, J.P., M.R. Kanost, and T. Trenczek, *Biological mediators of insect immunity.* Annu Rev Entomol, 1997. **42**: p. 611-43.

56. Strand, M.R. and L.L. Pech, *Immunological basis for compatibility in parasitoid-host relationships.* Annu Rev Entomol, 1995. **40**: p. 31-56.

57. Lavine, M. and M. Strand, *Insect hemocytes and their role in cellular immune responses.* Insect Biochem Mol Biol, 2002. **32**: p. 1237-1242.

58. Burke, G.R. and M.R. Strand, *Systematic analysis of a wasp parasitism arsenal.* Mol Ecol, 2014. **23**(4): p. 890-901.
59. Bitra, K., R.J. Suderman, and M.R. Strand, *Polydnavirus Ank Proteins Bind NF-κB Homodimers and Inhibit Processing of Relish.* PLOS Pathogens, 2012. **8**(5): p. e1002722.

60. Cooper, T.H., et al., *Identification of an in vitro interaction between an insect immune suppressor protein (CrV2) and G alpha proteins.* J Biol Chem, 2011. **286**(12): p. 10466-75.

61. Falabella, P., et al., *Protein tyrosine phosphatases of Toxoneuron nigriceps bracovirus as potential disrupters of host prothoracic gland function.* Arch Insect Biochem Physiol, 2006. **61**(3): p. 157-69.

62. Prasad, S.V., R. Hepat, and Y. Kim, *Selectivity of a translation-inhibitory factor, CpBV15β, in host mRNAs and subsequent alterations in host development and immunity.* Dev Comp Immunol, 2014. **44**(1): p. 152-62.

63. Strand, M.R. and E.A. Wong, *The growth and role of Microplitis demolitor teratocytes in parasitism of Pseudoplusia includens.* J Insect Physiol, 1991. **37**(7): p. 503-515.

64. Braunagel, S.C. and M.D. Summers, *Autographa californica nuclear polyhedrosis virus, PDV, and ECV viral envelopes and nucleocapsids: structural proteins, antigens, lipid and fatty acid profiles.* Virology, 1994. **202**(1): p. 315-28.

65. Coffman, K.A., T.C. Harrell, and G.R. Burke, *A Mutualistic Poxvirus Exhibits Convergent Evolution with Other Heritable Viruses in Parasitoid Wasps.* J Virol, 2020. **94**(8): p. e02059-19.

66. Clark, K.D., A. Witherell, and M.R. Strand, *Plasmatocyte spreading peptide is encoded by an mRNA differentially expressed in tissues of the moth Pseudoplusia includens.* Biochem Biophys Res Commun, 1998. **250**(2): p. 479-85.

## 2.6 Figures and Tables

### Table 2.1: MdBV gene products identified in virion envelope and capsid fractions[a]

| MdBV gene | Envelope | | | Nucleocapsid | | | | Other viruses | | | |
|---|---|---|---|---|---|---|---|---|---|---|---|
| | R1 | R2 | Σ | R1 | R2 | Σ | Assignment | Bac | aNV | bNV | BV |
| P74/Pif-0 | 37 | 36 | 73 | 0 | 0 | 0 | E | (E)+ | + | + | + |
| Pif-1 | 19 | 16 | 35 | 2 | 4 | 6 | E | (E)+ | + | + | + |
| Pif-2 | 11 | 12 | 23 | 2 | 3 | 5 | E | (E)+ | + | + | + |
| Pif-3 | 11 | 7 | 18 | 2 | 0 | 2 | E | (E)+ | + | + | + |
| Pif-4 | 9 | 5 | 14 | 0 | 0 | 0 | E | (E)+ | + | + | + |
| Pif-5-1 | 21 | 13 | 34 | 0 | 2 | 2 | E | (E)+[b] | + | + | + |
| Pif-5-2 | 8 | 6 | 14 | 0 | 0 | 0 | E | | | | |
| Pif-5-3 | 12 | 9 | 21 | 6 | 13 | 19 | E/N | | | | |
| Pif-6 | 5 | 4 | 9 | 0 | 0 | 0 | E | (E)+ | + | + | + |
| Vp91/Pif-8 | 35 | 44 | 79 | 3 | 3 | 6 | E | (E)+ | + | + | + |
| ODV-E66-1 | 33 | 39 | 72 | 3 | 8 | 11 | E | (E)+[b] | + | + | + |
| ODV-E66-2 | 6 | 4 | 10 | 0 | 0 | 0 | E | | | | |
| ODV-E66-3 | 22 | 24 | 46 | 0 | 25 | 25 | E | | | | |
| ODV-E66-4 | 6 | 5 | 11 | 0 | 4 | 4 | E/N | | | | |
| ODV-E66-5 | 23 | 29 | 52 | 4 | 5 | 9 | E | | | | |
| ODV-E66-6 | 50 | 50 | 100 | 13 | 22 | 35 | E | | | | |
| ODV-E66-7 | 19 | 24 | 43 | 3 | 3 | 6 | E | | | | |
| ODV-E66-10 | 19 | 34 | 53 | 0 | 14 | 14 | E | | | | |
| ODV-E66-12 | 35 | 33 | 68 | 10 | 8 | 18 | E | | | | |
| ODV-E66-13 | 13 | 12 | 25 | 0 | 0 | 0 | E | | | | |
| ODV-E66-14 | 38 | 35 | 73 | 17 | 19 | 36 | E | | | | |
| ODV-E66-15 | 19 | 16 | 35 | 2 | 3 | 5 | E | | | | |
| ODV-E66-16 | 29 | 25 | 54 | 12 | 10 | 22 | E | | | | |
| ODV-E66-17 | 23 | 20 | 43 | 0 | 5 | 5 | E | | | | |
| ODV-E66-19 | 21 | 26 | 47 | 0 | 0 | 0 | E | | | | |
| ODV-E66-20 | 28 | 28 | 56 | 0 | 4 | 4 | E | | | | |
| 38K | 7 | 7 | 14 | 10 | 13 | 23 | E/N | (N)+ | + | + | + |
| Vp39 | 5 | 9 | 14 | 14 | 17 | 31 | N | (N)+ | + | + | + |
| Vlf-1a | 0 | 0 | 0 | 6 | 12 | 18 | N | (N)+[b] | + | + | + |
| Vlf-1b-1 | 0 | 0 | 0 | 4 | 5 | 9 | N | | | | |
| Vlf-1b-2 | 0 | 0 | 0 | 7 | 12 | 19 | N | | | | |
| Ac92-like-1 | 2 | 3 | 5 | 0 | 2 | 2 | E/N | (E)+ | + | + | + |
| Ac92-like-2 | 0 | 2 | 2 | 0 | 3 | 3 | E/N | | | | |
| Int-1 | 0 | 0 | 0 | 8 | 15 | 23 | N | - | +[b] | +[b] | + |
| HzNVorf94-like | 13 | 11 | 24 | 2 | 0 | 2 | E | - | - | + | + |
| HzNVorf93-like | 0 | 0 | 0 | 2 | 3 | 5 | N | - | - | + | + |
| HzNVorf9-like-1 | 3 | 4 | 7 | 11 | 18 | 29 | N | - | - | + | + |
| HzNVorf9-like-2 | 1 | 5 | 6 | 10 | 14 | 24 | N | | | | |
| HzNVorf106-like | 0 | 3 | 3 | 10 | 12 | 22 | N | - | - | + | + |
| HzNVorf118-like | 0 | 3 | 3 | 7 | 8 | 15 | N | - | - | + | + |
| HzNVorf128-like | 0 | 0 | 0 | 0 | 4 | 4 | N | - | - | + | + |
| HzNVorf64-like (MdBVe46) | 13 | 10 | 23 | 0 | 6 | 6 | E | - | - | + | + |
| 17a | 9 | 8 | 17 | 10 | 10 | 20 | E/N | - | - | - | + |
| 27b-like-1 | 0 | 2 | 2 | 7 | 9 | 16 | N | - | - | + | + |
| 35a-2 | 18 | 18 | 36 | 15 | 16 | 31 | E/N | - | - | - | + |
| 35a-4 | 3 | 5 | 8 | 13 | 11 | 24* | N | | | | |
| 35a-5 | 12 | 4 | 16 | 13 | 29 | 42* | N | | | | |
| 35a-6 | 33 | 25 | 58 | 13 | 25 | 38 | E | | | | |
| 35a-7 | 51 | 22 | 73 | 34 | 47 | 81 | E/N | | | | |
| 35a-8 | 43 | 33 | 76 | 28 | 31 | 59 | E/N | | | | |
| 35a-10 | 13 | 9 | 22 | 10 | 17 | 27 | E/N | | | | |
| 35a-11 | 18 | 10 | 28 | 13 | 13 | 26 | E/N | | | | |
| 35a-12 | 16 | 11 | 27 | 9 | 8 | 17 | E/N | | | | |
| 35a-13 | 61 | 18 | 79 | 62 | 78 | 140 | N | | | | |
| 35a-14 | 43 | 32 | 75 | 36 | 52 | 88 | E/N | | | | |
| Cc50C22.5-like | 25 | 22 | 47 | 12 | 16 | 28 | E | - | - | - | + |
| Cc50C22.6-like-1 | 6 | 6 | 12 | 3 | 10 | 13 | E/N | - | - | - | + |
| K425_450 | 9 | 8 | 17 | 0 | 0 | 0 | E | - | - | - | + |
| K425_456 | 18 | 16 | 34 | 8 | 13 | 21 | E | - | - | - | + |
| K425_459 | 0 | 4 | 4 | 5 | 7 | 12 | N | - | - | - | + |
| K425_461 | 6 | 6 | 12 | 3 | 5 | 8 | E/N | - | - | - | + |

[a]For each gene product, the number of unique peptides detected in the envelope or nucleocapsid fraction in each replicate (R1 and R2) and summed (Σ) is shown. Products were assigned as envelope- (E) or nucleocapsid- associated (N) if peptide counts significantly deviated from an expected distribution of 0.5 or E/N-associated if they did not. To the right indicates identifiable homologs are present (+) or absent (-) in all other sequenced baculoviruses (Bac), alphanudiviruses (aNV), betanudiviruses (bNV) or bracoviruses (BV). For baculoviruses, E indicates the homologous product is preferentially detected in the envelope fraction of occlusion-derived virus while N indicates the product in preferentially detected in the nucleocapsid fraction (see main text).

[b]Indicates these genes are single copy in baculoviruses or nudiviruses but form multimember families in MdBV.

## Table 2.2: qPCR and dsRNA primer sequences

| Target | Accession numbers | Primer name | Sequence 5'-3' |
|---|---|---|---|
| **dsRNA synthesis primers** | | | |
| HzNVorf64 | MDEMTmpGB000093 | HzNVorf64_F_RNAi | TAATACGACTCACTATAGGGATAACCGATGCGTTACAGAC |
| | | HzNVorf64_R_RNAi | TAATACGACTCACTATAGGGATTGAAGCAAGAAAACAGGA |
| **qPCR primers** | | | |
| HzNVorf64 | MDEMTmpGB000093 | HzNVorf64_F_qPCR | TAATTGATCTGCTGTCTGATCG |
| | | HzNVorf64_R_qPCR | GAAATCTCGGTAATTGGTTTCTATG |
| ef1-α | | EF1aMdFqPCR | ATTGAAGGCCGAGCGTGAAC |
| | | EF1aMdRqPCR | CCGAGGGTGAAAGCAAGGAG |
| vp91 | MDEMTmpGB000004 | PIF-8/VP91_F_qPCR | TTGAACTTGAGCGAAGCAAA |
| | | PIF-8/VP91_R_qPCR | CAATAATTTCGACCGGGTTT |
| vlf-1a | MDEMTmpGB000094 | VLF-1a_F_qPCR | AACATTGAAAACGCACAACG |
| | | VLF-1a_R_qPCR | TTGTCAAAGACGGTTGGATG |
| p74 | MDEMTmpGB000024 | p74F* | TCGGTAATTGATTGGGGAGA |
| | | p74R* | TGCAGCACCAAACAAACAAT |
| vp39 | MDEMTmpGB000082 | VP39_F_qPCR | CGCTACACGCTATCGATTTG |
| | | VP39_R_qPCR | CACTGACTGTGCACAAAATTCA |
| lef-4 | MDEMTmpGB000092 | lef4qPCRF* | ACCCTTCACCAGGACAACTG |
| | | lef4qPCRR* | AAATAGTACGCGCCACCTTG |
| lef-8 | MDEMTmpGB000102 | lef-8qPCRF | TTTACGACCCACCTGACACA |
| | | lef-8qPCRR | CATGTGCTTTCCAATCATGC |
| Segment O | NW_014464327.1 | Segment_O_F | TTGCCAGGCCAGAAATTTTCAACATTACAATCTA |
| | | Segment_O_R | TACCCCTATAAGTAGTCCATCAAAAAGAACTGTGG |
| Segment R | NW_014464373.1 | Segment_R_Inside_F | CACACCCACACATTCGGATA |
| | | Segment_R_Inside_R | CCGTGCATTTTCTGTTCTGA |
| Segment S | NW_014463823.1 | Segment_S_Inside_F | TTGGTCAATTCTTGCGACTG |
| | | Segment_S_Inside_R | TACGGGTGGCTAAAATGGAG |

**Figure 2.1: *MdBVe46* is a late structural core gene that is preferentially detected in the MdBV envelope fraction.** (A) Mean transcript abundance ± SE in *M. demolitor* ovaries from stage 4 pupae and day 1 adults as determined by qPCR. The y axis shows copy number per ug of total RNA isolated from ovaries. Values at the bottom of each bar indicate the number of ovary pairs that were examined from each wasp stage. (B) Immunoblot showing that MDBVE46 is preferentially detected in the envelope fraction of MdBV virions. The total number of virions present in calyx fluid from a newly emerged adult female were either isolated as intact virions or partitioned into an envelope and nucleocapsid fraction. One tenth of each sample was then loaded per lane of an SDS-PAGE gel followed by immunoblot analysis using an MdBV anti-MdBVe46 antibody (1:2500). Molecular mass markers are indicated to the left.

**A**

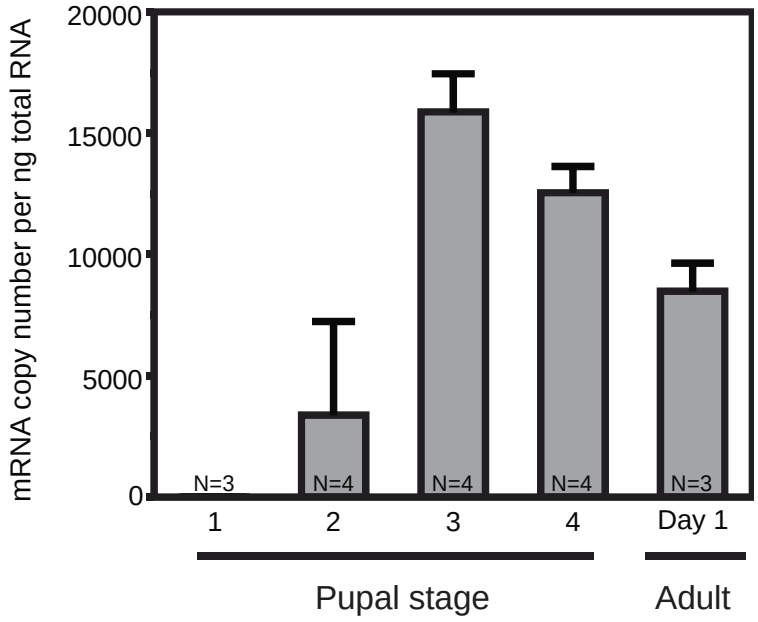
mRNA copy number per ng total RNA
20000
15000
10000
5000
0
N=3
N=4
N=4
N=4
N=3
1
2
3
4
Day 1
Pupal stage
Adult

**B**

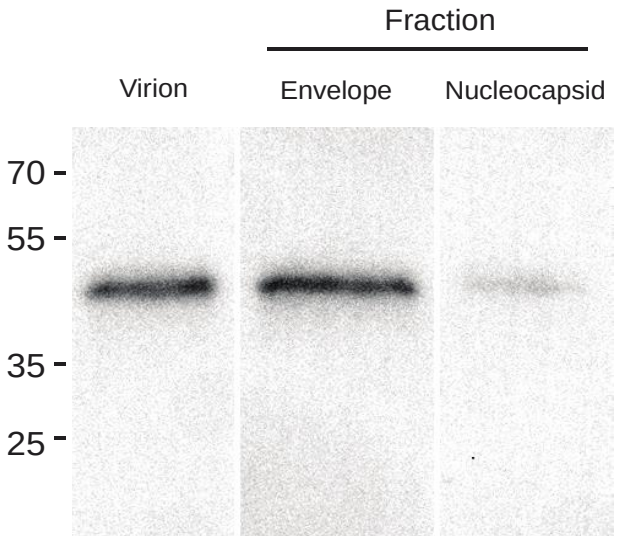
Fraction
Virion
Envelope
Nucleocapsid
70
55
35
25

**Figure 2.2: RNAi knockdown of *MdBVe46.*** *M. demolitor* were injected with double-stranded RNA (dsRNA) specific for *MdBVe46* (treatment) or ds-*e*GFP (control) followed by dissection of ovaries from individual, newly emerged females, isolation of total RNA and determination of total copy number ± SE for (A) *MdBVe46,* (B) *p74,* (C) *pif-8,* (D) *vp39.* Four asterisks (****) indicates copy number strongly differed between treatment and control females ($p \leq 0.0001$) while ns indicates no significant difference ($p > 0.05$). Values at the bottom of each bar indicates sample size for each treatment. (E) A one tenth aliquot of protein from the ovaries of four newly emerged females injected at stage 1 with ds-*e*GFP (left) or four newly emerged females (right) injected at stage 1 with ds-*MdBVe46* was loaded in each lane of an SDS-PAGE gel followed by immunoblot analysis using anti-MDBVE46 (1:2500). A second blot loaded with the same amount of protein but probed with an anti-actin antibody (1:1000) served as the loading control. Molecular mass markers are indicated to the left.

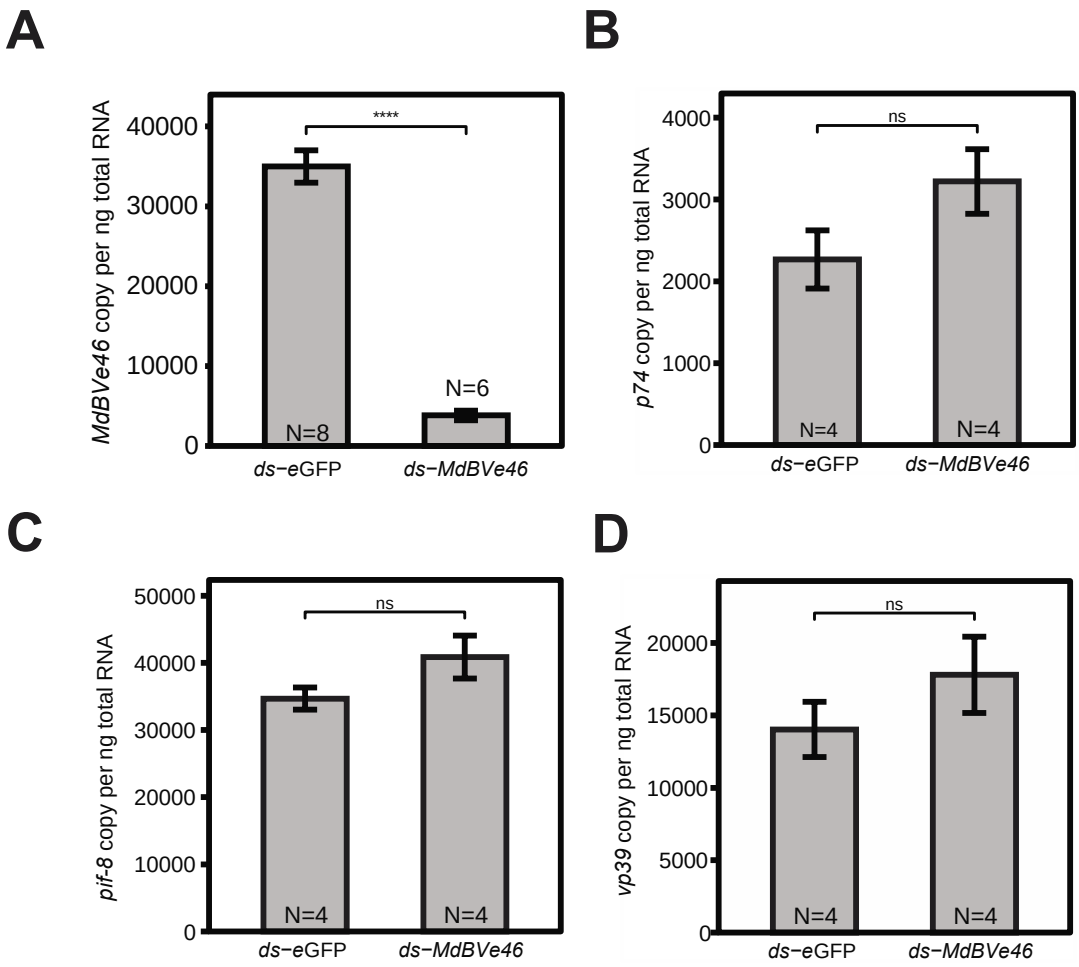
A
B
C
D
E
MdBVe46 copy per ng total RNA
p74 copy per ng total RNA
pif-8 copy per ng total RNA
vp39 copy per ng total RNA
****
ns
N=8
N=6
N=4
ds−eGFP
ds−MdBVe46
kDa
55
35
MdBVe46
F-Actin

**Figure 2.3: Electron microscopy analysis shows defects in MdBV morphogenesis after knockdown of *MdBVe46*.** *M. demolitor* were injected with ds-*e*GFP (control) or ds-*MdBVe46* (treatment) followed by isolation, fixation and thin sectioning of ovaries from different pupal stages or adults. (A) Image of a calyx cell nucleus from an early stage 3 control pupa showing the de novo appearance of envelope profiles (E) and electron-dense nucleocapsids (N). Scale bar = 180 nm. (B) Image of a calyx cell nucleus from a late stage 3 control pupa showing envelopes in the process of surrounding individual nucleocapsids (arrows) and parallel arrays of assembled virions in virogenic stroma that each consist of an electron-dense nucleocapsid and an elongated envelope (asterisks). (C). Image of calyx fluid in the calyx lumen of a newly emerged control adult female showing an abundance of virions that each consist of a single nucleocapsid surrounded by an envelope of uniform width but varying length. B and C are at the same magnification with the scale bar in C = 300 nm. (D) Image of a calyx cell nucleus from an early stage 3 treatment pupa showing the *de novo* appearance of electron-dense nucleocapsids (N) but no envelopes. (E and F). Images of calyx cell nuclei from different late stage 4 treatment pupae showing a predominance of nucleocapsids in virogenic stroma with no envelope (arrowhead) and individual nucleocapsids surrounded by a single rounded envelope. Note that nucleocapsids with and without envelopes do not form parallel arrays. (G) Image of calyx fluid in the calyx lumen from a newly emerged treatment adult female showing morphologically variable particles that include a virion with five nucleocapsids surrounded by a single rounded envelope (arrowhead), a single nucleocapsid surrounded by a rounded envelop (arrow) or a nucleocapsid with no envelop (asterisk). D-G are at the same magnification with the scale bar in G = 310 nm.

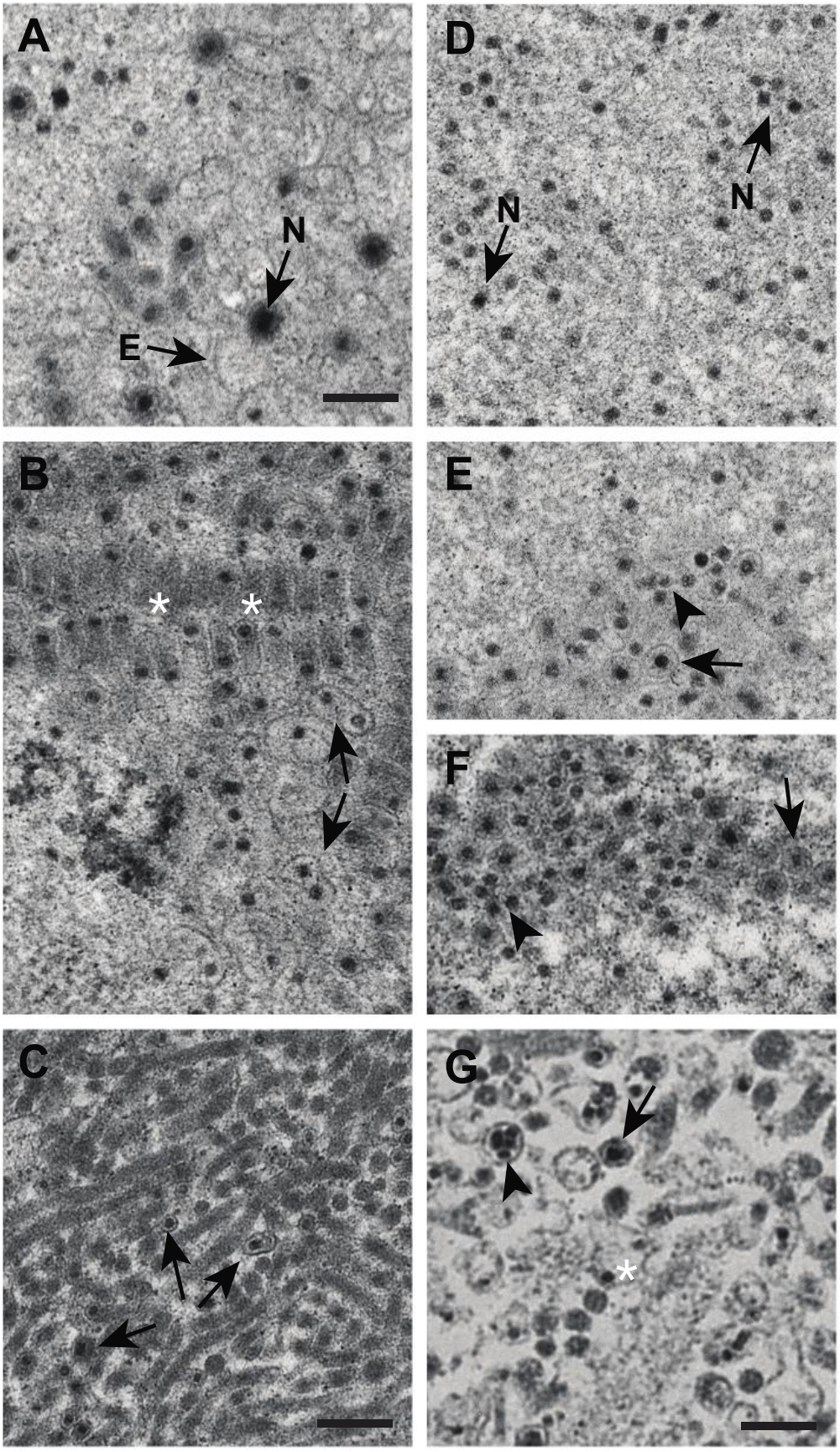
A
N
E
D
N
N
B
*
*
E
F
C
G
*

**Figure 2.4: Knockdown of *MdBVe46* reduces virion abundance in calyx fluid.** Stage 1 *M. demolitor* were injected with or ds-*eGFP* (control) or ds-*MdBVe46* (treatment) followed by collection of ovaries from newly emerged adult females. (A) Graph showing particle density ± SE in TEM sections from control wasps was higher than in treatment wasps. (B). Mean copy number ± SE of MdBV segments O, R or S in calyx fluid collected from control and treatment wasps. (C). Mean copy number ± SE of MdBV segments O, R, S, in calyx fluid from treatment wasps that were or were not pretreated with DNase before DNA extraction. N values at the bottom of each bar indicate the number of ovary pairs that were analyzed. Statistical significance is indicated by asterisks: *, p≤0.05; **, p≤0.01; ***, p≥ 0.001; ****, p≥0.0001; ns, not significant.

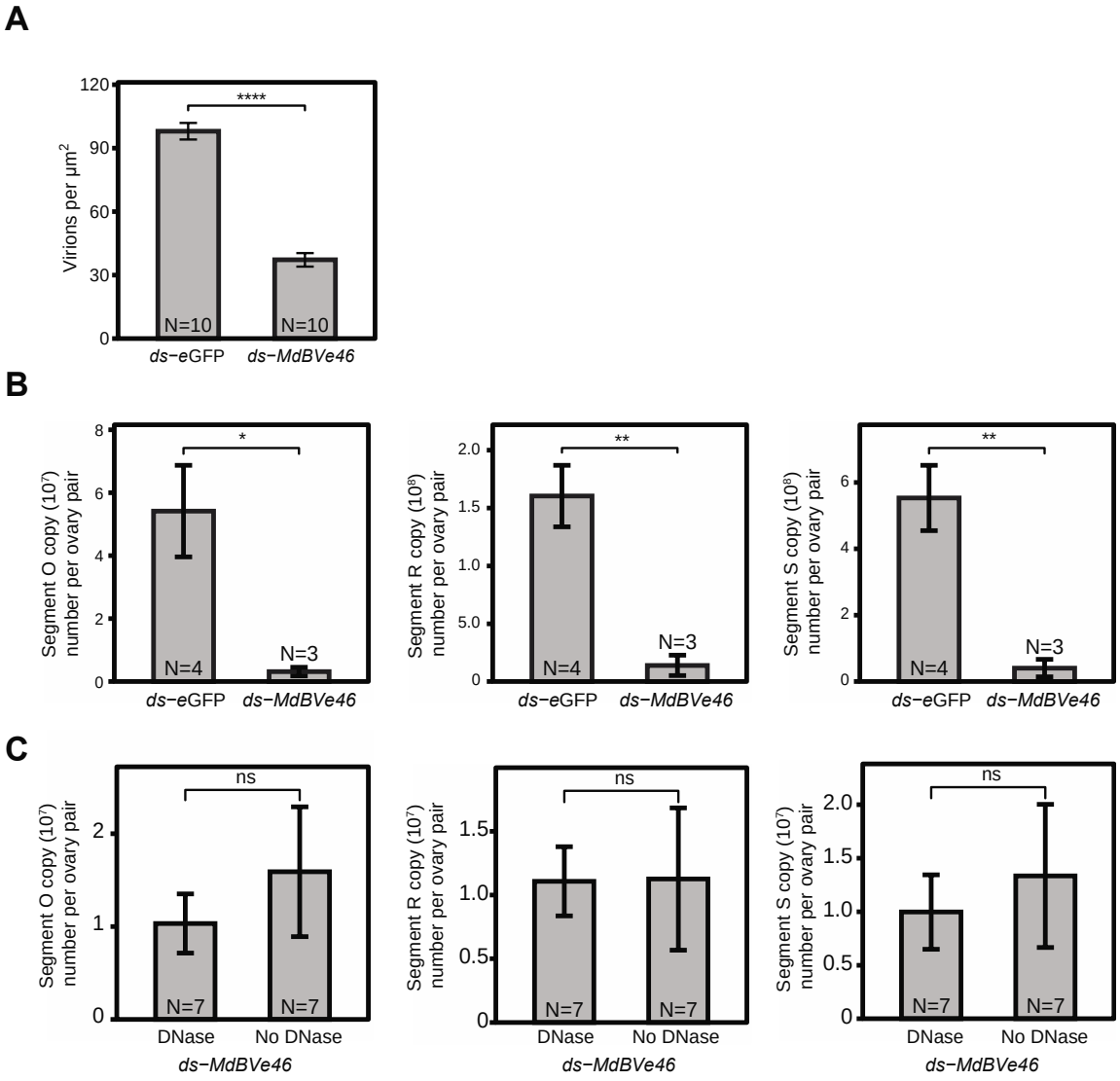
A
120
90
60
30
0
Virions per µm2
****
N=10
N=10
ds−eGFP
ds−MdBVe46
B
Segment O copy (10^7) number per ovary pair
*
N=4
N=3
Segment R copy (10^6) number per ovary pair
**
N=4
N=3
Segment S copy (10^6) number per ovary pair
**
N=4
N=3
C
Segment O copy (10^7) number per ovary pair
ns
N=7
N=7
DNase
No DNase
ds−MdBVe46
Segment R copy (10^7) number per ovary pair
ns
N=7
N=7
DNase
No DNase
ds−MdBVe46
Segment S copy (10^7) number per ovary pair
ns
N=7
N=7
DNase
No DNase
ds−MdBVe46

**Figure 2.5: Knockdown of *MdBVe46* reduces MdBV infection of *C. includens* hemocytes and fat body.** *M. demolitor* were injected with *ds-e*GFP (control) or *ds-MdBVe46* (treatment). Adult females were then allowed to parasitize three to four *C. includens* larvae from which DNA and total RNA was isolated from hemocytes or fat body and pooled. (A) Mean copy number ± SE of MdBV segments O, R, and S per hemocyte or fat body cell from control and treatment hosts. (B) Mean copy number ± SE of *glc1.8* per ug of total RNA in hemocytes or fat body from control or treatment hosts. The number of wasps examined for each treatment is indicated by the N value at the bottom of each bar. Statistical significance is indicated by asterisks: *, p≤0.05; **, p≤0.01; ***, p≥ 0.001; ****, p≥0.0001; ns, not significant.

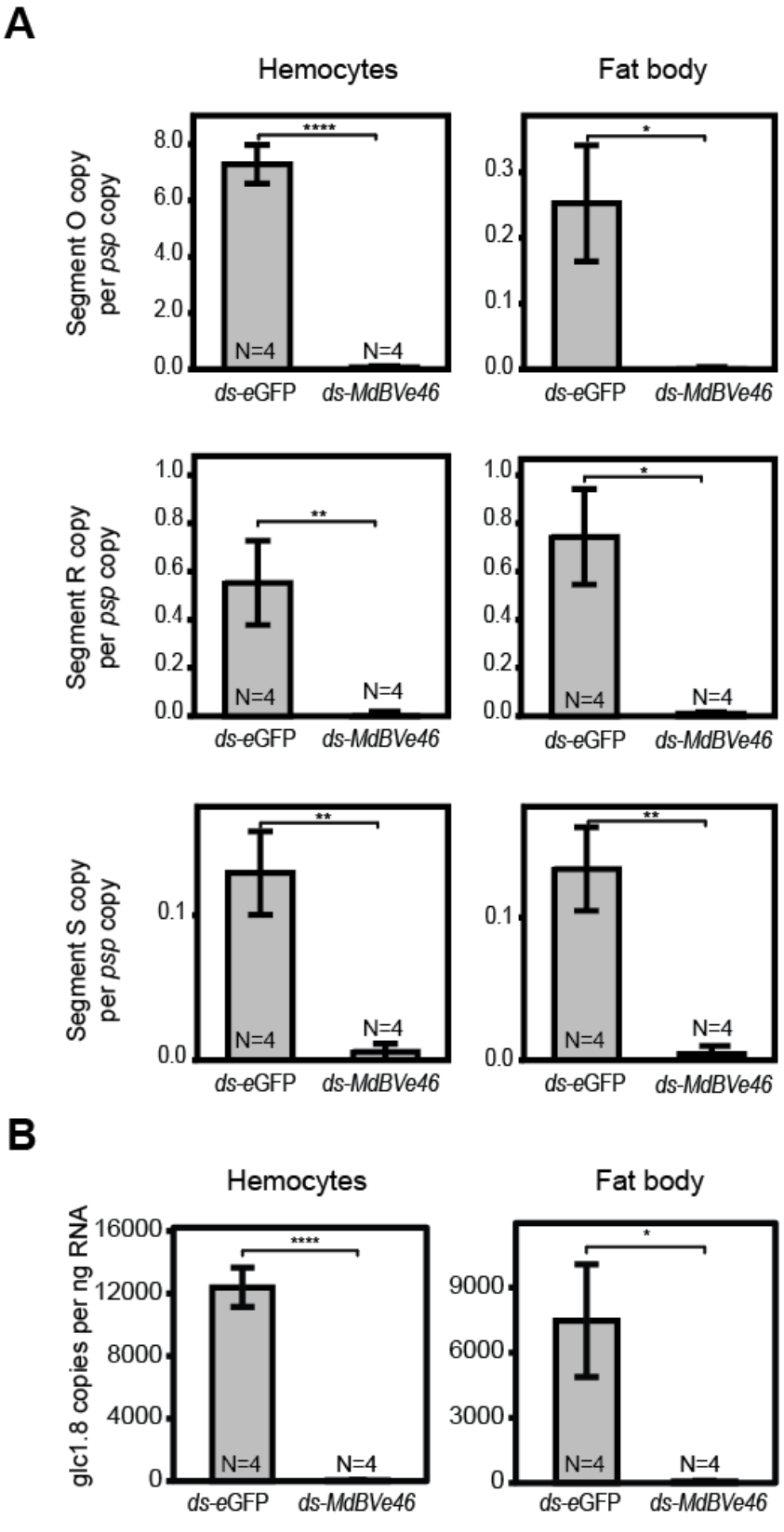
A
Hemocytes
Fat body
Segment O copy per psp copy
Segment R copy per psp copy
Segment S copy per psp copy
****
*
**
N=4
ds-eGFP
ds-MdBVe46
B
glc1.8 copies per ng RNA

**Figure 2.6: Knockdown of *MdBVe46* reduces parasitism of *C. includens* by *M. demolitor*.** *M. demolitor* were injected with *ds-e*GFP (control) or *ds-HzNVorf64* (treatment). Eight control and 7 treatment adult females were then allowed to parasitize 10-15 *C. includens* larvae. Bars indicate the proportion of hosts that: produced a mature wasp larva (parasitized) (=P), died without pupating but produced no wasp larva (symptomatic) (=S), or pupated (non-parasitized) (=N). The values at the bottom of each bar indicates the total number of treatment and control hosts that were classified as P, S or N.

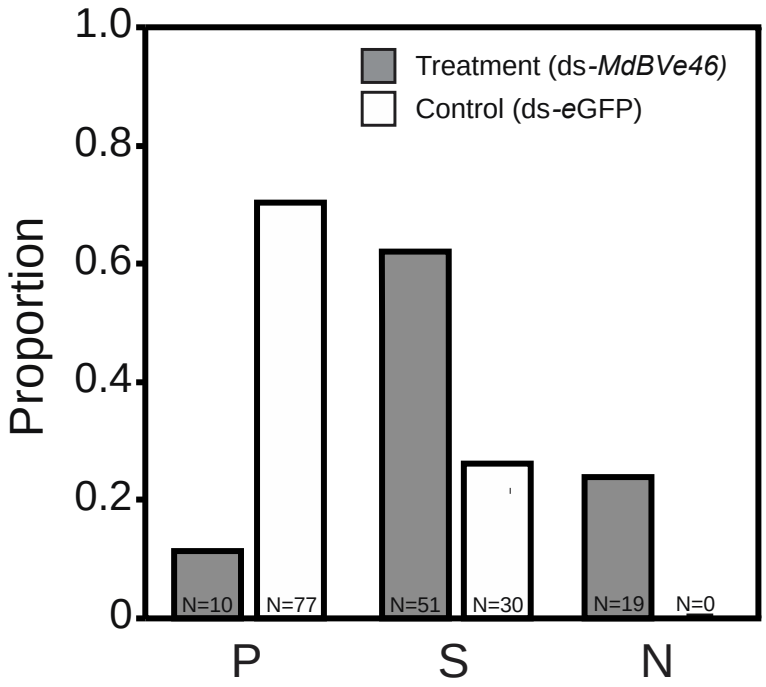
1.0
0.8
0.6
0.4
0.2
0
Proportion
Treatment (ds-*MdBVe46)*
Control (ds-*e*GFP)
N=10
N=77
N=51
N=30
N=19
N=0
P
S
N

# 3. PER OS ORAL INFECTIVITY GENES AFFECT MORPHOGENESIS AND INFECTIVITY OF *MICROPLITIS DEMOLITOR* BRACOVIRUS VIRIONS

## 3. 1 Introduction

The results from the preceding chapter identified one envelope gene which appears to be critical for the formation of viral envelopes. Another group of MdBV genes that are clearly identified as envelope components in my analysis are homologs of *per os* infectivity factors (PIFs). PIFs are known to exist in baculoviruses, nudiviruses, hytrosaviruses, and whispoviruses, all of which infect orally [1-4]. Most functional insights about PIF gene function derive from studies of baculoviruses where PIF genes are known envelope components of baculovirus occlusion-derived virus particles (ODVs). As discussed in previous chapters, baculoviruses are well studied and share a set of core genes, many of which have been functionally characterized and are conserved in nudiviruses and BVs [5]. The baculovirus life cycle [reviewed in [5] broadly consists of two phases, each characterized by different virion morphotype, associated proteins, and mode of infection. Insects first become infected with baculoviruses by ingesting occlusion bodies, which are protective protein matrices in which are embedded ODVs, the first morphotype. Baculovirus ODV morphotypes are released from occlusion bodies in the insect midgut, after which they infect midgut epithelial cells [6]. During the initial phase of infection, infected midgut cells produce budded virus particles, the secondary baculovirus virion morphotype. Insect midgut cells are thus the entry point for baculovirus infection. The

secondary virion morphotype spreads the infection systemically throughout the insect, similar to BV infection. During later stages of infection, ODVs are produced in the nuclei of infected cells where they derive their envelope from nuclear membranes before being occluded. To infect insect midgut cells after ingestion by caterpillars, ODVs require a set of proteins specific to ODV envelopes, namely the PIFs [1, 7]. Each PIF is essential for oral infection by baculoviruses and knockout of PIFs results in a failure of ODVs to infect orally through insect midgut cells. In contrast, ODV infection of other host cell types does not require PIFs. ODVs with one or more PIF gene knockouts have no trouble infecting cells elsewhere in the insect.

A total of nine baculovirus PIFs have been identified, namely *pif-0* [8, 9], *pif-1* [10, 11], *pif-2* [12, 13], *pif-3* [10, 14], *pif-4* [15, 16], *pif-5* [17, 18], *pif-6* [19], *pif-7* [20], and *pif-8* [21]. With the exception of *pif-5*, evidence shows that all PIF gene products physically interact with each other in the form of a highly stable complex on the surface of ODV virions, which is thought to play a critical role in midgut cell entry [22]. While their sequences differ from one another greatly, PIFs share certain characteristics. All PIFs have hydrophobic transmembrane domains [1, 7]. For Pif-1, Pif-2, Pif-3, Pif-4, Pif-6, and Pif-8 these are N-terminal domains identified as inner nuclear membrane sorting motif (INM-SM) that has been shown to be crucial for routing proteins to the inner nuclear membrane [1, 14, 23, 24]. In Pif-0, Pif-5, and Pif-6 their hydrophobic domain is present in the C-terminal region, and for Pif-5 this region has been shown to be required for translocation to the baculovirus ODV envelope [1, 25]. Another feature shared by PIFs is the presence of highly conserved cysteine domains, which are found in all PIFs except Pif-6 and Pif-7 [7].

Microgastroid wasps inject BV virions directly into hemocoel of host insects where they infect hemocytes, fat body and select other tissues [26, 27]. Unlike baculoviruses, BVs do not need to infect midgut epithelial cells prior to systemic infection. Despite this, MdBV encodes 10 PIF genes; *pif-0/p74*, *pif-1*, *pif-2*, *pif-3*, *pif-4*, *pif-5-1*, *pif-5-2*, *pif-5-3*, *pif-6*, and *pif-8* (Fig. 3.1). These PIF homologs were initially identified during transcriptomic analysis of *M. demolitor* ovaries and are upregulated during MdBV replication [28]. In previous work, MdBV *pif-8* and *pif-6* are known as *vp91* and *Cc50C22.3*, respectively [28]. Gene products of all MdBV PIFs are present in MdBV virions [29]. Functional studies using RNAi to knock down *pif-0* and *pif-1* in *Microplitis demolitor* bracovirus (MdBV) showed that PIFs are not required for infection of host cells but did significantly reduce the expression of select virulence genes, suggesting that loss of PIFs from the MdBV envelope results in improper translocation of MdBV to host cell nuclei, where virulence genes are expressed [29].

Given that BVs are passed from wasp carriers to their hosts by being injected directly into the host hemocoel during parasitism, it is not clear why genes known to be oral infectivity factors should be conserved. While the two MdBV PIFs studied so far do not support an obvious critical role in BV infection, many PIFs remain to be investigated. In this study I further examined MdBV PIFs and assessed their homology to baculovirus PIFs. In addition, I performed functional studies on a core complex PIF homolog (*pif-2*), a complex-associated PIF homolog (*pif-8*), and three homologs of a PIF not known to be associated with the PIF entry complex and the only PIF that has expanded into a multimember gene family in BVs (*pif-5-1*, *pif-5-2*, and *pif-5-3*). I knocked down selected MdBV PIFs in wasps and performed experiments that tested knockdown virion structural

integrity, morphogenesis, and ability to infect host cells and live hosts. I found little evidence that MdBV PIFs are essential for infection of host cells and tissues. I did find evidence that some of the selected PIFs could be involved in translocation of viral DNA to the nucleus, mirroring previous MdBV PIF work. In addition, I found that some PIFs, primarily *pif-8*, is involved in virion morphogenesis in wasp calyx cell nuclei.

## 3.2 Results

### 3.2.1 *Per os* infectivity factors are present in BVs

The percent shared identity of MdBV PIF genes with corresponding predicted proteins from the closest known nudivirus-relative, *Heliothis zea* nudivirus-1 (HzNV-1) are as follows: *pif-0/p74* (27%), *pif-1* (28%), *pif-2* (30%), *pif-3* (34%), *pif-4* (27%), *pif-5-1* (27%), *pif-5-2* (23%), *pif-5-3* (23%), and *pif-6* (25%), *pif-8* (23%). I performed a MUSCLE alignment of MdBV PIF peptide sequences to homologs from all virus families in which they have been identified (Table 3.1). My results indicated that all MdBV PIFs retain most of the highly conserved PIF cysteine residues previously identified in their baculovirus homologs as being highly conserved (Fig. 3.2) [7]. Cysteines are potentially significant in forming disulfide bonds and determining overall protein structure and folding, however no information is currently available on how this might work in baculoviruses or any other virus. These alignments further indicated that peptide regions containing previously identified transmembrane domains are conserved in all MdBV PIFs (Fig. 3.3 and Fig. 3.4). One exception is *pif-5-1*, in which the second domain is truncated (Fig. 3.3) [1]. I performed my own analysis of these regions in MdBV PIF peptide sequences using protein structure prediction tools TMHMM (Server v. 2.0,

http://www.cbs.dtu.dk/services/TMHMM/)[30] and Phobius (http://phobius.sbc.su.se/)[31] and found results largely congruent with my protein sequence comparison (Fig. 3.5 and Fig. 3.6). P74/Pif-0 showed mixed results in the analysis, with only the Phobius analysis showed transmembrane domains in the same relative locations as seen in Fig. 3.4. I found that most MdBV PIFs have a predicted topology that matches topologies of baculovirus homologs from both my own analysis and those recently performed by others [1, 7]. Exceptions to this are Pif-3, which is predicted to be non-cytoplasmic (facing outward on the virion envelope) in MdBV virions and cytoplasmic (facing inward on the virion envelope, toward the nucleocapsid) in baculoviruses, and Pif-4, for which there is no prior consensus in baculoviruses across two recent analyses, but which is predicted to be cytoplasmic in MdBV [1, 7].

Previous work on baculovirus *pif-8* implicates it in the formation of the cell entry complex, which is suggested to be facilitated by three zinc finger domains [21]. Only one of the three predicted zinc finger domains found in AcMNPV are present in MdBV *pif-8* (Fig. 3.7A). Other MdBV PIFs do not have recognizable zinc finger domains. In addition, *pif-8* has been shown to be required for baculovirus ODV and budded virus nucleocapsid assembly in addition to being an oral infectivity factor [24, 32]. Recent work has identified a domain required for nucleocapsid assembly in AcMNPV [21]. While not containing predicted structures or motifs, I found that this domain appears generally conserved in MdBV *pif-8* (Fig. 3.7B).

Using RAxML, I produced maximum-likelihood tree topologies for each MdBV PIF rooted to baculoviruses or WSSV (Fig. 3.8 and Fig. 3.9). The phylogeny I generated with *pif-2* shows MdBV *pif-2* being sister to α nudiviruses and nested in the β nudiviruses.

However, bootstrap support for these nodes is low. Note the clustering of LbFV and hytrosaviruses (MdSGHV and GpSGHV) which have been shown to be distantly related to baculoviruses [33]. The generated phylogeny of *pif-5* homologs show that MdBV *pif-5* duplicates branch out as sister to the whole of nudiviruses, with MdBV *pif-5-2* and *pif-5-3* isolated on a long branch that originates at the base of the betanudivirus *pif-5* clade, suggesting that this duplication is older than the nudivirus endogenization event that created bracoviruses. In collecting viral protein sequences for this analysis, I found that duplication of *pif-5* has happened in four nudiviruses. Tree topology suggests, with adequate bootstrap support, that duplication of *pif-5* was an early event in nudivirus history. This PIF is the only one that has undergone such duplication in MdBV or other viruses. MdBV *pif-8* appears sister to nudivirus *pif-8*. All other MdBV PIFs are nested among the nudiviruses (Fig. 3.8 and Fig. 3.9). The gene tree topologies I generated correspond to topologies generated by other authors using larger subsets of nudivirus and baculovirus core genes to clarify evolutionary relationships between virus groups [2, 34, 35].

### 3.2.2 MdBV PIF proteins localize to the MdBV viral envelope

Prior proteomic analysis detected all MdBV PIFs in MdBV virions [29]. In chapter 2 I report that all PIF genes preferentially localized to the envelope fraction except Pif-5-3 that was detected in both the capsid and envelope fraction.

### 3.2.3 MdBV PIF genes are efficiently knocked down by RNAi

Previous functional assays for MdBV PIFs were restricted to *pif-0/p74* and *pif-1*, both of which were suggested to play a role in translocation of MdBV to host cell nuclei. To further characterize PIF function in MdBV, I selected five additional MdBV PIFs for investigation; *pif-2*, *pif-8*, and all three *pif-5* duplicates, *pif-5-1*, *pif-5-2*, *pif-5-3*. In baculoviruses, each of these genes has been found to be required for oral infection of insects [12, 17, 21]. In baculoviruses occlusion derived virions (ODV), *pif-2* has been shown to be involved in virion binding to, and fusion with midgut cells [10]. In addition, *pif-2* has been shown to be critical for formation of the PIF cell entry complex [36-38]. As mentioned previously, *pif-8* is implicated in nucleocapsid formation and PIF complex formation and has retained some of its critical peptide domains in MdBV. Finally, baculovirus *pif-5* appears to function independently from the PIF entry complex during primary infection of insect midgut cells, though is implicated in interacting with *pif-3* [37, 39, 40]. MdBV has three pif-5 homologs that are transcribed and found as virion components [28, 29]. One additional homolog, *pif-5-4*, can be found in the MdBV genome, however this pseudogene is severely truncated and its gene products were not found to be part of MdBV virions (AgDataCommons accession number MDEMTmpGB000064) [29]. The presence of multiple copies of *pif-5* in the genomes of nudiviruses and BVs suggests neofunctionalization relative to baculovirus *pif-5*.

Like other MdBV genes, the PIF genes I selected are expressed in *M. demolitor* ovaries during virion replication, which starts in the pupal stage of the wasp [28]. Previously, methods were developed for knocking down viral genes in *M. demolitor* using RNAi [29]. In short I injected gene specific dsRNAs into wasp larvae after they emerged

from host caterpillars and spun cocoons. I then used qPCR to compare the abundance of each target transcript in newly emerged adult wasps relative to treatment with *ds-e*GFP, a non-specific dsRNA. My results show a reduction of transcript abundance of 70-90% for each targeted gene (Fig. 3.10).

### 3.2.4 Knockdown of select PIFs reduces virion density in calyx fluid

As part of this study I examined virion assembly morphology of MdBV in calyx cell nuclei. Previous work has shown that calyx cells progress from smaller cells into larger cells while slowly moving toward the lumen of the ovary and away from the ovarioles [41]. As calyx cells progress in development, their nuclei expand and fill with virions, followed by cell lysis, which releases virions into the lumen of the ovary to form densely packed calyx fluid [29, 42]. Previous imaging with TEM show that virion morphogenesis begins with *de novo* formation of viral envelopes in calyx cell nuclei followed by nucleocapsid formation. Nucleocapsids are then surrounded by envelopes, which elongate to mark virion maturation. Mature virions are organized into arrays and stored in calyx cell nuclei until the cells lyse, after which virions end up in the lumen of the ovary [29]. To observe the effect of MdBV PIF knockdown on virion assembly morphology, I produced thin sections of ovaries from wasps injected with dsRNA and compared them using TEM. In the control (*ds-e*GFP) ovaries I found typical envelope and capsid formation, including the surrounding of nucleocapsids by viral envelopes (Fig. 3.11A). Virions appeared to form normal aggregates in calyx cell nuclei (Fig. 3.11B) and collected into a dense fluid in the lumen of the calyx (Fig. 3.11C). Knockdown of *pif-2* and *pif-5-1* resulted in normal capsid and envelope formation (Fig. 3.11D and G) and mature virion aggregation (Fig. 3.11E

and H), as well as typical calyx fluid (Fig. 3.11F and I). Knockdown of *pif-5-2* resulted in the normal formation of capsids, though showed atypical aggregation of mature envelopes and a rounding of viral envelopes (Fig. 3.11J). However, aggregation of mature virions appears disorganized and virion envelopes poorly defined (Fig. 3.11K and L). Knockdown of *pif-5-3* and *pif-8* both show mostly normal formation of capsid and envelope (Fig. 3.11M, N, P and Q). In the *pif-5-3* knockdown images I found that clustering of mature virions looked slightly different than in the control: envelopes were rounder and less densely packed. Notably, the calyx fluid for both *pif-5-3* and *pif-8* knockdowns appear significantly less dense (Fig. 3.11O and R). By counting virions in randomly selected fields of view from treatment and control wasp sections, I found that calyx fluid from wasps treated with *ds-pif-5-3* and *ds-pif-8* contained a lower density (15% and 50% reduction, respectively) of virions relative to wasps treated with *ds-e*GFP (Fig. 3.12).

### 3.2.5 Knockdown of PIFs does not compromise MdBV virion nucleocapsid structural integrity

Based on previous studies, the baculovirus PIFs have been assigned as viral envelope proteins, though *pif-8* products have been found in small amounts in nucleocapsids [21, 24, 43, 44]. Knockout of *pif-0*, *pif-5*, or *pif-6* produced phenotypically normal virus particles [8, 40]. In contrast, *pif-8* knockouts cause aberrant formation of nucleocapsids where they appear elongated and empty of viral genomes [32, 44]. Previous work on MdBV viral genes has revealed baculovirus gene homologs that encode structural components of MdBV nucleocapsids [29]. The proteomics data I generated in chapter 2 (Table 2.1) suggest that MdBV PIF proteins are not capsid components, localizing mainly to the viral

envelope. However, one exception to this is MdBV *pif-5-3*, of which protein products are also found in nucleocapsids. In addition, my EM data show that *pif-8* appears to be involved in the formation of virions, potentially by playing some role in MdBV nucleocapsid formation as is suggested by the conserved protein domain shown to be involved in nucleocapsid assembly in baculoviruses. These data suggest that some MdBV PIFs could be nucleocapsid structural components or required for nucleocapsid integrity. To further investigate potential PIF involvement in capsid integrity, I performed DNase protection assays on PIF knockdown virions. After knocking down *pif-2*, *pif-5-1*, *pif-5-2*, *pif-5-3*, or *pif-8* in *M. demolitor*, I measured DNase sensitivity of packaged genomic DNAs as described in chapter 2, section 2.4.3. My results indicated that the abundance of Segment O did not change for any of the individual PIF gene knockdown virions versus control virions (Fig. 3.13).

### 3.2.6 Knockdown of PIFs disrupts typical MdBV viral infection

Unlike baculoviruses, BV virions don't infect host insects orally, but instead infect host cells after being injected into the insect hemocoel where they bind to and fuse their envelope with host cell plasma membranes [45]. Previous work has found that MdBV primarily infects insect hemocytes, where proviral DNA segments are integrated into the host cell genome and viral genes are expressed [46-49]. My ability to knock down individual PIF genes in MdBV provides us with an opportunity to explore the role these genes might play in BV infection. To that end, I individually knocked down the selected PIF genes and assessed how well knockdown MdBV virions infected host cells in vitro and in vivo. First, I knocked down each PIF in *M. demolitor* using RNAi as described

previously. After extracting knockdown virions from emerged wasp ovaries, I used them to infect CiE1 cells, which are a hemocyte-like cell line established from *C. includens* and are permissive to infection by MdBV [48, 50]. Previous work determined that infection of CiE1 cell cultures with normal MdBV virions results in the presence of viral DNA segments, suggesting virions have entered cells, followed by expression of viral genes, which starts 2 hours post infection (hpi) [50]. Previous work also showed that knockdown of *p74*/*pif-0* and *pif-1* knockdowns resulted in reduced expression of MdBV virulence genes in infected CiE1 cells, without any reduction in detected proviral segment DNA [29]. For my assays I selected MdBV proviral segment O, a high abundance proviral segment, and the viral gene *glc1.8*, which is encoded on segment O [26]. Previous work established that *M. demolitor* females contain on roughly 1 x $10^{10}$ MdBV virions and that they inject 0.01 to 0.1 wasp equivalents of MdBV into hosts during natural parasitism [26]. In previous work, infecting CiE1 cells at a viral multiplicity of infection of 100 (100 virions per cell) results in ~60% of the sample to be infected [50]. In order to mimic natural parasitism, MdBV virions were allowed to infect the cells for 2 hours at an MOI of 100, after which they were incubated for an additional 22 hours before sampling (24 hpi total). Total DNA and RNA were extracted from washed cells to quantify intracellular proviral genome presence and activity. First, I determined by qPCR the abundance of proviral Segment O associated with CiE1 cells. Relative to virions from *ds-e*GFP treated wasps, my results showed a 48% reduction of viral segment O per $10^5$ cells infected with *pif-2* knockdown MdBV (Fig. 3.14A). The knockdown of *pif-5-1* resulted in a 47% reduction of viral segment O per $10^5$ cells infected with knockdown virions relative to the *ds-e*GFP control virions (Fig. 3.14C). In contrast, knockdown of *pif-5-2* or *pif-5-3* resulted in an increase of viral

segment O of 331% and 343%, respectively (Fig. 3.14E and G). There was no statistically significant difference in viral segment O in CiE1 cells between infection with *ds-e*GFP control or *pif-8* knockdown virions (Fig. 3.14I).

In addition to Segment O copy number, I measured expression of *glc1.8* in the same cell samples. This viral gene is encoded on Segment O and is expressed as early as 2 hpi [50]. My results show that viral gene expression is reduced in CiE1 cells infected with MdBV virions with *pif-5-1* or *pif-8* knocked down, 81% and 60%, respectively (Fig. 3.14D and J). Knockdown of *pif-2*, *pif-5-2*, and *pif-5-3* produced no such statistically significant results (Fig. 3.14B, F, and H). These same experiments performed at a lower MOI of 1 showed similar patterns in response to PIF knockdown, though not all with the same statistical significance (Fig. 3.15). MOI infected cells were infected with the same knockdown virions used to inoculate MOI 100 infected cells.

### 3.2.7 In Vivo effects of PIF knockdown

The preceding assays suggested that knockdown of certain PIFs altered MdBV infection of CiE1 cells. To determine if this effect was reproducible *in vivo*, I investigated the effect of select PIF knockdowns on MdBV infectivity of *C. includens* caterpillars. Individual wasps injected with dsRNA specific to *pif-5-1*, *pif-5-2*, or *pif-5-3* were allowed to parasitize fourth instar caterpillars to allow for adequate hemocyte collection, one parasitism each for 3 to 4 individuals. After 24 hours, caterpillars were dissected for their gut tissue, fat body, and hemolymph, which were pooled together for each wasp to maximize DNA yield. From this sample pool I extracted total RNA and DNA. I used qPCR to determine Segment O copy number and *glc1.8* expression levels. Segment O copy number was normalized

to host genome copies using the *psp* gene. Similar to previous studies, my results showed that *C. includens* hemocytes are preferentially infected by MdBV, followed by fat body tissue and gut (Fig. 3.16) [26]. Notably, in caterpillars infected with *pif-5-1* knockdown wasps I found hemocyte expression of *glc1.8* reduced by 72% relative to the control (Fig. 3.16F), echoing my *in vitro* results (Fig. 3.14D and Fig. 3.15D). Additionally, I found that fat body expression of glc1.8 increased by 200% in the knockdown of *pif-5-3* (Fig. 3.16B). These data mirror my in vitro results showing increased viral DNA present in cells infected with *pif-5-3* knockdown (Fig. 3.14G and Fig. 3.15G). All other samples showed no change in the treatment group relative to the control.

### 3.2.8 Knockdown of *pif-2* inhibits MdBV DNA from entering CiE1 cell nuclei

Previous data indicate that *pif-2* and *pif-5-1* knockdown causes fewer MdBV proviral segments to end up in CiE1 cells (Fig. 3.14A and C), as well as reduction in *glc1.8* expression though this is only statistically significant for pif-5-1 (Fig. 3.14B and D). Data also indicate that *pif-8* knockdown reduced *glc1.8* expression without affecting entry of proviral DNA into cells (Fig. 3.14I and J). To investigate whether PIFs could play a role in translocating MdBV particles to host cell nuclei after infection of host cells, I separated infected cells into nuclear and cytoplasmic fractions and measured *glc1.8* and proviral segment O copies as described above. For this experiment I infected cells at an MOI of 10 after determining this was optimal for the sensitivity of the qPCR assay. My results show that knockdown of *pif-5-1* or *pif-8* did not affect how much proviral segment O gets into the nuclear fraction of the CiE1 cells (Fig. 3.17C and E). In contrast, knockdown of *pif-2* caused a reduction of nuclear segment O of roughly 51%

(Fig. 3.17A). There was no real effect overall on cytoplasmic segment O copy number between treatment and control for any of the three PIF knockdowns (Fig. 3.17B, D, and F).

### 3.3 Discussion

BVs evolved from a betanudivirus ancestor roughly 100 MYA [51]. Baculoviruses and nudiviruses maintain a conserved set of core genes involved in basic virus functions such as virion structural components and virion assembly machinery [5]. ODVs, the orally infectious stage of baculoviruses, infect insects via the midgut where they fuse with midgut epithelial cell membranes at the microvilli [6]. ODV virions bind to a specific, yet uncharacterized receptor [52, 53]. So far, 9 baculovirus ODV envelope proteins collectively referred to as PIF genes have been implicated in oral infection of hosts with most also being shown to form a complex [1, 22]. Baculovirus PIFs are essential for ODV midgut cell infection but are not needed for cell to cell spreading of systemic infection by ODVs. BV virions do not infect orally, and they primarily infect hemocytes and fat body tissue [26]. Despite the difference in biology, BVs encode 8 of the 9 PIF genes that are encoded by baculoviruses and nudiviruses [28]. My analyses further suggest MdBV PIFs retain most domain features recognized in baculovirus PIFs. With the exception of the truncation of a *pif-5* duplicate, MdBV PIFs have retained key transmembrane domains necessary for transferring PIFs to inner nuclear membranes during virion replication [14, 24]. This suggests that routing of virus proteins to the nuclear membrane in calyx cells uses a similar mechanism. From my phylogenetic analysis, patterns of diversification of PIFs from various virus species matches the current consensus on virus evolution,

showing a high degree of conservation and suggesting strict evolutionary constraint among PIFs [54]. Notable exception to this appears to be *pif-5* which has duplicated in both nudiviruses and BVs [28, 54-56]. The clustering of two *pif-5* duplicates on a long and isolated branch in my phylogenetic analysis suggests a recent duplication of *pif-5* in BVs. Baculovirus *pif-8* possesses 3 zinc finger domains that have been shown to be critical for PIF complex formation, as well as a domain required for nucleocapsid formation [21, 57]. The single zinc finger domain and nucleocapsid assembly domain found in MdBV *pif-8* suggests that *pif-8* might still perform this role, although PIF complex formation in BVs has not yet been investigated.

Without functional investigation into BV PIFs I cannot determine what role they might play in BV biology. However, the above analysis of MdBV PIF sequences shows that many previously recognized peptide domains are still shared with PIFs from other viruses. Proteomics results further indicate most MdBV PIFs are envelope proteins. The one exception, *pif-5-3*, localizes to both MdBV capsid and envelope fractions. Analysis using predictive software shows that MdBV PIFs, apart from truncated *pif-5-1*, have transmembrane-signal peptides in domains conserved from baculovirus/nudivirus PIFs. Given their previously established involvement in translocating viral proteins to viral envelopes, I expect that they might play a similar role in BVs [14, 24].

Previous work has shown that MdBV homologs of baculovirus core genes are involved in MdBV capsid assembly and structural integrity [29]. Knockdown of *vp39* and *vlf-1a* in MdBV caused defects in morphogenesis and infectivity consistent with their characterized role in baculoviruses [5]. The phenotypic effects I observed in the knockdowns indicate that *pif-2* and *pif-5-1* are unlikely to be capsid components, nor are

they required for morphogenesis in calyx cells based on EM analysis. Morphology of *pif-5-2* virion envelopes is not typical, though virion density appears unaffected. Reduced virion density in calyx fluid for *pif-5-3* and *pif-8* knockdowns suggest they play a role in virion replication. In baculoviruses *pif-8* has previously been shown to be involved in nucleocapsid formation and the embedding of baculoviruses into occlusion bodies, so my data are consistent with the baculovirus literature [32, 44]. Reduction of virion density in *pif-5-3* knockdown ovaries is small in magnitude, though combined with evidence that *pif-5-3* gene products are found in capsids suggests it could play some role in virion replication.

Knockdown of *p74*/*pif-0* and *pif-1* were previously shown to inhibit viral gene expression in cells infected with MdBV, but showed no defects in copy number of MdBV DNA detected in infected cells [29]. My *in vitro* assays showed that knockdown of *pif-2* and *pif-5-1* reduced the abundance of MdBV segment O in infected cells across different MOIs. Though this is in parallel with current understanding of baculovirus PIF function, the effects don't have the same magnitude as they do in baculoviruses and it would be premature to characterize these genes as infectivity factors [1, 7]. Similar to previous work on *p74*/*pif-0* and *pif-1*, I also saw a reduction of *glc1.8* expression cells infected with *pif-2*, *pif-5-1*, or *pif-8* knockdown virions [29]. For *pif-2* these results were trending towards significance but not statistically significant. The *in vivo* infection assay with *pif-5-1* knockdown wasps showed a reduction of *glc1.8*, corroborating my *in vitro* results. Counterintuitively, I saw an increase of proviral DNA segment O associated with cells infected with *pif-5-2* and *pif-5-3* knockdown virions. This result was also seen *in vivo*, but only for *pif-5-3*. Notably, I found increased expression of viral gene *glc1.8* corresponding

with the increase in viral segment O. These results are surprising as I would expect knockdowns to disrupt virus function rather than enhance virulence effects. Knockdown of PIFs does not cause DNA packaged in MdBV virions to become more sensitive to DNase treatment, indicating that MdBV PIFs are not essential for structural integrity of nucleocapsids. In the knockdown of *pif-8*, the reduction in virion density is only mirrored in viral gene expression of cells infected with knockdown virions, and not the entry of viral DNA into cells. The results from previous experiments characterizing MdBV PIFs suggested that they were involved in translocation of MdBV virions to host cell nuclei [29]. The separation of infected CiE1 cells into nuclear and cytoplasmic fractions showed that *pif-2* knockdown causes a reduction of viral DNA segments in the nucleus of CiE1 cells. This result was not seen for *pif-5-1*, and *pif-8* knockdowns.

Baculovirus PIFs play a critical role as oral infectivity factors in that they are required for infection of insect midgut cells. What characterizes Baculovirus PIFs is that disabling them blocks baculovirus ODV ability to infect host cells [1]. The results from PIF knockdowns do not strongly support MdBV PIFs in their role as a potential infectivity factor. However, my experiments do show that select PIF knockdowns inhibit MdBV virion infection of host cells and subsequent gene expression. I showed that *pif-2* might play a role in delivering MdBV proviral segments to CiE1 cells and CiE1 cell nuclei. My data also show *pif-5-1* knockdown resulted in reduced viral gene expression both *in vivo* and *in vitro*. My electron microscopy data further provide evidence that *pif-5-2*, *pif-5-3,* and *pif-8* are involved in MdBV virion morphogenesis.

More experimental work is needed to determine how MdBV PIFs play a role in bracovirus biology. There are currently no data on whether bracovirus PIFs form a

complex. Steps could be taken to determine this by generating antibodies to various PIFs. In addition, the assays performed in this chapter did not involve all of the MdBV PIFs, and a few of them have yet to be characterized at all. In order to form a complete understanding of bracovirus PIFs I strongly suggest continuing the work performed by expanding the work to all MdBV PIFs as well as any other envelope genes potentially involved in infecting host cells.

## 3.4 Methods

### 3.4.1 Insect rearing and staging

*M. demolitor* females parasitize larval stage lepidopteran species, including *Chrysodeixis includens* [58]. Both parasitoid and host were reared at 27°C, with a 16 h light and 8 h dark photoperiod [59]. *M. demolitor* typically take 11 days to develop from egg into adult. After being injected in the host, *M. demolitor* hatches and feeds as a larva for 6 days, after which the last larval instar emerges from the host to spin a cocoon within [58]. Spinning a cocoon takes several hours, after which the wasps spend an additional time (nine-12 hours) as larvae, before starting their pupation. [29]. Adult wasps were maintained in constant dark at 18°C. Rearing and staging of *C. includens* for parasitism was done as previously described [60].

### 3.4.2 Proteomic analysis of virions

Proteomic analysis of virions was performed as described in chapter two.

### 3.4.3 RNAi knockdowns and quantification of target gene expression

For targeted knockdown of individual genes I used gene-specific primers which are prefixed with T7 promoter adaptor sequence to generate 300-400 bp templates for double stranded RNA (dsRNA) synthesis. Previous work describes generating dsRNA Primers for *e*GFP [29]. I generated dsRNA primers for *pif-5-1*, *pif-5-2*, *pif-5-3*, *pif-2*, and *pif-8* (Table 3.2). I generated PCR products from adult wasp ovary cDNA and used those as templates for the MegaScript RNAi Kit (Ambion) to produce dsRNA. Larval stage wasp cocoons were selected and injected as previously described [29]. In short, I injected individual wasp larvae in abdomen with 0.5-1 µl of 400-500 ng/µl dsRNA. Control wasps were injected with a non-specific dsRNA probe (bacterial *e*GFP). After emerging as adults, females were allowed 2 h parasitism each day for 5 days before being used in RNAi phenotype assays. To check the knockdown efficiency of MdBV PIFs, half-ovaries from each wasp used in the assays were extracted and separated. One half-ovary was frozen at -80°C for RNA extraction. Total RNA extraction from wasp ovaries was performed using the Quick-RNA MiniPrep (Zymo Research). cDNA was synthesized from total RNA using Nanodrop-determined (Fischer) RNA concentrations to normalize across samples, as described previously [29]. I used quantitative PCR (qPCR) to measure differences in gene expression across samples. To do this, I generated qPCR primers for *pif-5-1*, *pif-5-2*, *pif-5-3*, *pif-2*, and *pif-8* (Table 3.2). I cloned the PCR product of this primer set into pSC-A-amp/kan, isolated and sequenced the plasmid, and generated an absolute standard curve by determining copy numbers from serially diluted amounts of plasmid ($10^2$ to $10^7$ copies). I used a Rotor-Gene Q with the Rotor-Gene SYBR Green PCR kit in conjunction with the qPCR primers. Cycling conditions were the same for each PIF primer

combination: 5 min initial denaturation step at 95 °C, followed by 50 cycles of 5 s denaturation at 95 °C and 20 s annealing at 60 °C. Data were acquired during the extension step and analyzed with the Rotor-Gene application software (Version 6.0.27).

### 3.4.4 Electron microscopy

Electron microscopy was performed as in [61] with slight modification. Half-ovaries from dsRNA-injected wasps were fixed in 3% glutaraldehyde in phosphate buffer (pH7.0) at 4°C. Fixed ovaries were rinsed with buffer and post-fixed using 1% osmium tetroxide. Ovaries were then block stained using 0.5% uranyl acetate before being dehydrated in graded ethanol solutions, 100% acetone, and 100% propylene oxide. Ovaries were embedded in Spurr's resin and sectioned on a Reichert Ultracut S (Leica). Sections were stained with lead citrate and examined with JEM-1011 Transmission Electron Microscope (JOEL). At least two samples were generated per knockdown wasp, with multiple sections prepared from each sample. Virion fluid density was measured by counting the number of virions in randomly selected fields of view from treatment and control wasps sections.

### 3.4.5 *In vitro* infectivity assay

Previous work describes how the CiE1 cell line was generated and maintained [50]. To measure the infectivity of MdBV virions I counted copies of proviral Segment O present in CiE1 cells 24 h post-infection [50]. In addition, I quantified viral gene transcription by measuring expression of *glc1.8*. To prepare virus samples for in vitro infection, newly emerged dsRNA injected female wasps were allowed to parasitize first or second instar *C. includens* individuals for two hours a day for 5 days. Wasps had access to 10% sucrose

in water during these 5 days. After the final parasitism on day 5, virions were collected as previously described [29]. Virions in suspension were added to CiE1 cells in 24-well cell culture plates at an estimated MOI of 1 and 100 based on previous estimates for calyx fluid virion density [26, 29]. For the extraction of both total RNA and DNA from the infected cells, I used a joint DNA and RNA extraction protocol based on the RNA extraction protocol described in [62]. In brief, I suspended cells from each well in 550 µl room temperature guanidine thiocyanate lysis buffer [4 M guanidine thiocyanate, 2% Sarkosyl, 50 mM Tris (pH 7.6), 10 mM EDTA] for 10 minutes. Next, I added 250 µg proteinase K (QIAGEN), followed by incubation at 62°C for 10 minutes. Samples were then phenol:chloroform extracted and precipitated using isopropanol/ethanol in the presence of 0.3 M sodium acetate and glycogen (3.3 µl per sample). DNA and RNA were dissolved in 100 µl DNase/RNase free water and split into an RNA and DNA fraction. For DNA isolation, RNase A (6.6 µg/µl) was added to the DNA fraction followed by phenol-chloroform extraction and reprecipitation while for total RNA isolation DNase was added to the RNA fraction using the Turbo DNA-free kit (Ambion) followed by elution in water. The DNA fraction was used to measure segment O copies, and the RNA fraction was used to synthesize cDNA. See Table 3.2 for qPCR primer sets for *glc1.8* and segment O.

### 3.4.6 In vivo infectivity assay

As with the *in vitro* infectivity assay, dsRNA injected wasp females were allowed to feed freely and parasitize for 2 hours a day for 5 days post emergence, with minor modification. On the 5$^{th}$ day individual wasp females parasitized 4$^{th}$ instar *C. includens* caterpillars. The caterpillars were then kept at 27°C for 24 hours, after which they were bled to remove

hemolymph and dissected in PBS, where I sampled gut and fat body tissue. These tissues were first frozen at -80°C, after which they were homogenized in guanidine thiocyanate lysis buffer for joint DNA/RNA extraction as described above. I measured proviral segment O and expression of *glc1.8* using qPCR as described above. To account for inconsistencies in tissue extraction of caterpillars I used a *C. includens* gene encoding plasmatocyte spreading peptide (*psp*). See Table 3.2 for qPCR primer set for *psp*.

### 3.4.7 Quantification of Segment O in ovaries and calyx fluid

I measured the titer of MdBV virions with DNase-protected episomes of MdBV segment O using qPCR. One half ovary from each individual wasp was homogenized in 100 µl of DNase buffer from the Roche HighPure RNA isolation kit, and Nonidet P-40 substitute (Roche) to a concentration 0.1% to solubilize virion envelopes. After 20 minutes of gentle rocking at room temperature, I added 1 µl TURBO DNase from the Ambion DNA free kit and incubated the samples at 37°C for 40 minutes. After incubation, I added EDTA (10 mM) to inactivate DNase, I added 250 µg of proteinase K (Roche) and 2% sarcosyl, followed by incubation at 62°C for 1h, and continued with phenol:chloroform extraction and ethanol precipitation as described above. I then performed qPCR on the extracted DNA to measure copies of segment O.

### 3.4.8 CiE1 nuclear and cytoplasmic fractionation

CiE1 cells were infected in 1.7 microcentrifuge tubes using knockdown virions at room temperature. After a two hour incubation time on a shaker, cell medium was replaced and tubes were placed in an incubator at 27°C. To separate infected CiE1 cells into nuclear

and cytoplasmic fractions, I performed the Rapid, Efficient And Practical (REAP) method as described here [63] with slight modification. In brief, I centrifuged infected cells in 1.7 ml microcentrifuge tubes at 500 rcf for 5 minutes at 4°C and discarded the supernatant. I washed and resuspended the cell pellet in ice cold 1xPBS and centrifuged the suspension. This and all following centrifugation steps were performed for 10 s at 16,100 rcf and at 4°C. After removing the supernatant, I resuspended the pellet in 900 µl ice cold 1xPBS with 0.01% Nonidet P-40 substitute. Next, I pipetted this cell suspension forcefully 10 times, inverting the tube twice. Then I removed 300 µl of this whole cell lysate for later processing. I centrifuged the remaining 600 µl cell suspension and removed 300 µl of the supernatant as cytosolic cell lysate and discarded the remaining supernatant. The remaining pellet was washed and resuspended in 1000 µl ice cold 1xPBS with 0.01% Nonidet P-40 substitute and centrifuged again. The supernatant was then discarded, and the pellet saved as the nuclear cell fraction. Next, I treated each fraction with 250 µg of proteinase K (Roche) and 2% sarcosyl, followed by incubation at 62°C for 1h, phenol:chloroform extraction and ethanol precipitation as described above. I performed qPCR on extracted DNA using segment O primers.

### 3.4.9 Computer and statistical analysis

In my analysis using qPCR I averaged the number of copies of gene or DNA product for all technical replicates within a biological sample. For functional assays, I calculated means from experimental values from biological replicates. Each biological replicate represents and individual wasp or virions from one wasp ovary. JMP v14 was used for statistical analyses. Differences between means of biological replicates were tested using

a *t*-test assuming equal variances or ANOVA. I used RAxML for the maximum-likelihood based phylogenetic inference of each MdBV PIF sequence [64]. For analysis of PIF transmembrane domains I used TMHMM, a software designed for predicting transmembrane domains and signal peptide sequences [65, 66]. Thanks to NetNGlyc 1.0 Server, University of Denmark. Thanks to NetPhos 3.1 Server, University of Denmark.

### 3.5 References


1. Boogaard, B., M.M. van Oers, and J.W.M. van Lent, *An Advanced View on Baculovirus per Os Infectivity Factors.* Insects, 2018. **9**(3).

2. Bezier, A., et al., *The genome of the nucleopolyhedrosis-causing virus from Tipula oleracea sheds new light on the Nudiviridae family.* J Virol, 2015. **89**(6): p. 3008-25.

3. Kariithi, H.M., et al., *Virology, Epidemiology and Pathology of Glossina Hytrosavirus, and Its Control Prospects in Laboratory Colonies of the Tsetse Fly, Glossina pallidipes (Diptera; Glossinidae).* Insects, 2013. **4**(3): p. 287-319.

4. Sánchez-Paz, A., *White spot syndrome virus: an overview on an emergent concern.* Vet Res, 2010. **41**(6): p. 43-43.

5. Rohrmann, G.F., *Baculovirus Molecular Biology*. 4th ed. 2019, Bethesda (MD): National Center for Biotechnology Information (US).

6. Granados, R.R. and K.A. Lawler, *In vivo pathway of Autographa californica baculovirus invasion and infection.* Virology, 1981. **108**(2): p. 297-308.

7. Wang, X., et al., *Per os infectivity factors: a complicated and evolutionarily conserved entry machinery of baculovirus.* Sci China Life Sci, 2017. **60**(8): p. 806-815.

8. Faulkner, P., et al., *Analysis of p74, a PDV envelope protein of Autographa californica nucleopolyhedrovirus required for occlusion body infectivity in vivo.* J Gen Virol, 1997. **78**(12): p. 3091-3100.

9. Kuzio, J., R. Jaques, and P. Faulkner, *Identification of p74, a gene essential for virulence of baculovirus occlusion bodies.* Virology, 1989. **173**(2): p. 759-63.

10. Ohkawa, T., et al., *Specific Binding of Autographa californica M Nucleopolyhedrovirus Occlusion-Derived Virus to Midgut Cells of Heliothis virescens Larvae Is Mediated by Products of pif Genes Ac119 and Ac022 but Not by Ac115.* J Virol, 2005. **79**(24): p. 15258-15264.

11. Kikhno, I., et al., *Characterization of pif, a gene required for the per os infectivity of Spodoptera littoralis nucleopolyhedrovirus.* J Gen Virol, 2002. **83**(12): p. 3013-3022.

12. Pijlman, G.P., A.J.P. Pruijssers, and J.M. Vlak, *Identification of pif-2, a third conserved baculovirus gene required for per os infection of insects.* J Gen Virol, 2003. **84**(8): p. 2041-2049.

13. Fang, M., et al., *Open reading frame 132 of Heliocoverpa armigera nucleopolyhedrovirus encodes a functional per os infectivity factor (PIF-2).* J Gen Virol, 2006. **87**(9): p. 2563-2569.

14. Li, X., et al., *The N-terminal hydrophobic sequence of Autographa californica nucleopolyhedrovirus PIF-3 is essential for oral infection.* Arch Virol, 2007. **152**(10): p. 1851-1858.

15. Xu, H.J., et al., *Bombyx mori nucleopolyhedrovirus ORF79 encodes a 28-kDa structural protein of the ODV envelope.* Arch Virol, 2006. **151**(4): p. 681-95.

16. Fang, M., et al., *Autographa californica Multiple Nucleopolyhedrovirus Core Gene ac96 Encodes a Per Os Infectivity Factor (pif-4).* J Virol, 2009. **83**(23): p. 12569-12578.

17. Xiang, X., et al., *The Bombyx mori nucleopolyhedrovirus (BmNPV) ODV-E56 envelope protein is also a per os infectivity factor.* Virus Res, 2010. **155**(1): p. 69-75.

18. Harrison, R.L., W.O. Sparks, and B.C. Bonning, *Autographa californica multiple nucleopolyhedrovirus ODV-E56 envelope protein is required for oral infectivity and can be substituted functionally by Rachiplusia ou multiple nucleopolyhedrovirus ODV-E56.* J Gen Virol, 2010. **91**(Pt 5): p. 1173-82.

19. Nie, Y., et al., *Analysis of the Autographa californica Multiple Nucleopolyhedrovirus Overlapping Gene Pair lef3 and ac68 Reveals that AC68 Is a Per Os Infectivity Factor and that LEF3 Is Critical, but Not Essential, for Virus Replication.* J Virol, 2012. **86**(7): p. 3985-3994.

20. Jiantao, L., et al., *The Autographa californica multiple nucleopolyhedrovirus ac110 gene encodes a new per os infectivity factor.* Virus Res, 2016. **221**: p. 30-7.

21. Javed, M.A., et al., *Autographa californica Multiple Nucleopolyhedrovirus AC83 is a Per Os Infectivity Factor (PIF) Protein Required for Occlusion-Derived Virus (ODV) and Budded Virus Nucleocapsid Assembly as well as Assembly of the PIF Complex in ODV Envelopes.* J Virol, 2017. **91**(5): p. e02115-16.

22. Wang, X., et al., *Baculovirus Per Os Infectivity Factor Complex: Components and Assembly.* J Virol, 2019. **93**(6).

23. Braunagel, S.C., et al., *Trafficking of ODV-E66 is mediated via a sorting motif and other viral proteins: facilitated trafficking to the inner nuclear membrane.* Proc Natl Acad Sci U S A, 2004. **101**(22): p. 8372-7.

24. Zhu, S., et al., *The Baculovirus Core Gene ac83 Is Required for Nucleocapsid Assembly and Per Os Infectivity of Autographa californica Nucleopolyhedrovirus.* J Virol, 2013. **87**(19): p. 10573-10586.

25. Braunagel, S.C., et al., *Identification and analysis of an Autographa californica nuclear polyhedrosis virus structural protein of the occlusion-derived virus envelope: ODV-E56.* Virology, 1996. **217**(1): p. 97-110.

26. Beck, M.H., R.B. Inman, and M.R. Strand, *Microplitis demolitor bracovirus genome segments vary in abundance and are individually packaged in virions.* Virology, 2007. **359**(1): p. 179-89.

27. Chevignon, G., et al., *Functional annotation of Cotesia congregata bracovirus: identification of viral genes expressed in parasitized host immune tissues.* J Virol, 2014. **88**(16): p. 8795-812.

28. Burke, G.R. and M.R. Strand, *Deep sequencing identifies viral and wasp genes with potential roles in replication of Microplitis demolitor Bracovirus.* J Virol, 2012. **86**(6): p. 3293-306.

29. Burke, G.R., et al., *Mutualistic polydnaviruses share essential replication gene functions with pathogenic ancestors.* PLoS Pathog, 2013. **9**(5): p. e1003348.

30. Krogh, A., et al., *Predicting transmembrane protein topology with a hidden markov model: application to complete genomes11Edited by F. Cohen.* J Mol Biol, 2001. **305**(3): p. 567-580.

31. Käll, L., A. Krogh, and E.L.L. Sonnhammer, *A Combined Transmembrane Topology and Signal Peptide Prediction Method.* J Mol Biol, 2004. **338**(5): p. 1027-1036.

32. Xiang, X., et al., *Bombyx mori nucleopolyhedrovirus BmP95 plays an essential role in budded virus production and nucleocapsid assembly.* J Gen Virol, 2013. **94**(Pt 7): p. 1669-79.

33. Lepetit, D., et al., *Genome Sequencing of the Behavior Manipulating Virus LbFV Reveals a Possible New Virus Family.* Genome Biol Evol, 2016. **8**(12): p. 3718-3739.

34. Theze, J., et al., *Paleozoic origin of insect large dsDNA viruses.* Proc Natl Acad Sci U S A, 2011. **108**(38): p. 15931-5.

35. Cheng, R.L., et al., *Brown planthopper nudivirus DNA integrated in its host genome.* J Virol, 2014. **88**(10): p. 5310-8.

36. Peng, K., et al., *Baculovirus Per Os Infectivity Factors Form a Complex on the Surface of Occlusion-Derived Virus.* J Virol, 2010. **84**(18): p. 9497-9504.

37. Peng, K., et al., *Characterization of Novel Components of the Baculovirus Per Os Infectivity Factor Complex.* J Virol, 2012. **86**(9): p. 4981-4988.

38. Zheng, Q., et al., *Protein–protein interactions of the baculovirus per os infectivity factors (PIFs) in the PIF complex.* J Gen Virol, 2017. **98**(4): p. 853-861.

39. Boogaard, B., et al., *The baculovirus Ac108 protein is a per os infectivity factor and a component of the ODV entry complex.* J Gen Virol, 2019. **100**(4): p. 669-678.

40. Sparks, W.O., R.L. Harrison, and B.C. Bonning, *Autographa californica multiple nucleopolyhedrovirus ODV-E56 is a per os infectivity factor, but is not essential for binding and fusion of occlusion-derived virus to the host midgut.* Virology, 2011. **409**(1): p. 69-76.

41. Stoltz, D.B. and S.B. Vinson, *Baculovirus-like particles in the reproductive tracts of female parasitoid wasps II: the genus Apanteles.* Can J Microbiol, 1977. **23**(1): p. 28-37.

42. Stoltz, D.B., S.B. Vinson, and E.A. MacKinnon, *Baculovirus-like particles in the reproductive tracts of female parasitoid wasps.* Can J Microbiol, 1976. **22**(7): p. 1013-23.

43. Hou, D., et al., *Comparative Proteomics Reveal Fundamental Structural and Functional Differences between the Two Progeny Phenotypes of a Baculovirus.* J Virol, 2013. **87**(2): p. 829-839.

44. Zhou, F., et al., *The cysteine-rich region of a baculovirus VP91 protein contributes to the morphogenesis of occlusion bodies.* Virology, 2019. **535**: p. 144-153.

45. Strand, M.R., *Microplitis Demolitor Polydnavirus Infects and Expresses in Specific Morphotypes of Pseudoplusia Includens Haemocytes.* J Gen Virol, 1994. **75**(11): p. 3007-3020.

46. Beck, M.H. and M.R. Strand, *A novel polydnavirus protein inhibits the insect prophenoloxidase activation pathway.* Proc Natl Acad Sci U S A, 2007. **104**(49): p. 19267-72.

47. Pruijssers, A.J. and M.R. Strand, *PTP-H2 and PTP-H3 from Microplitis demolitor Bracovirus Localize to Focal Adhesions and Are Antiphagocytic in Insect Immune Cells.* J Virol, 2007. **81**(3): p. 1209-1219.

48. Beck, M.H., et al., *The encapsidated genome of Microplitis demolitor bracovirus integrates into the host Pseudoplusia includens.* J Virol, 2011. **85**(22): p. 11685-96.

49. Bitra, K., S. Zhang, and M.R. Strand, *Transcriptomic profiling of Microplitis demolitor bracovirus reveals host, tissue and stage-specific patterns of activity.* J Gen Virol, 2011. **92**(Pt 9): p. 2060-71.

50. Johnson, J.A., et al., *The UGA-CiE1 cell line from Chrysodeixis includens exhibits characteristics of granulocytes and is permissive to infection by two viruses.* Insect Biochem Mol Biol, 2010. **40**(5): p. 394-404.

51. Murphy, N., et al., *Phylogeny of the parasitic microgastroid subfamilies (Hymenoptera: Braconidae) based on sequence data from seven genes, with an improved time estimate of the origin of the lineage.* Mol Phylogenet Evol, 2008. **47**(1): p. 378-95.

52. Haas-Stapleton, E.J., J.O. Washburn, and L.E. Volkman, *P74 Mediates Specific Binding of Autographa californica M Nucleopolyhedrovirus Occlusion-Derived Virus to Primary Cellular Targets in the Midgut Epithelia of Heliothis virescens Larvae.* J Virol, 2004. **78**(13): p. 6786-6791.

53. Horton, H.M. and J.P. Burand, *Saturable attachment sites for polyhedron-derived baculovirus on insect cells and evidence for entry via direct membrane fusion.* J Virol, 1993. **67**(4): p. 1860-8.

54. Hill, T. and R.L. Unckless, *The dynamic evolution of Drosophila innubila Nudivirus.* Infect Genet Evol, 2018. **57**: p. 151-157.

55. Bezier, A., et al., *Qualitative proteomic analysis of Tipula oleracea nudivirus occlusion bodies.* J Gen Virol, 2017. **98**(2): p. 284-295.

56. Bezier, A., et al., *Polydnaviruses of braconid wasps derive from an ancestral nudivirus.* Science, 2009. **323**(5916): p. 926-30.

57. Javed, M.A., et al., *AcMNPV AC83 is a PIF protein required for ODV and BV nucleocapsid assembly as well as assembly of the PIF complex in ODV envelopes.* J Virol, 2016.

58. Strand, M.R., J.A. Johnson, and J.D. Culin, *Developmental interactions between the parasitoid Microplitis demolitor (Hymenoptera: Braconidae) and its host Heliothis virescens (Lepidoptera: Noctuidae).* Ann Entomol Soc Am, 1988. **81**(5): p. 822-830.

59. Strand, M.R. and T. Noda, *Alterations in the hemocytes of Pseudoplusia includens after parasitism by Microplitis demolitor.* J. Insect Physiol., 1991. **37**(11): p. 839-850.

60. Strand, M.R., *Characterization of Larval Development in Pseudoplusia includens (Lepidoptera: Noctuidae).* Ann Entomol Soc Am, 1990. **83**(3): p. 538-544.

61. Strand, M.R., et al., *Persistence and expression of Microplitis demolitor polydnavirus in Pseudoplusia includens.* J Gen Virol, 1992. **73 ( Pt 7)**: p. 1627-35.

62. Coffman, K.A., T.C. Harrell, and G.R. Burke, *A mutualistic poxvirus exhibits convergent evolution with other heritable viruses in parasitoid wasps.* J Virol, 2020.

63. Suzuki, K., et al., *REAP: A two minute cell fractionation method.* BMC Research Notes, 2010. **3**(1): p. 294.

64. Stamatakis, A., *RAxML version 8: a tool for phylogenetic analysis and post-analysis of large phylogenies.* Bioinformatics, 2014. **30**(9): p. 1312-1313.

65. Krogh, A., et al., *Predicting transmembrane protein topology with a hidden Markov model: application to complete genomes.* J Mol Biol, 2001. **305**(3): p. 567-80.

66. Sonnhammer, E.L., G. von Heijne, and A. Krogh, *A hidden Markov model for predicting transmembrane helices in protein sequences.* Proc Int Conf Intell Syst Mol Biol, 1998. **6**: p. 175-82.

## 3.6 Figures and Tables

### Table 3.1: Virus abbreviations and genome accession numbers.

| Virus name | Abbreviaton | Accession no. |
|---|---|---|
| *Heliothis zea* NV-1 | HzNV1 | AF451898.1 |
| *Tipula oleracea* NV | ToNV | NC_026242.1 |
| *Gryllus bimaculatus* NV | GbNV | NC_009240.1 |
| *Venturia canescens* NV | VcENV | KP972599.1 |
| *Oryctes rhinoceros* NV | OrNV | NC_011588.1 |
| *Venturia canescens* NV | DiNV | MF966379.1 |
| Kallithea virus | DmNV Kal | KX130344.1 |
| *Autographa californica* MNPV | AcMNPV | NC_001623.1 |
| *Bombyx mori* NPV | BmNPV | NC_001962.1 |
| *Cydia pomonella* GV | CpGV | NC_002816.1 |
| *Culex nigripalpus* NPV | CuniNPV | NC_003084.1 |
| *Neodiprion lecontei* NPV | NeleNPV | NC_005906.1 |
| *Musa domestica* SGHV | MdSGHV | EU522111.1 |
| *Glossina pallidipes* SGHV | GpSGHV | KU050077.1 |
| *Leptopilina boulardi* FV | LbFV | GCF_002005725.1.1 |
| White spot syndrome virus | WSSV | AF369029.2 |

MNPV, multiple nucleopolyhedrovirus; NPV, nucleopolyhedrovirus; GV, granulovirus; NV, nudivirus; SGHV, salivary gland hypertrophy virus; FV, filamentous virus. MdBV *pif* sequence files are available at AgDataCommons (http://dx.doi.org/10.15482/USDA.ADC/1432667).

## Table 3.2: PCR and dsRNA primer sets for selected MdBV sequences.

| Genomic Segment | Orientation | Sequence |
|---|---|---|
| Segment O qPCR* | Forward | 5′-TTGCCAGGCCAGAAATTTTCAACATTACAATCTA-3′ |
| | Reverse | 5′-TACCCCTATAAGTAGTCCATCAAAAAGAACTGTGG-3′ |
| glc1.8 qPCR* | Forward | 5′-ACTACTACCCACCATGAAGAC-3′ |
| | Reverse | 5′-ATGCAATACGGAAAGGCAG-3′ |
| psp qPCR* | Forward | 5′-GCACCAACCGTGGCGACTAATG-3′ |
| | Reverse | 5′-GGCGAGACAGCCACCGTTGAA-3′ |
| 18S rRNA qPCR* | Forward | 5′-CAGTGATGGGATGAGTGCTTTTATTAGAT-3′ |
| | Reverse | 5′-AGGCCCTCCGTCGATTGGTTTT-3′ |
| PIF-5-1 RNAi | Forward | 5'-TAATACGACTCACTATAGGGGTTTGGACGAATCTGAATGT-3' |
| | Reverse | 5'-TAATACGACTCACTATAGGGACTCAAATCAACACCCATGT-3' |
| PIF-5-1 qPCR | Forward | 5'-CGACATTGATGACGGAGAAG-3' |
| | Reverse | 5'-CGGGAACTTCGGATAATAACA-3' |
| PIF-5-2 RNAi | Forward | 5'-TAATACGACTCACTATAGGGCATGGAAGACCAGACATCTT-3' |
| | Reverse | 5'-TAATACGACTCACTATAGGGAAAAGAAACAGCGTAACCAA-3' |
| PIF-5-2 qPCR | Forward | 5'-CAGGTGCTGCTGTTGGAGTA-3' |
| | Reverse | 5'-AATTGCGTGAAAGCATTTGG-3' |
| PIF-5-3 RNAi | Forward | 5'-TAATACGACTCACTATAGGGACGAAATATCATCGGAATTG-3' |
| | Reverse | 5'-TAATACGACTCACTATAGGGTTATTCCAATAGCAGCACCT-3' |
| PIF-5-3 qPCR | Forward | 5'-TCGAATGCCGCAATCAATA-3' |
| | Reverse | 5'-CAAAGAAAGTGCCGAAGAAAG-3' |
| PIF-2 RNAi | Forward | 5'-TAATACGACTCACTATAGGGGTCGTTTTCATCCGATTCGT-3' |
| | Reverse | 5'-TAATACGACTCACTATAGGGAAAAGTGGCATTTTCCAACG-3' |
| PIF-2 qPCR | Forward | 5'-TATGACAAAGGGTGCGAAAA-3' |
| | Reverse | 5'-ACCGTTCATTGTCATGATGG-3' |
| PIF-8/VP91 RNAi | Forward | 5'-TAATACGACTCACTATAGGGCATAGGAGCGATGGTTTTGAA-3' |
| | Reverse | 5'-TAATACGACTCACTATAGGGCCTTCGGGAAAATCTTGACA-3' |
| PIF-8/VP91 qPCR | Forward | 5'-TTGAACTTGAGCGAAGCAAA-3' |
| | Reverse | 5'-CAATAATTTCGACCGGGTTT-3' |

*Thermal profile for qPCR quantification of glc1.8 and segment O are described in [46]

**Figure 3.1: Conserved MdBV PIFs superimposed onto model of baculovirus ODV PIF entry complex**. MdBV maintains key PIF proteins involved in viral entry complex formation, however no evidence exists of MdBV PIFs forming a protein complex. This diagram shows the proposed model for PIF complex found in baculoviruses, adapted from and modified for comparison with MdBV PIFs. Pif-1, Pif-2, Pif-3, and Pif-4 make up the core of the PIF complex, with Pif-0/P74, Pif-6, Pif-7, and Pif-8 more loosely associated with the complex. Pif-5 is not associated with the complex. MdBV does not encode Pif-7. Pif-3, predicted to cytoplasmic (Facing inside the viral envelope) in topology in baculoviruses (shown in figure), is contrastingly predicted to be non-cytoplasmic in MdBV. Pif-4, predicted to non-cytoplasmic (Facing outside the viral envelope) in topology in baculoviruses (shown in figure), is contrastingly predicted to be cytoplasmic in MdBV.

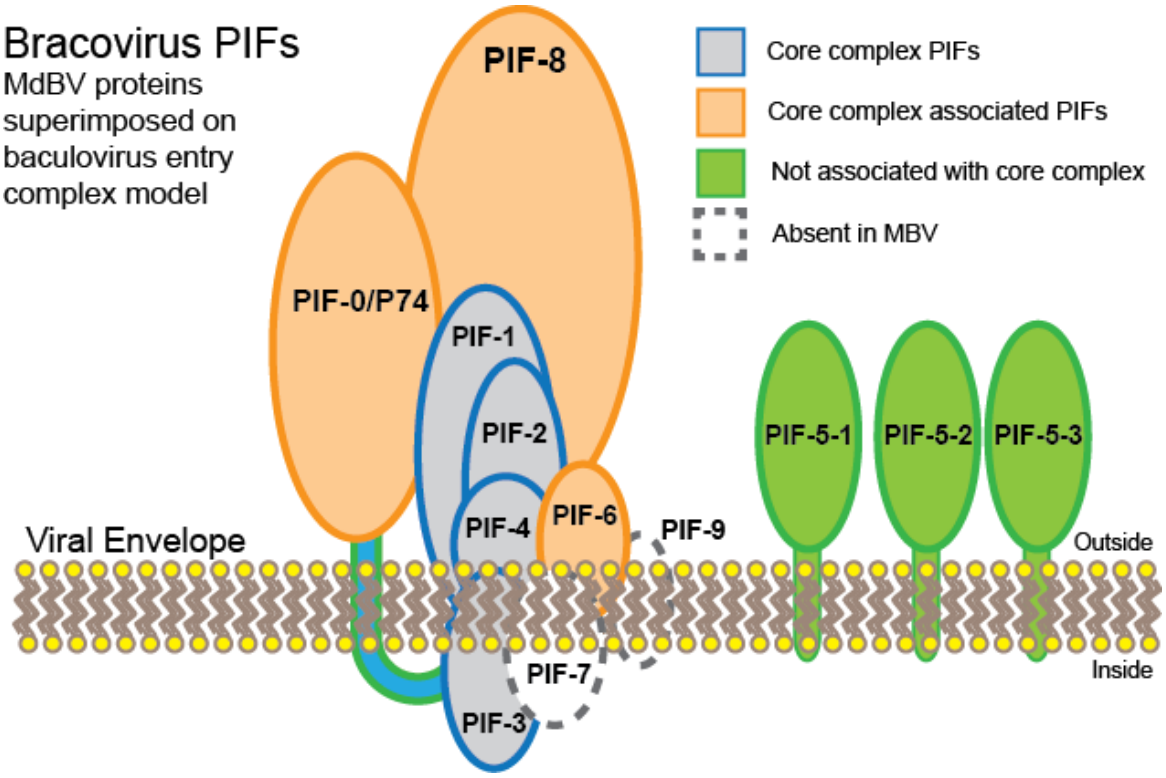
Bracovirus PIFs
MdBV proteins superimposed on baculovirus entry complex model
Core complex PIFs
Core complex associated PIFs
Not associated with core complex
Absent in MBV
PIF-8
PIF-0/P74
PIF-1
PIF-2
PIF-4
PIF-6
PIF-9
PIF-5-1
PIF-5-2
PIF-5-3
Viral Envelope
Outside
Inside
PIF-7
PIF-3

**Figure 3.2: MdBV PIFs retain many key PIF characteristics, including transmembrane domains and highly conserved cysteines.** The schematic of each MdBV PIF protein. The N- and C-terminus is indicated for each, as well as total length. Transmembrane domains shown in blue. Cysteine residues conserved in all PIFs analyzed in this paper are shown by red vertical lines and their positions shown above are relative to the MdBV sequence. Transmembrane domain sequence analysis showed that Pif-5-1 has lost both transmembrane domains. No conserved cysteines were found in Pif-6.

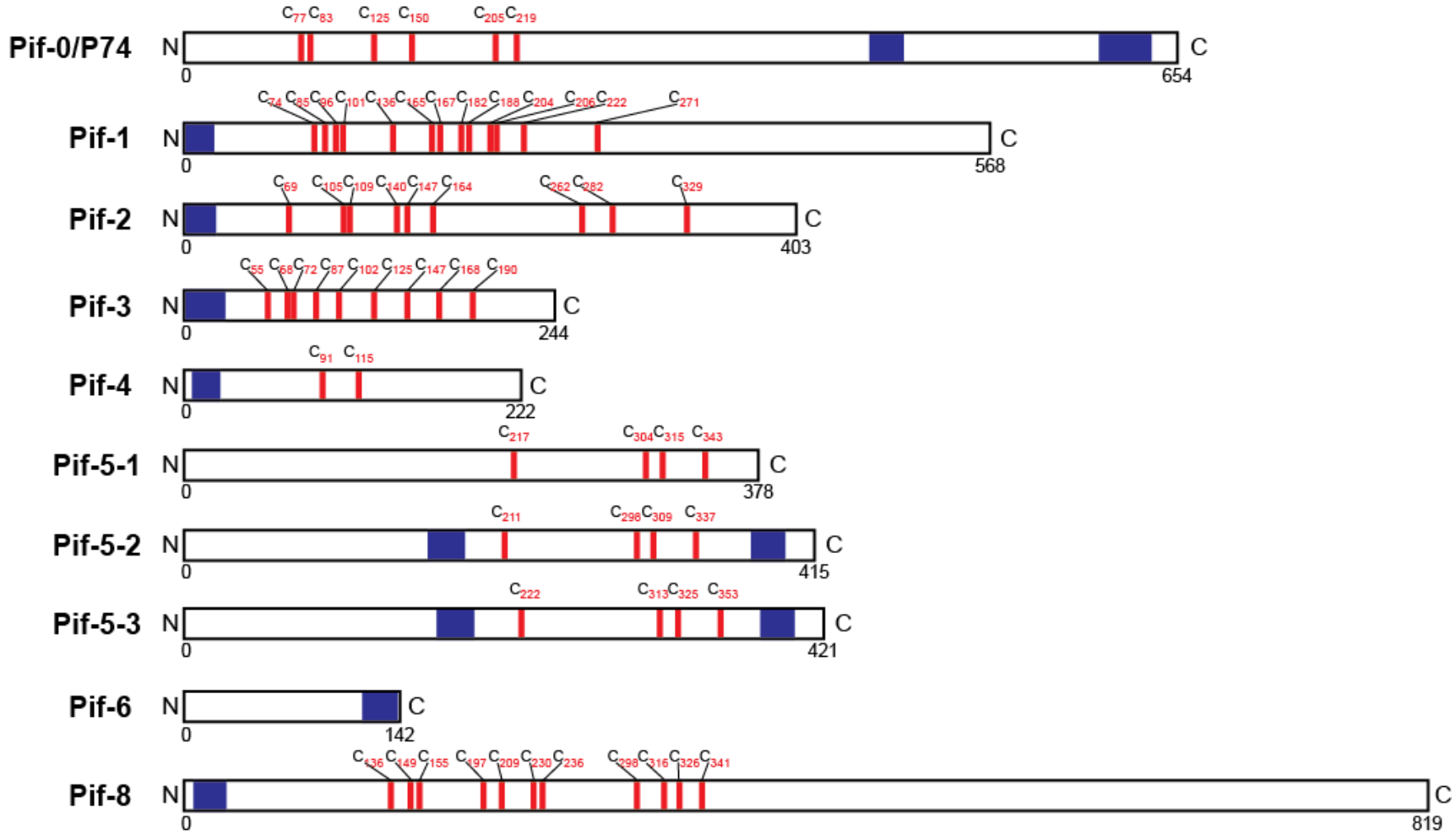
Pif-0/P74
N
C
0
654
C77 C83 C125 C150 C205 C219
Pif-1
N
C
0
568
C74 C85 C86 C101 C136 C155 C167 C182 C188 C204 C206 C222 C271
Pif-2
N
C
0
403
C69 C105 C109 C140 C147 C164 C262 C282 C329
Pif-3
N
C
0
244
C55 C68 C72 C87 C102 C125 C147 C168 C190
Pif-4
N
C
0
222
C91 C115
Pif-5-1
N
C
0
378
C217 C304 C315 C343
Pif-5-2
N
C
0
415
C211 C296 C309 C337
Pif-5-3
N
C
0
421
C222 C313 C325 C353
Pif-6
N
C
0
142
Pif-8
N
C
0
819
C136 C149 C155 C197 C209 C230 C236 C298 C316 C326 C341

**Figure 3.3: Alignment of MdBV Pif-2, Pif-5 duplicates and Pif-8 show conserved domains.** Alignment of MdBV Pif-2, Pif-5-1, Pif-5-2, Pif-5-3, Pif-8 family members to family members from select nudiviruses, baculoviruses, hytrosaviruses, LbFV, and WSSV (Table 3.1). Alignment shows the transmembrane domains in the PIFs. Note the truncation of Pif-5-1. Cysteine residues conserved in all baculoviruses and also present in MdBV PIFs are highlighted in red and labeled with their relative position in MdBV PIF protein sequences. MdBV PIF sequence files are available at AgDataCommons (http://dx.doi.org/10.15482/USDA.ADC/1432667). Accession numbers; Pif-2, MDEMTmpGB000099-RA; Pif-8, MDEMTmpGB000004-RA; Pif-5-1,, MDEMTmpGB000095-RA; Pif-5-2, MDEMTmpGB000022-RA; Pif-5-3, MDEMTmpGB000023-RA. Other viral peptide sequences are available through the NCBI RefSeq via accession numbers in parentheses. Red sequence name corresponds to MdBV, grey corresponds to β nudiviruses, green to α nudiviruses, blue to baculoviruses, brown to hytrosaviruses, black to WSSV and LbFV.

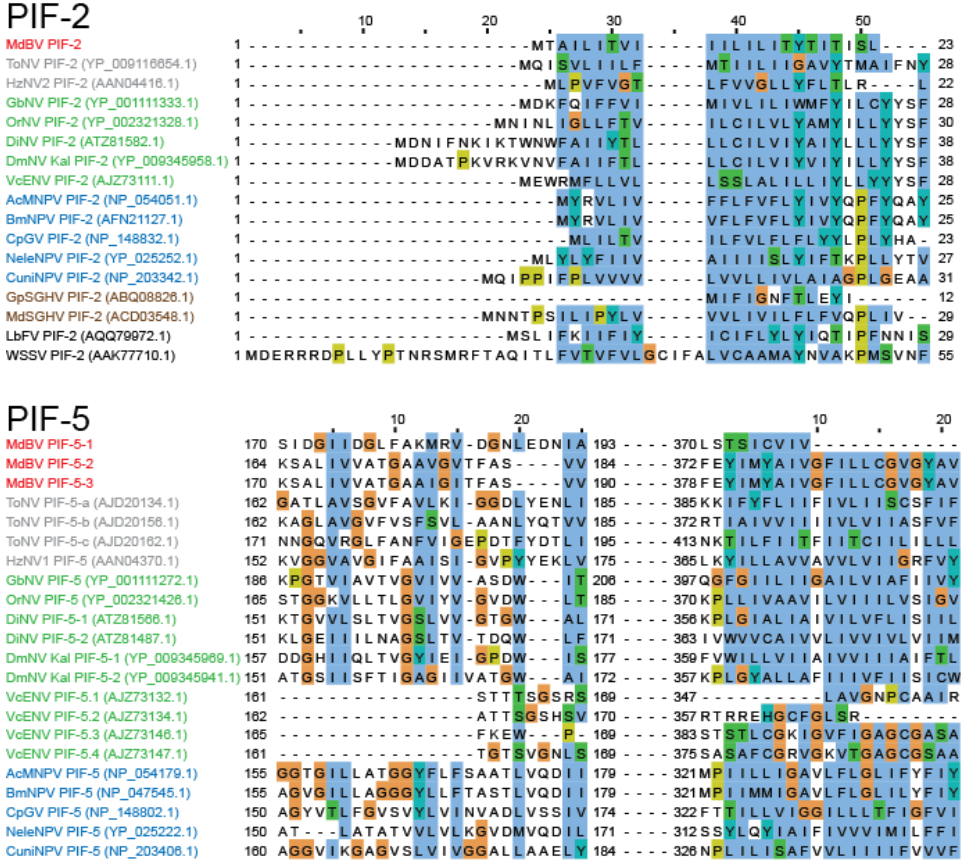
PIF-2
MdBV PIF-2
ToNV PIF-2 (YP_009116654.1)
HzNV2 PIF-2 (AAN04416.1)
GbNV PIF-2 (YP_001111333.1)
OrNV PIF-2 (YP_002321328.1)
DiNV PIF-2 (ATZ81582.1)
DmNV Kal PIF-2 (YP_009345958.1)
VcENV PIF-2 (AJZ73111.1)
AcMNPV PIF-2 (NP_054051.1)
BmNPV PIF-2 (AFN21127.1)
CpGV PIF-2 (NP_148832.1)
NeleNPV PIF-2 (YP_025252.1)
CuniNPV PIF-2 (NP_203342.1)
GpSGHV PIF-2 (ABQ08826.1)
MdSGHV PIF-2 (ACD03548.1)
LbFV PIF-2 (AQQ79972.1)
WSSV PIF-2 (AAK77710.1)
PIF-5
MdBV PIF-5-1
MdBV PIF-5-2
MdBV PIF-5-3
ToNV PIF-5-a (AJD20134.1)
ToNV PIF-5-b (AJD20156.1)
ToNV PIF-5-c (AJD20162.1)
HzNV1 PIF-5 (AAN04370.1)
GbNV PIF-5 (YP_001111272.1)
OrNV PIF-5 (YP_002321426.1)
DiNV PIF-5-1 (ATZ81566.1)
DiNV PIF-5-2 (ATZ81487.1)
DmNV Kal PIF-5-1 (YP_009345969.1)
DmNV Kal PIF-5-2 (YP_009345941.1)
VcENV PIF-5.1 (AJZ73132.1)
VcENV PIF-5.2 (AJZ73134.1)
VcENV PIF-5.3 (AJZ73146.1)
VcENV PIF-5.4 (AJZ73147.1)
AcMNPV PIF-5 (NP_054179.1)
BmNPV PIF-5 (NP_047545.1)
CpGV PIF-5 (NP_148802.1)
NeleNPV PIF-5 (YP_025222.1)
CuniNPV PIF-5 (NP_203406.1)
PIF-8
MdBV PIF-8
ToNV PIF-8 (YP_009116663.1)
HzNV1 PIF-8 (AAM45759.1)
GbNV PIF-8 (ABO45335.1)
OrNV PIF-8 (ACH96238.1)
DiNV PIF-8 (ATZ81573.1)
DmNV Kal PIF-8_(AQN78618.1)
VcENV PIF-8 (AJZ73135.1)
AcMNPV PIF-8 (NP_047486.1)
BmNPV PIF-8 (NP_047486.1)
CpGV PIF-8 (NP_148885.1)
NeleNPV PIF-8 (YP_025283.1)
CuniNPV PIF-8 (NP_203339.1)

**Figure 3.4: Alignment of MdBV P74/Pif-0, Pif-1, Pif-3, Pif-4, Pif-6 to homologs from other viruses.** Alignment of MdBV P74/Pif-0, Pif-1, Pif-3, Pif-4, and Pif-6 family members to family members from select nudiviruses, baculoviruses, hytrosaviruses, LbFV, and WSSV (Table 3.1). Alignment shows the transmembrane domains in the PIFs. Conserved residues are highlighted with background colors. MdBV PIF sequence files are available at AgDataCommons (http://dx.doi.org/10.15482/USDA.ADC/1432667). Accession numbers; P74/Pif-0, MDEMTmpGB000024-RA; Pif-1, MDEMTmpGB000100-RA; Pif-3, MDEMTmpGB000066-RA; Pif-4, MDEMTmpGB000063-RA; Pif-6, MDEMTmpGB000081-RA. Annotation for Pif-6 was found to be incomplete in the database, and was corrected for this analysis. Other viral PIF sequences are available through the NCBI RefSeq via accession numbers in parentheses. Red sequence name corresponds to MdBV, grey corresponds to β nudiviruses, green to α nudiviruses, blue to baculoviruses, brown to hytrosaviruses, black to WSSV and LbFV.

## P74

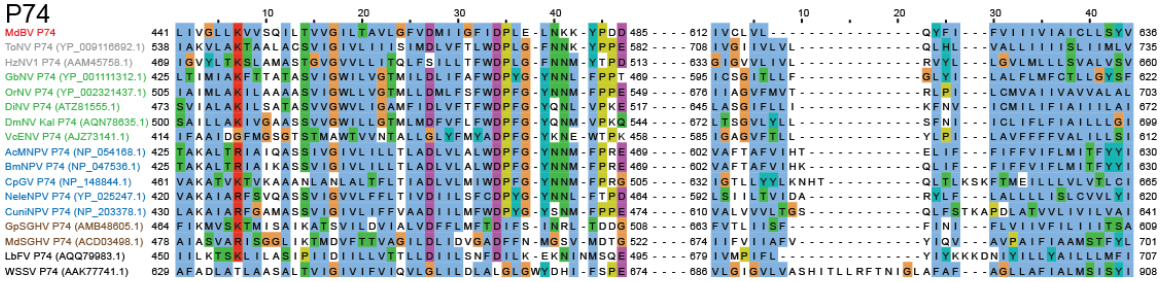


## PIF-1

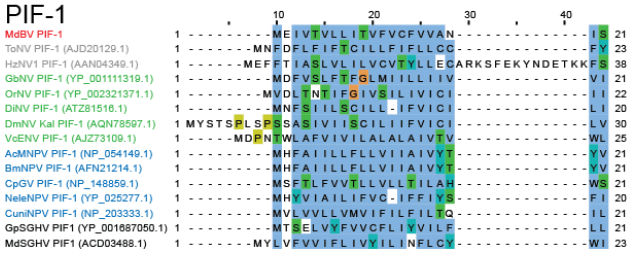


## PIF-3

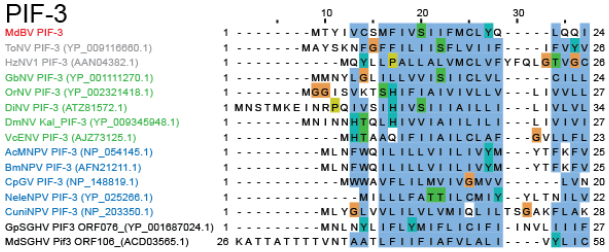


## PIF-4

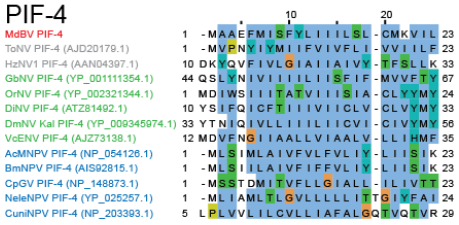


## PIF-6

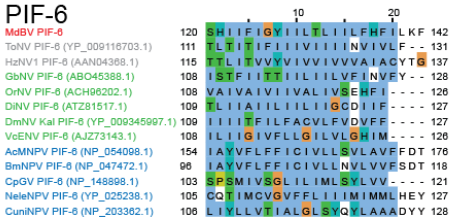

**Figure 3.5: Phobius prediction of presence of transmembrane domains and signal peptides in MdBV PIFs.** Sequence analysis using Phobius shows conserved transmembrane domains in MdBV PIFs (http://phobius.sbc.su.se/)[31].

P74/Pif-0

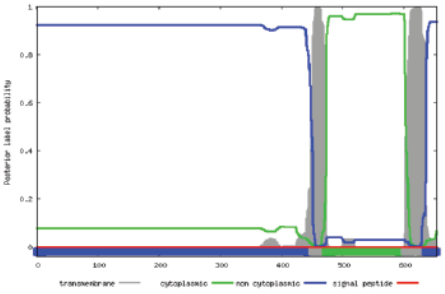


Pif-5-1

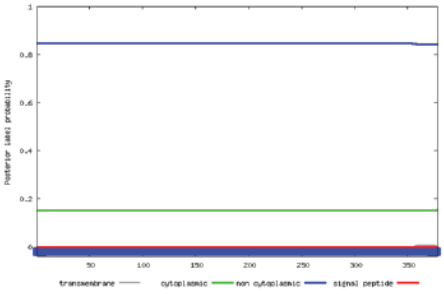


Pif-1

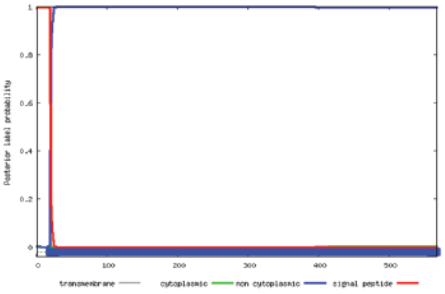


Pif-5-2

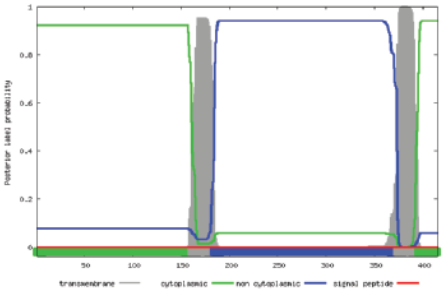


Pif-2

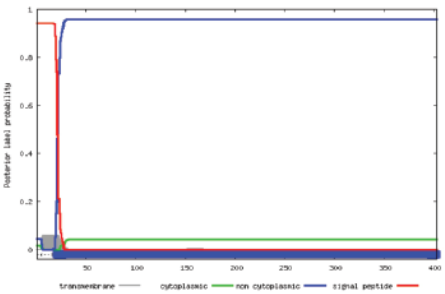


Pif-5-3

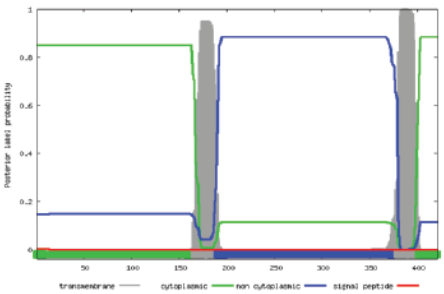


Pif-3

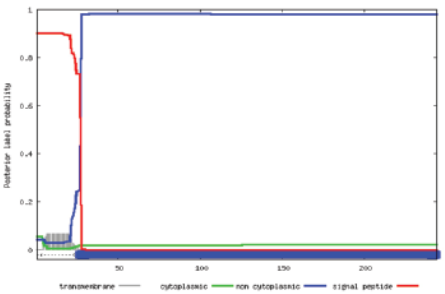


Pif-6

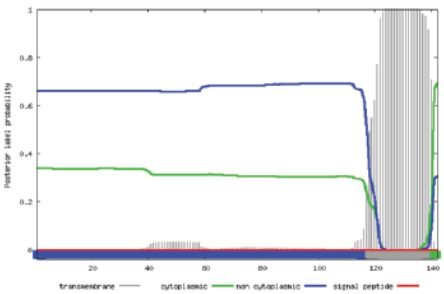


Pif-4

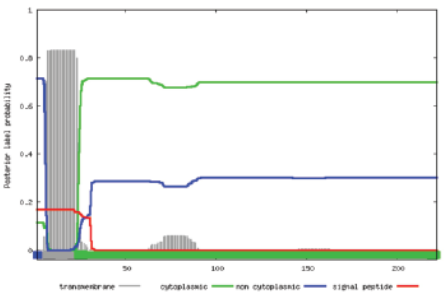


Pif-8

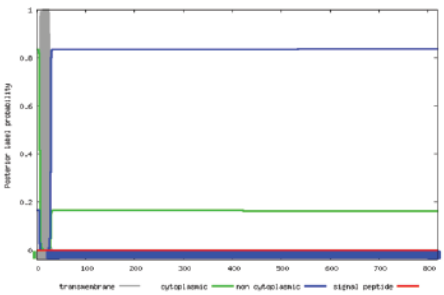

**Figure 3.6: TMHMM prediction of presence of transmembrane domains and signal peptides in MdBV PIFs.** Transmembrane domain prediction of MdBV PIF sequences using TMHMM (Server v. 2.0, http://www.cbs.dtu.dk/services/TMHMM/)[30].

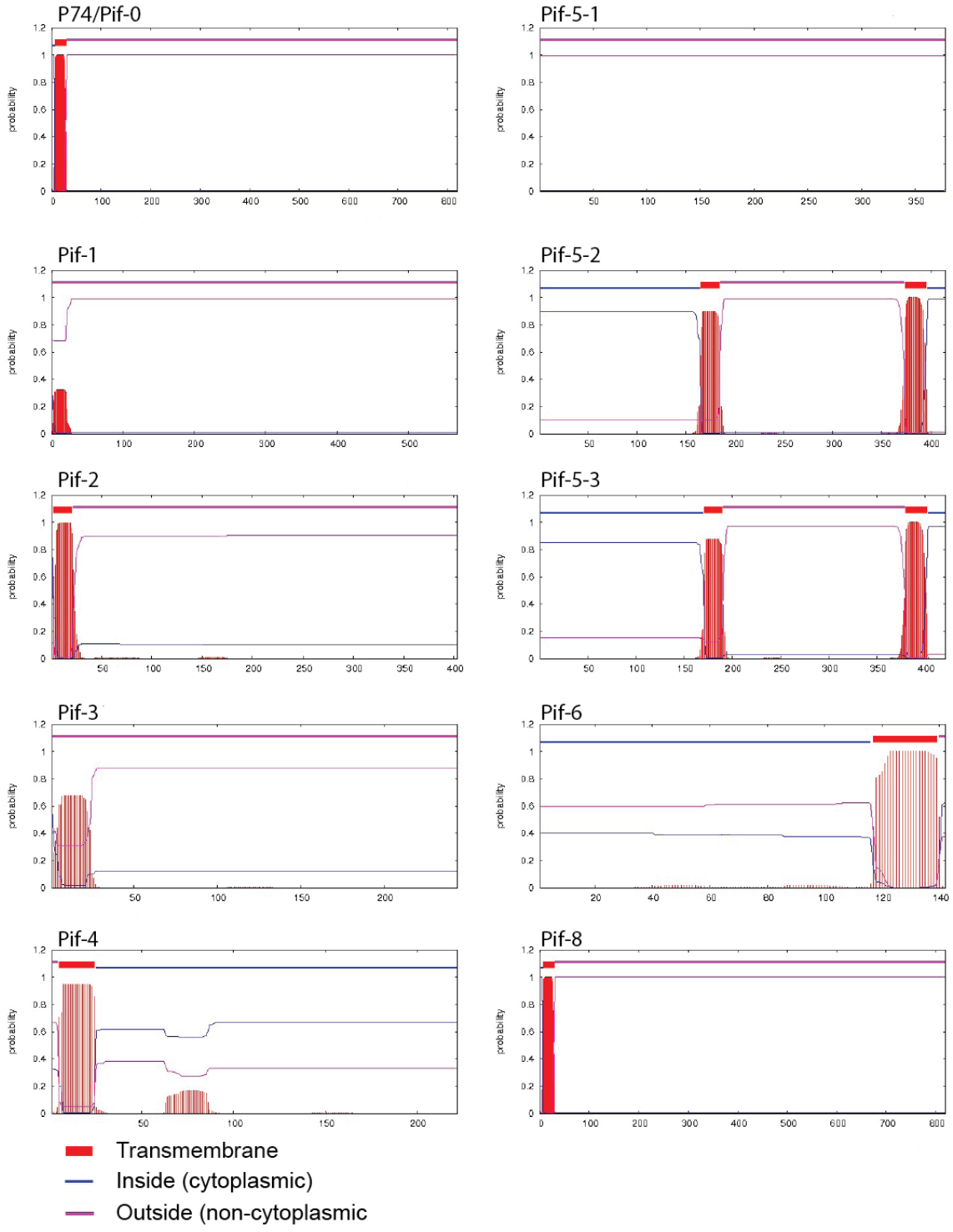
P74/Pif-0
Pif-5-1
Pif-1
Pif-5-2
Pif-2
Pif-5-3
Pif-3
Pif-6
Pif-4
Pif-8
probability
Transmembrane
Inside (cytoplasmic)
Outside (non-cytoplasmic)

**Figure 3.7: Alignment of MdBV Pif-8 shows conserved zinc finger and nucleocapsid assembly domains.** Alignment of Pif-8 from MdBV to homologs from select nudiviruses, baculoviruses, hytrosaviruses, LbFV, and WSSV (Table 3.1). (A) Alignment shows C2H2-type zinc finger domain first identified in AcMNPV [24, 32]. The zinc finger domain conforms to a C-X5-C-XnH-X6-C amino acid sequence patter, with X being any residue (arrows). (B) Nucleocapsid assembly domain first identified in baculoviruses [21]. Conserved residues are highlighted with background colors. MdBV PIF sequence files are available at AgDataCommons (http://dx.doi.org/10.15482/USDA.ADC/1432667). Accession numbers for Pif-8, MDEMTmpGB000004-RA. Other viral PIF sequences are available through the NCBI RefSeq via accession numbers in parentheses. Red sequence name corresponds to MdBV, grey corresponds to β nudiviruses, green to α nudiviruses, blue to baculoviruses, brown to hytrosaviruses, black to WSSV and LbFV.

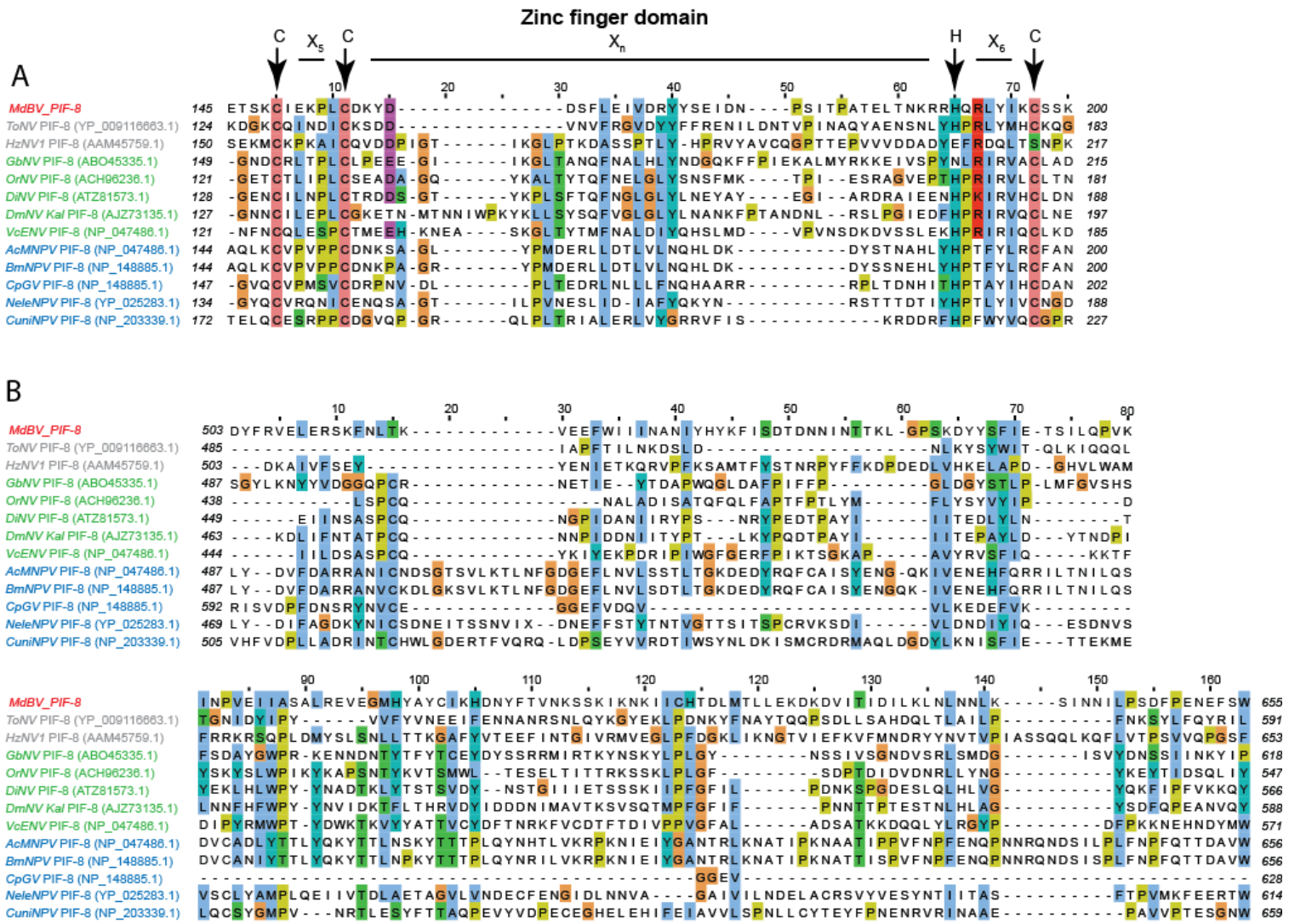
A
Zinc finger domain
C
X5
C
Xn
H
X6
C
MdBV_PIF-8
ToNV PIF-8 (YP_009116663.1)
HzNV1 PIF-8 (AAM45759.1)
GbNV PIF-8 (ABO45335.1)
OrNV PIF-8 (ACH96236.1)
DiNV PIF-8 (ATZ81573.1)
DmNV Kal PIF-8 (AJZ73135.1)
VcENV PIF-8 (NP_047486.1)
AcMNPV PIF-8 (NP_047486.1)
BmNPV PIF-8 (NP_148885.1)
CpGV PIF-8 (NP_148885.1)
NeleNPV PIF-8 (YP_025283.1)
CuniNPV PIF-8 (NP_203339.1)
B

**Figure 3.8: Phylogenetic relationship of MdBV Pif-2, Pif-5, and Pif-8 with homologs from free-living virus relatives.** The maximum-likelihood (ML) tree was generated with RAxML using ML inference analysis of available PIF protein sequences from baculoviruses, nudiviruses, hytrosaviruses, LbFV, and WSSV (Table 3.1) [64]. The Pif-2 tree is rooted to WSSV. The trees of Pif-5 and Pif-8 are outgroup rooted to baculoviruses. Numbers on nodes indicate ML bootstrap support (100 replicates). Red sequence name corresponds to MdBV, grey corresponds to β nudiviruses, green to α nudiviruses, blue to baculoviruses, brown to hytrosaviruses, black to WSSV and LbFV. Inset tree shows cladogram of current phylogenetic constructions of viruses related to Bracoviruses [2, 34, 35].

## Pif-2

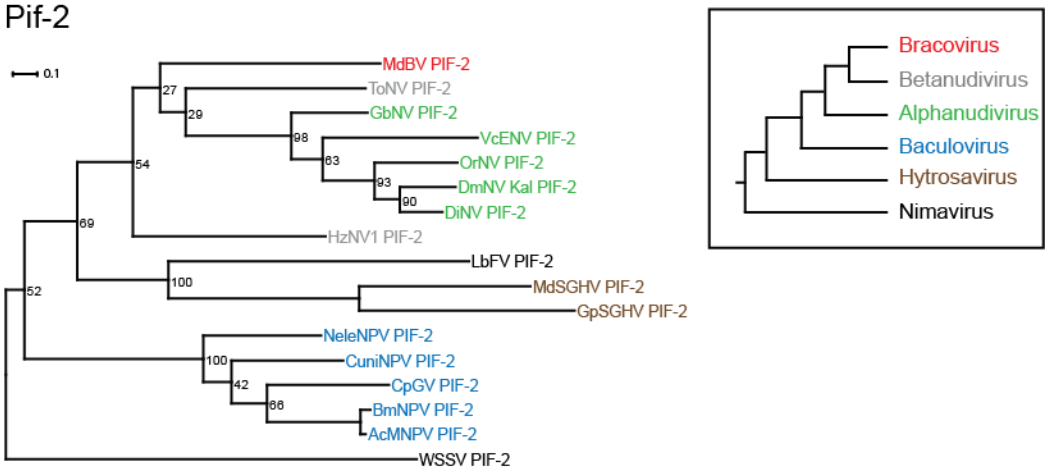


## Pif-5

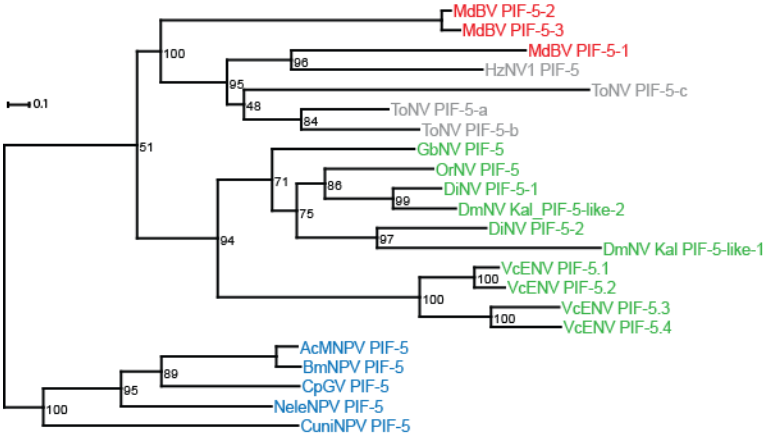


## Pif-8

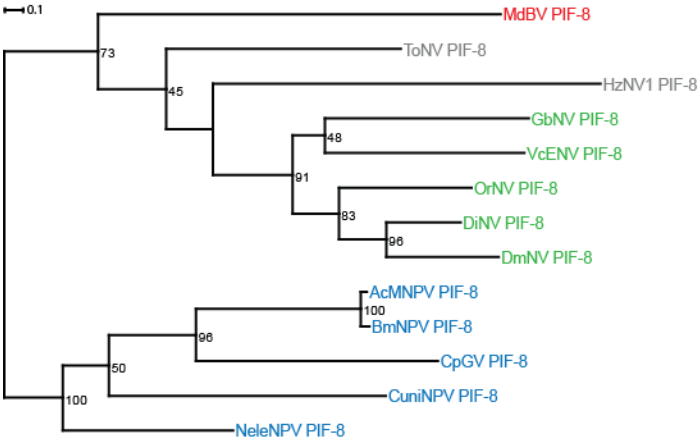

**Figure 3.9: Phylogenetic relationship of MdBV P74/Pif-0, Pif-1, Pif-3, Pif-4, Pif-6 with homologs from free-living virus relatives.** The maximum-likelihood (ML) tree was generated with RAxML using ML inference analysis of available PIF protein sequences from baculoviruses, nudiviruses, hytrosaviruses, LbFV, and WSSV (Table 1) [64]. The P74/Pif-0 tree is rooted to WSSV. The trees of Pif-1 and Pif-3 are outgroup rooted to hytrosaviruses. The trees of Pif-4 and Pif-6 are outgroup rooted to baculoviruses. Numbers on nodes indicate ML bootstrap support (100 replicates). Red sequence name corresponds to MdBV, grey corresponds to β nudiviruses, green to α nudiviruses, blue to baculoviruses, brown to hytrosaviruses, black to WSSV and LbFV. Inset tree shows cladogram of recent phylogenetic constructions of viruses related to Bracoviruses [2, 34, 35].

P74/Pif-0

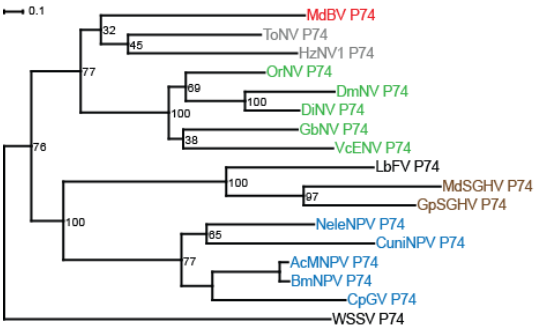


Pif-1

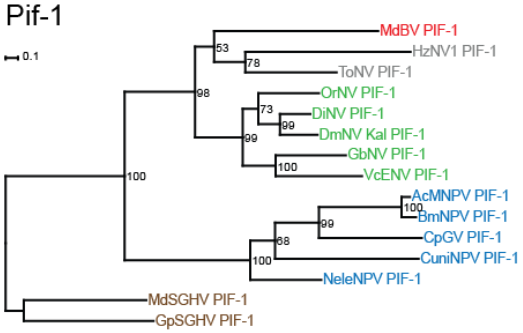


Pif-3

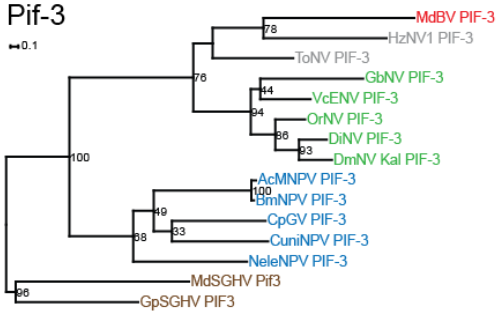


Pif-4

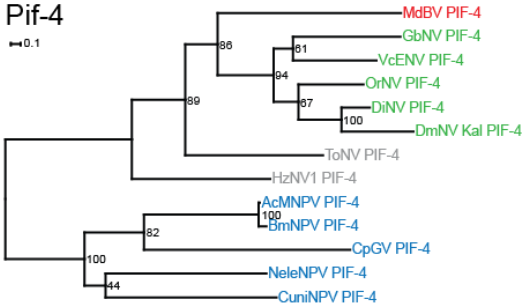


Pif-6

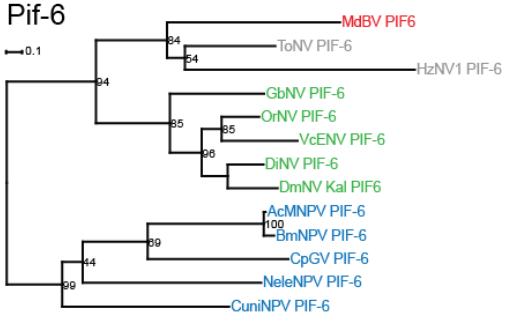


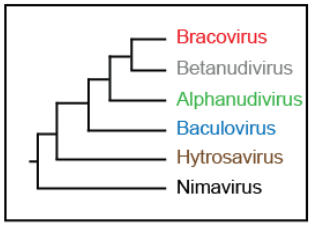

**Figure 3.10: Knockdown of *pif-2*, *pif-5-1*, *pif-5-2*, *pif-5-3*, *pif-8* in MdBV using RNAi.** M. demolitor larvae were injected with double stranded RNA (dsRNA) specific to (A) *pif-2*, (B) *pif-5-1*,(C) *pif-5-2*,(D) *pif-5-3*, or (E) *pif-8*. Control larvae were injected with *ds-e*GFP. Wasps were allowed to emerge, after which ovaries were dissected and total RNA was isolated from one half ovary. I used qPCR to measure MdBV PIF transcript copy number. Error bars represent one standard error from the mean. The number of individuals examined for each treatment is indicated by the N value at the bottom of each bar. Statistical significance is indicated by asterisks: *,p≤0.05; **, p≤0.01; ***, p≥0.001; ****, p≥0.0001; N. S., not significant.

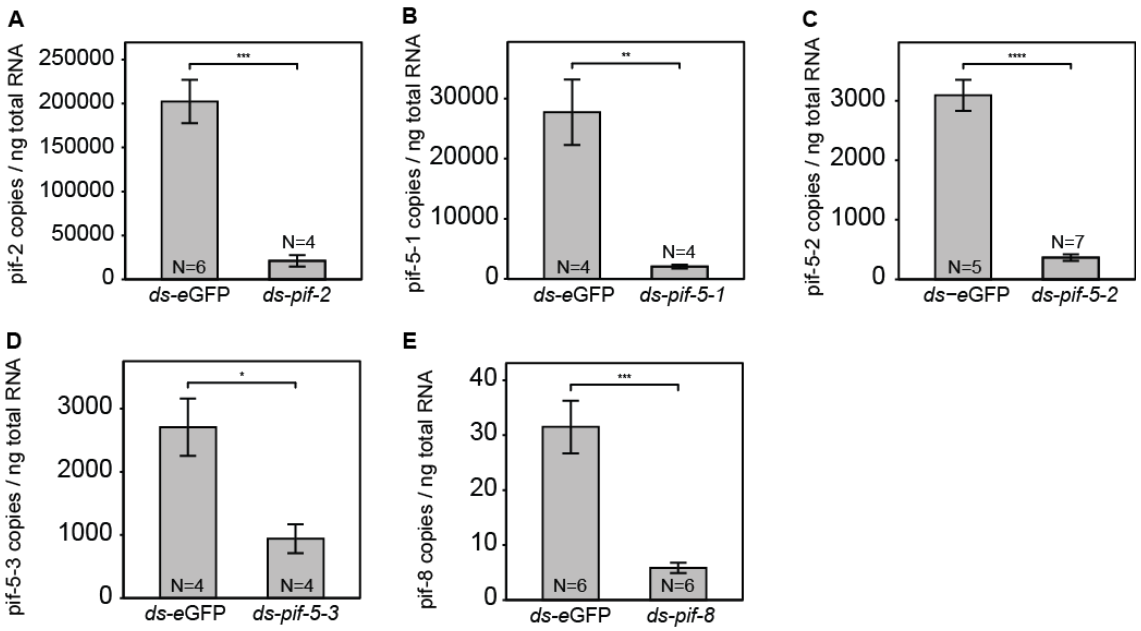
A
pif-2 copies / ng total RNA
250000
200000
150000
100000
50000
0
***
N=6
N=4
ds-eGFP
ds-pif-2
B
pif-5-1 copies / ng total RNA
30000
20000
10000
0
**
N=4
N=4
ds-eGFP
ds-pif-5-1
C
pif-5-2 copies / ng total RNA
3000
2000
1000
0
****
N=5
N=7
ds−eGFP
ds-pif-5-2
D
pif-5-3 copies / ng total RNA
3000
2000
1000
0
*
N=4
N=4
ds-eGFP
ds-pif-5-3
E
pif-8 copies / ng total RNA
40
30
20
10
0
***
N=6
N=6
ds-eGFP
ds-pif-8

**Figure 3.11: Electron microscopy analysis of MdBV PIF knockdowns**. Electron micrographs were taken from one wasp per knockdown. Calyx cells selected were all at the same developmental stage. Wasp ovaries from at least two separate individuals were examined to ensure that images were representative for the knockdown. Arrowheads indicate fully formed virions and nucleocapsids in the process of being enveloped. Arrow indicates virion with elongated envelope organized into an array. Scale bars in each panel equal 200 nm.

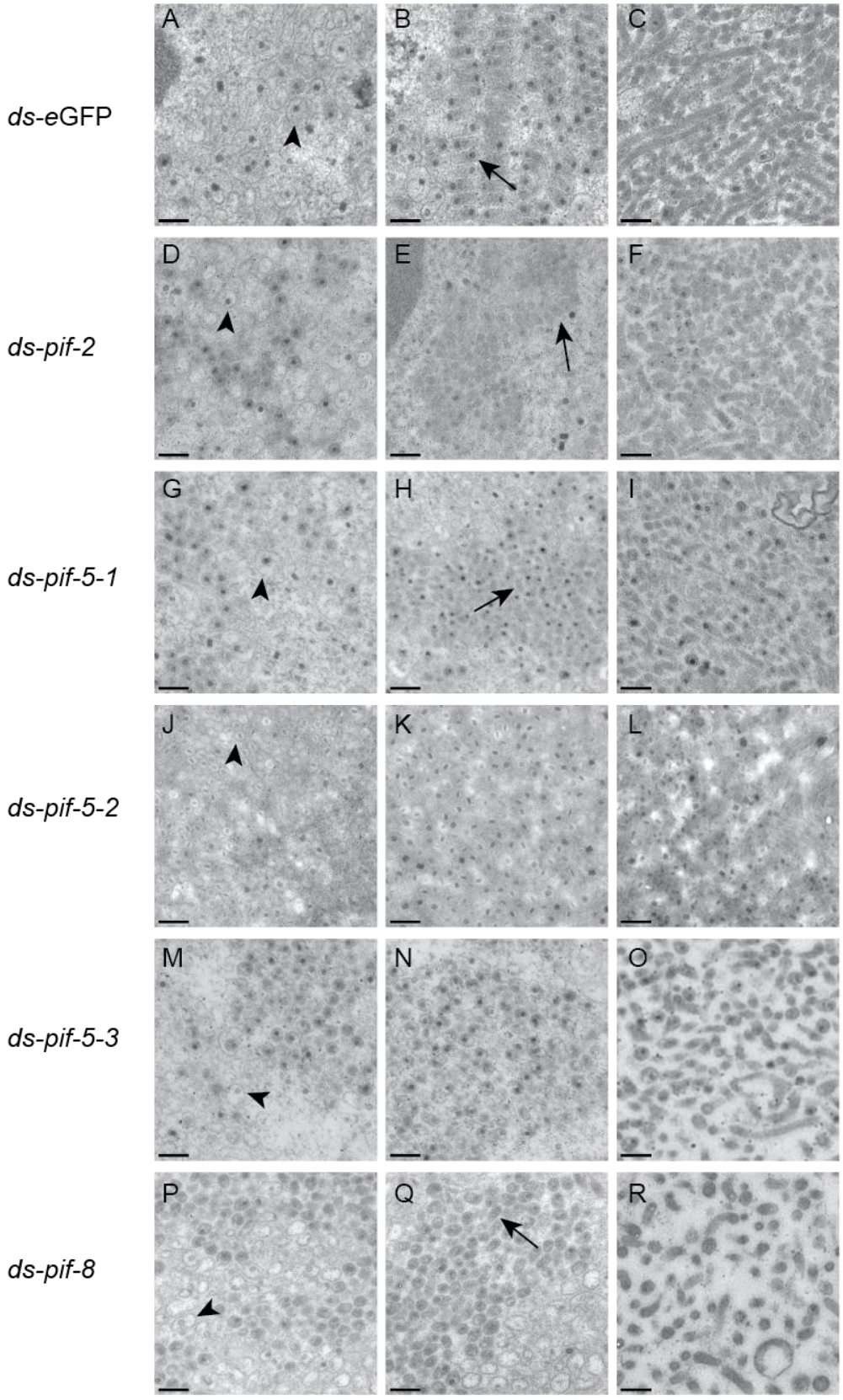
ds-eGFP
ds-pif-2
ds-pif-5-1
ds-pif-5-2
ds-pif-5-3
ds-pif-8
A
B
C
D
E
F
G
H
I
J
K
L
M
N
O
P
Q
R

**Figure 3.12: Virion density in calyx fluid from wasps treated with dsRNA corresponding to MdBV PIFs.** Density results were based on at least two wasps per knockdown. Knockdown of *pif-5-3* and *pif-8* resulted in significantly lower virion density relative to d*s-e*GFP control wasps. Error bars, N values, and statistical significance are indicated as defined in Fig. 3.10.

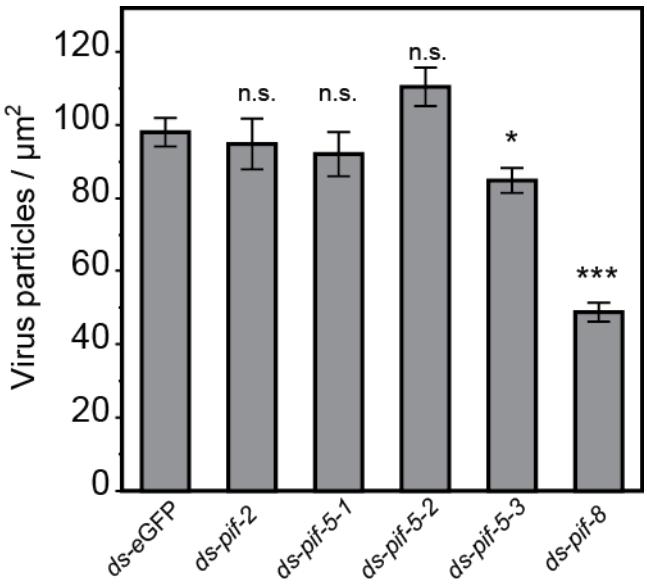
Virus particles / µm²
120
100
80
60
40
20
0
n.s.
n.s.
n.s.
*
***
ds-eGFP
ds-pif-2
ds-pif-5-1
ds-pif-5-2
ds-pif-5-3
ds-pif-8

**Figure 3.13: Knockdown of *pif-2*, *pif-5-1*, *pif-5-2*, *pif-5-3*, or *pif-8* does not increase DNase sensitivity of MdBV virions.** To confirm that none of the MdBV PIFs are necessary for virion structural integrity, I tested whether viral DNAs packaged into knockdown virion nucleocapsid were protected from DNase treatment. *M. demolitor* larvae were injected with *ds-pif-2*, *ds-pif-5-1*, *ds-pif-5-2*, *ds-pif-5-3* or *ds-pif-8*. After adult emergence, half of the reproductive tract was removed and treated with NP-40 to solubilize virion nucleocapsids and treated with DNase. Panels show copy number of DNase-protected viral DNA segment O remaining per ovary for wasps treated with (A) *ds-pif-2*, (B) *ds-pif-5-1*, (C) *ds-pif-5-2*, (D) *ds-pif-5-3* or (E) *ds-pif-8*, relative to the control. Error bars, N values, and statistical significance are indicated as in Fig. 3.10.

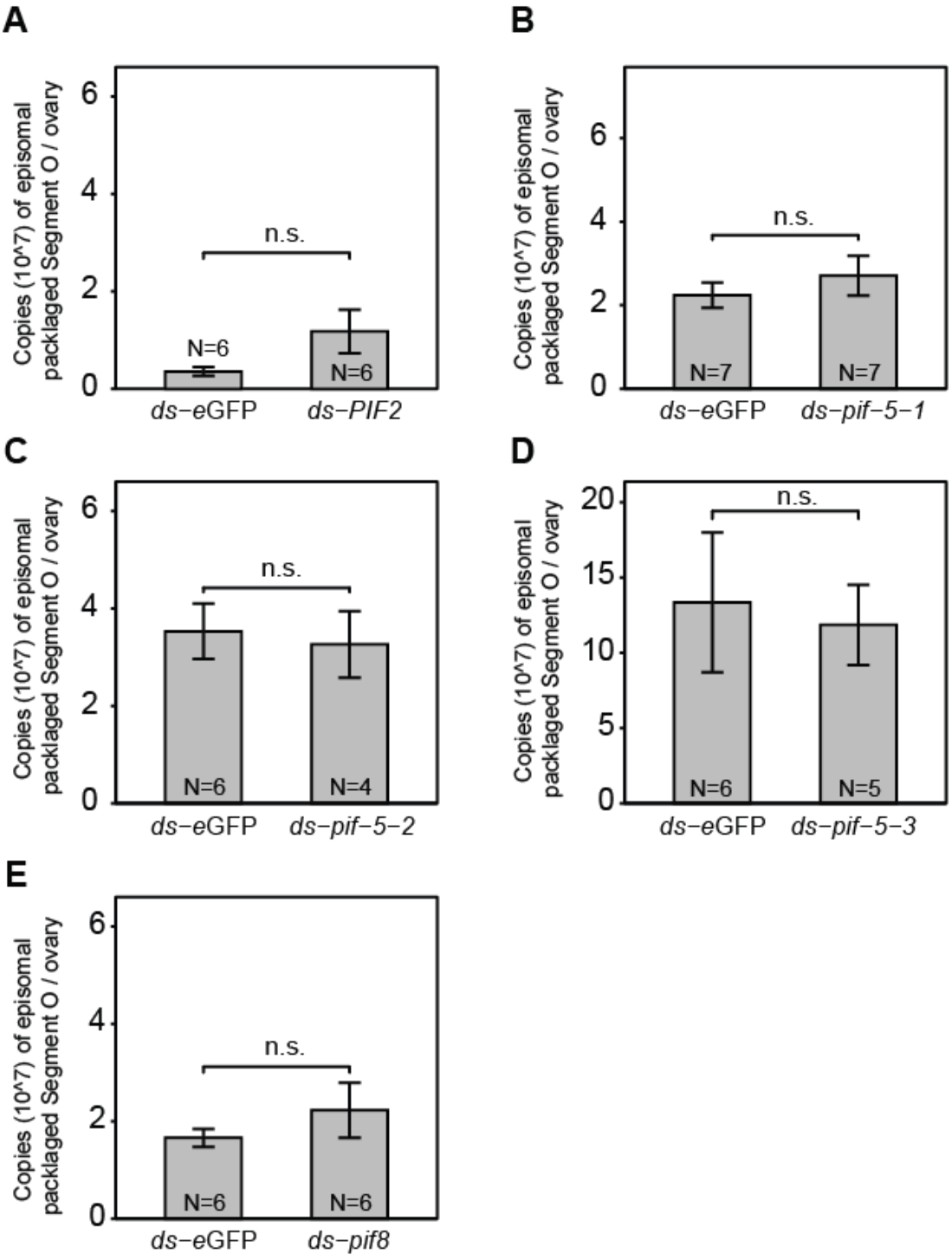
A
Copies (10^7) of episomal packlaged Segment O / ovary
6
4
2
0
n.s.
N=6
N=6
ds−eGFP
ds−PIF2
B
Copies (10^7) of episomal packlaged Segment O / ovary
6
4
2
0
n.s.
N=7
N=7
ds−eGFP
ds−pif−5−1
C
Copies (10^7) of episomal packlaged Segment O / ovary
6
4
2
0
n.s.
N=6
N=4
ds−eGFP
ds−pif−5−2
D
Copies (10^7) of episomal packlaged Segment O / ovary
20
15
10
5
0
n.s.
N=6
N=5
ds−eGFP
ds−pif−5−3
E
Copies (10^7) of episomal packlaged Segment O / ovary
6
4
2
0
n.s.
N=6
N=6
ds−eGFP
ds−pif8

**Figure 3.14: Knockdown of PIFs disrupts typical viral infection *in vitro*.** *M. demolitor* larvae were injected with *ds-pif-2*, *ds-pif-5-1*, *ds-pif-5-2*, *ds-pif-5-3* or *ds-pif-8*. Wells of 200,000 CiE1 cells were infected (MOI 100) with virions extracted from PIF knockdown wasps. DNA and RNA were extracted from CiE1 cells 24 h post infection. Left panels show copy number of viral DNA segment O in CiE1 cells infected with virions from wasps with knockdown of (A) *pif-2*, (C) *pif-5-1*, (E) *pif-5-2*, (G) *pif-5-3*, or (I) *pif-8*. Right panels show copy number of *glc1.8* per ng RNA in CiE1 cells infected with virions from wasps with knockdown of (B) *pif-2*, (D) *pif-5-1*, (F) *pif-5-2*, (H) *pif-5-3*, or (J) *pif-8*. Error bars, N values, and statistical significance are indicated as in Fig. 3.10.

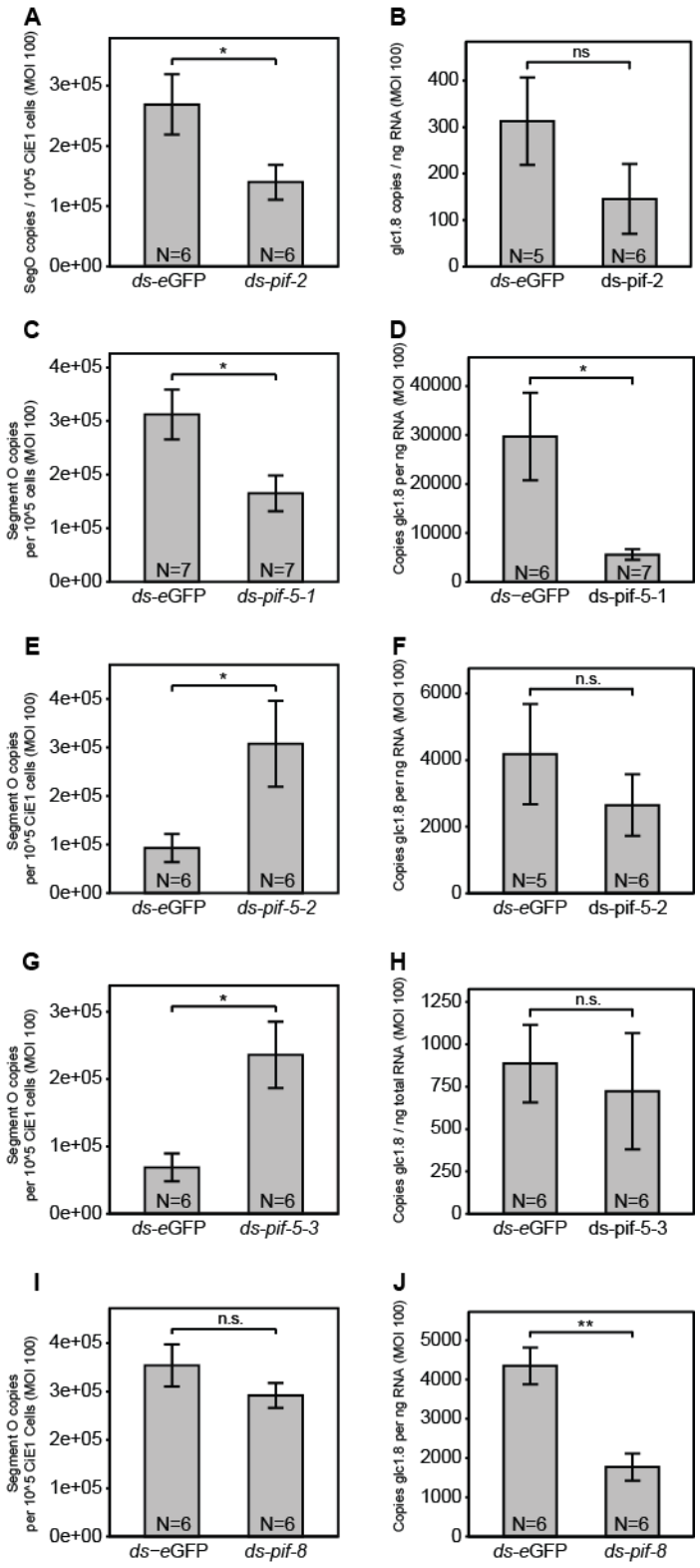
A
SegO copies / 10^5 CiE1 cells (MOI 100)
3e+05
2e+05
1e+05
0e+00
*
N=6
N=6
ds-eGFP
ds-pif-2
B
glc1.8 copies / ng RNA (MOI 100)
400
300
200
100
0
ns
N=5
N=6
ds-eGFP
ds-pif-2
C
Segment O copies per 10^5 cells (MOI 100)
4e+05
3e+05
2e+05
1e+05
0e+00
*
N=7
N=7
ds-eGFP
ds-pif-5-1
D
Copies glc1.8 per ng RNA (MOI 100)
40000
30000
20000
10000
0
*
N=6
N=7
ds−eGFP
ds-pif-5-1
E
Segment O copies per 10^5 CiE1 cells (MOI 100)
4e+05
3e+05
2e+05
1e+05
0e+00
*
N=6
N=6
ds-eGFP
ds-pif-5-2
F
Copies glc1.8 per ng RNA (MOI 100)
6000
4000
2000
0
n.s.
N=5
N=6
ds-eGFP
ds-pif-5-2
G
Segment O copies per 10^5 CiE1 cells (MOI 100)
3e+05
2e+05
1e+05
0e+00
*
N=6
N=6
ds-eGFP
ds-pif-5-3
H
Copies glc1.8 / ng total RNA (MOI 100)
1250
1000
750
500
250
0
n.s.
N=6
N=6
ds-eGFP
ds-pif-5-3
I
Segment O copies per 10^5 CiE1 Cells (MOI 100)
4e+05
3e+05
2e+05
1e+05
0e+00
n.s.
N=6
N=6
ds−eGFP
ds-pif-8
J
Copies glc1.8 per ng RNA (MOI 100)
5000
4000
3000
2000
1000
0
**
N=6
N=6
ds-eGFP
ds-pif-8

**Figure 3.15: Knockdown of PIFs disrupts typical viral infection *in vitro*.** *M. demolitor* larvae were injected with *ds-pif-2*, *ds-pif-5-1*, *ds-pif-5-2*, *ds-pif-5-3* or *ds-pif-8*. Wells of 200,000 CiE1 cells were infected (MOI 1) with virions extracted from PIF knockdown wasps. DNA and RNA were extracted from CiE1 cells 24 h post infection. Left panels show copy number of viral DNA segment O in CiE1 cells infected with virions from wasps with knockdown of (A) *pif-2*, (C) *pif-5-1*, (E) *pif-5-2*, (G) *pif-5-3*, or (I) *pif-8*. Right panels show copy number of *glc1.8* per ng RNA in CiE1 cells infected with virions from wasps with knockdown of (B) *pif-2*, (D) *pif-5-1*, (F) *pif-5-2*, (H) *pif-5-3*, or (J) *pif-8*. Error bars, N values, and statistical significance are indicated as defined in Fig. 3.10.

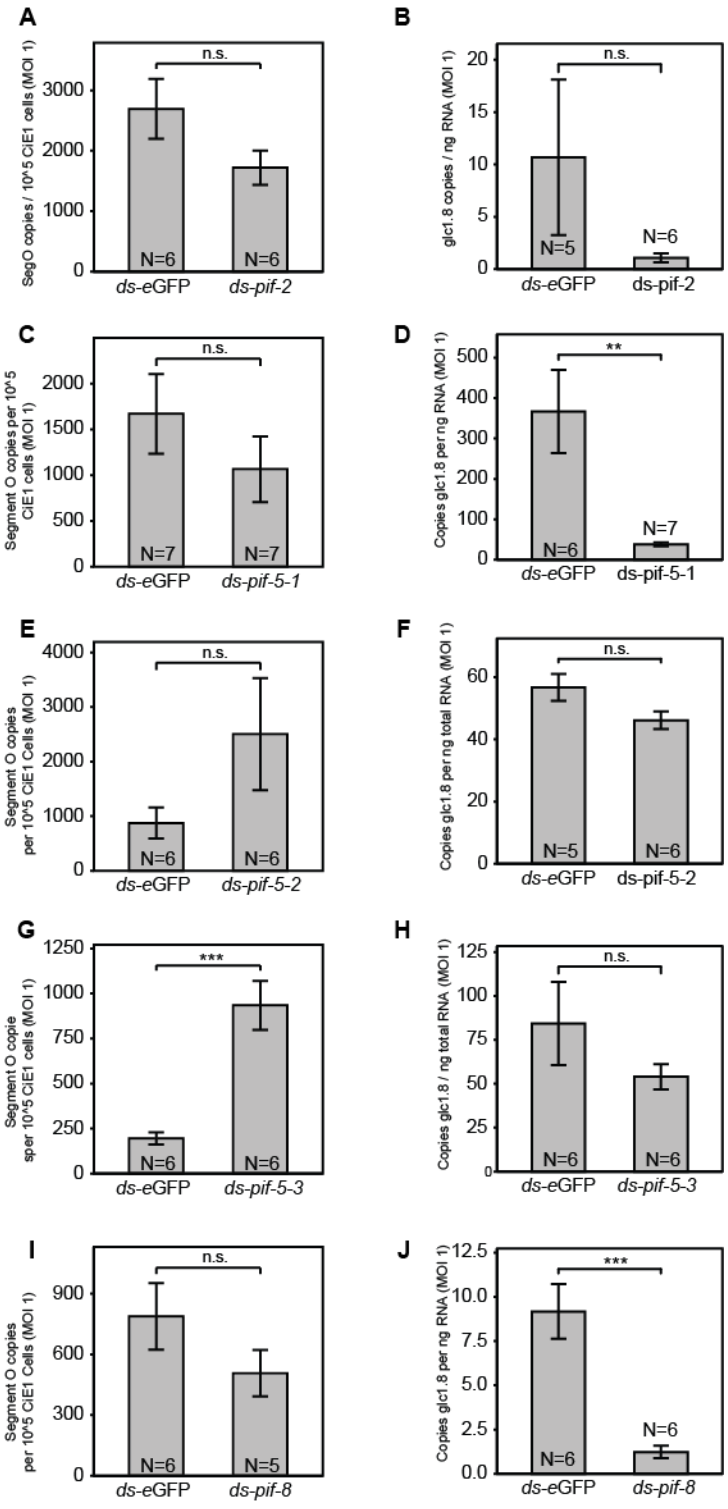
A
SegO copies / 10^5 CiE1 cells (MOI 1)
n.s.
N=6
N=6
ds-eGFP
ds-pif-2
B
glc1.8 copies / ng RNA (MOI 1)
n.s.
N=5
N=6
ds-eGFP
ds-pif-2
C
Segment O copies per 10^5 CiE1 cells (MOI 1)
n.s.
N=7
N=7
ds-eGFP
ds-pif-5-1
D
Copies glc1.8 per ng RNA (MOI 1)
**
N=6
N=7
ds-eGFP
ds-pif-5-1
E
Segment O copies per 10^5 CiE1 Cells (MOI 1)
n.s.
N=6
N=6
ds-eGFP
ds-pif-5-2
F
Copies glc1.8 per ng total RNA (MOI 1)
n.s.
N=5
N=6
ds-eGFP
ds-pif-5-2
G
Segment O copie sper 10^5 CiE1 cells (MOI 1)
***
N=6
N=6
ds-eGFP
ds-pif-5-3
H
Copies glc1.8 / ng total RNA (MOI 1)
n.s.
N=6
N=6
ds-eGFP
ds-pif-5-3
I
Segment O copies per 10^5 CiE1 Cells (MOI 1)
n.s.
N=6
N=5
ds-eGFP
ds-pif-8
J
Copies glc1.8 per ng RNA (MOI 1)
***
N=6
N=6
ds-eGFP
ds-pif-8

**Figure 3.16: Viral gene expression and viral DNA segments in *C. includens* larval tissues parasitized using knockdown wasps.** *M. demolitor* larvae were injected with *ds-pif-5-1*, *ds-pif-5-2* or *ds-pif-5-3*. Knockdown wasps were allowed to parasitize a pool (3 to 4 individuals) of 4th instar *C. includens* larvae. I extracted DNA and total RNA from hemocytes, gut tissue, and fat body tissue 24 hours post parasitism. I used qPCR to measure viral DNA segment copy and viral gene expression in each tissue. Copy number of *glc1.8* per ng RNA in parasitized (B) fat body, (D) gut, (F) hemocytes. Copy number of viral DNA segment O in parasitized (A) fat body, (C) gut, and (E) hemocytes. Error bars, N values, and statistical significance are indicated as defined in Fig. 3.10.

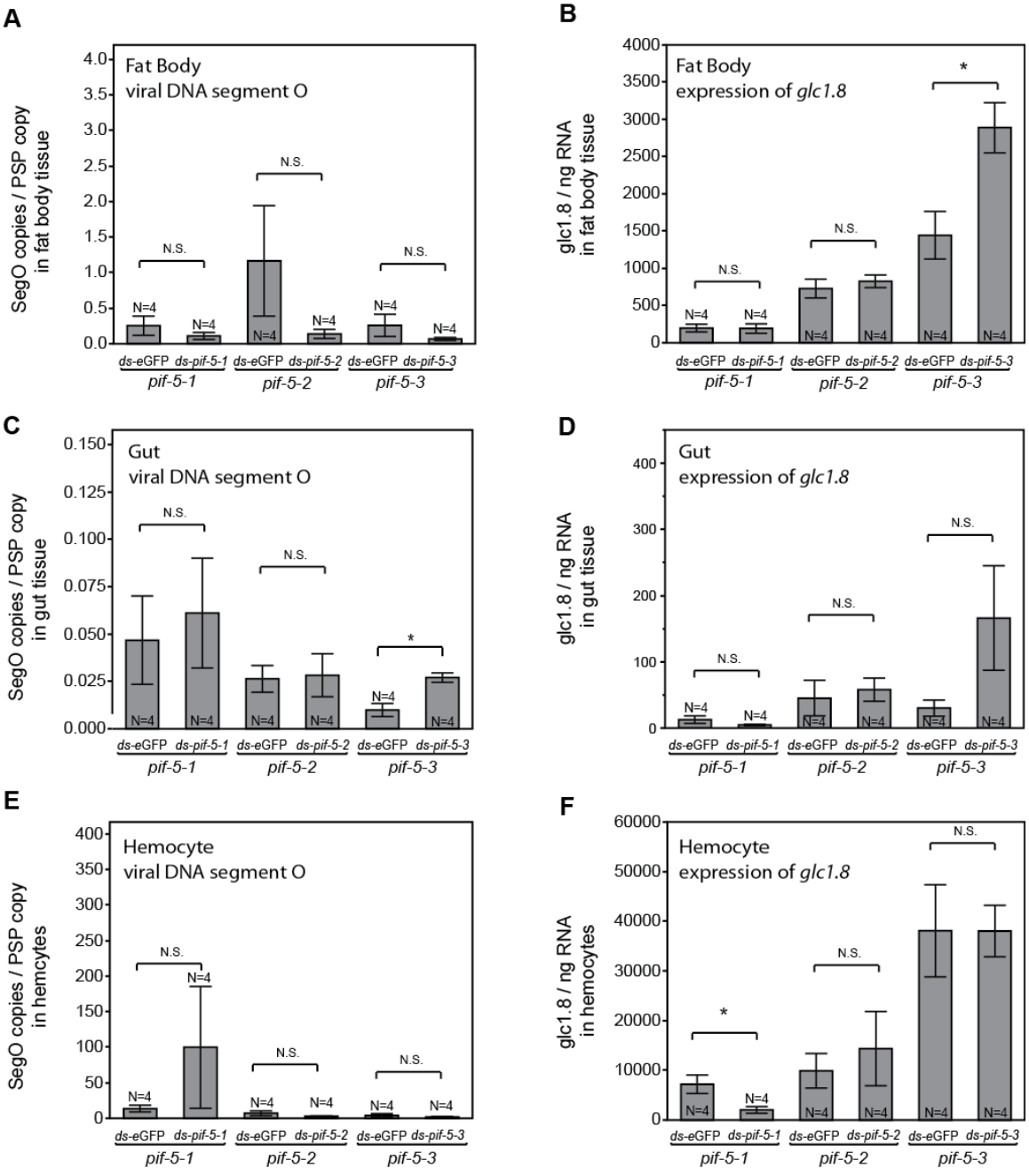
A
Fat Body
viral DNA segment O
SegO copies / PSP copy
in fat body tissue
B
Fat Body
expression of glc1.8
glc1.8 / ng RNA
in fat body tissue
C
Gut
viral DNA segment O
SegO copies / PSP copy
in gut tissue
D
Gut
expression of glc1.8
glc1.8 / ng RNA
in gut tissue
E
Hemocyte
viral DNA segment O
SegO copies / PSP copy
in hemcytes
F
Hemocyte
expression of glc1.8
glc1.8 / ng RNA
in hemocytes
N.S.
*
N=4
ds-eGFP ds-pif-5-1 ds-eGFP ds-pif-5-2 ds-eGFP ds-pif-5-3
pif-5-1
pif-5-2
pif-5-3

**Figure 3.17: Viral DNA segment O found in the nuclei of CiE1 cells infected with knockdown virions.** *M. demolitor* larvae were injected with *ds-pif-2*, *ds-pif-5-1*, or ds-*pif-8*. Tubes of 200,000 CiE1 cells were infected (MOI 10) with virions extracted from PIF knockdown wasps. These cells were then separated into nuclear and cytoplasmic fractions, and segment O abundance was measured for both fractions for (A,B) *pif-2*, (C,D) *pif-5-1*, and (E,F) *pif-8* knockdown virion infections. Note that infection with *pif-2* knockdown virions (A) resulted in significantly fewer copies of Segment O present in the nucleus relative to the control. Error bars, N values, and statistical significance are indicated as defined in Fig. 3.10.

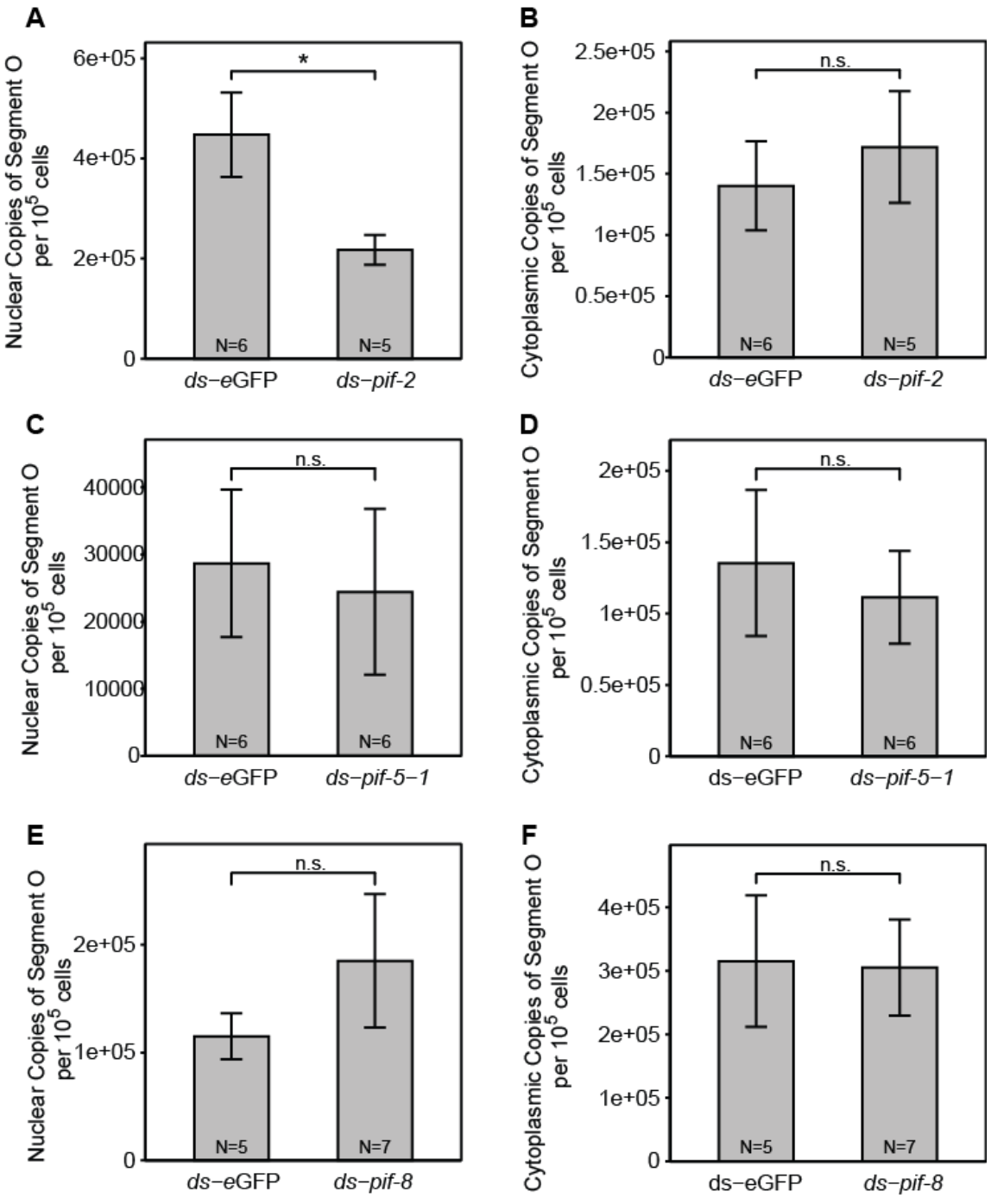
A
Nuclear Copies of Segment O per 10^5 cells
6e+05
4e+05
2e+05
0
*
N=6
N=5
ds−eGFP
ds−pif-2
B
Cytoplasmic Copies of Segment O per 10^5 cells
2.5e+05
2e+05
1.5e+05
1e+05
0.5e+05
0
n.s.
N=6
N=5
ds−eGFP
ds−pif-2
C
Nuclear Copies of Segment O per 10^5 cells
40000
30000
20000
10000
0
n.s.
N=6
N=6
ds−eGFP
ds−pif-5−1
D
Cytoplasmic Copies of Segment O per 10^5 cells
2e+05
1.5e+05
1e+05
0.5e+05
0
n.s.
N=6
N=6
ds−eGFP
ds−pif-5−1
E
Nuclear Copies of Segment O per 10^5 cells
2e+05
1e+05
0
n.s.
N=5
N=7
ds−eGFP
ds−pif-8
F
Cytoplasmic Copies of Segment O per 10^5 cells
4e+05
3e+05
2e+05
1e+05
0
n.s.
N=5
N=7
ds−eGFP
ds−pif-8

# 4. CONSERVED VIRAL TYROSINE RECOMBINASES PLAY A ROLE IN *MICROPLITIS DEMOLITOR* BRACOVIRUS VIRAL DNA PROCESSING

## 4. 1 Introduction

To propagate infection from cell to cell, typical viruses must amplify their genetic material and package it into newly replicated virions. The way this works depends on factors such as the physical attributes of the viral genome (RNA or DNA, linear or circular, etc) and where it is replicated in the infected cell (nucleus or cytoplasm). Viruses exploit host cell genetic machinery for genome replication, such as relying on a host cell DNA polymerase to replicate their genome. Many viruses also carry genes involved in DNA replication with them on their genomes. Baculoviruses, which are large, double stranded DNA (dsDNA) viruses, encode six essential genes for DNA amplification (*dnapol*, *helicase*, *lef-1*, *lef-2*, *lef-3* and *ie1*) [1]. Baculovirus genomes persist episomally and are amplified in a process that involves rolling circle amplification and recombination [2, 3]. Long strands of dsDNA are formed consisting of many multiples of a single viral genome. This amplified DNA is then processed resulting in circularized viral genomes that are packaged into baculovirus virions [1].

Like baculoviruses, bracoviruses (BVs) package circular dsDNAs into nucleocapsids during virion replication. Unlike baculoviruses, BVs have many different dsDNAs that are individually packaged, called proviral segments. Prior to packaging, viral DNA must be first amplified and processed. BVs also differ from baculoviruses in that

their genomes do not persist episomally but are integrated into the genomes of their wasp hosts [1]. As seen in previous chapters, BVs retain many genes from their baculovirus/nudivirus ancestors, some of which may have conserved functions in various BV processes. Notably absent from the BV genome are genes required for DNA amplification, such as a viral DNA polymerase (*dnapol*), DNA primases (*lef-1* and *lef-2*), and single-stranded binding protein (*lef-3*)[4]. *Microplitis demolitor* bracovirus (MdBV) has a total of 25 different proviral segments that must be amplified before they are individually packaged into virions [4]. Each of these segments is encoded on a specific locus in the *M. demolitor* genome. Some proviral segments are encoded singly on a locus whereas other segments share the same locus [5]**.** The loci encoding proviral segments are amplified from the wasp genome as part of a replication unit (RU) during viral DNA replication. RUs begin and end at discrete junctions and are strung together to form long double stranded DNAs [5]. RUs, and therefore proviral segments encoded on them, are amplified in one of two ways [5]. Some RUs are always amplified head-to-tail, resulting in replication units that are joined in sequence, with the end of one RU joined to the beginning of the next RU. Other RUs are amplified and concatemerized resulting in RU junctions alternating between head-to-head and tail-to-tail [5]. The exact mechanisms for BV DNA amplification is unknown, however the absence of known viral DNA replication genes suggests BV DNA amplification likely happens through wasp-regulated genetic machinery or under the influence of MdBV nudivirus-like genes, of which many remain uncharacterized.

In order to package discrete viral genomes into virions, baculoviruses must process amplified DNA [1]. Implicated in this step in baculoviruses is *vlf-1*, member of a

family of site specific tyrosine recombinases known as λ integrases that are known to mediate integration and excision of bacteriophage genomes with the genomes of bacteria [6, 7]. Integrases form tetramers that bind to DNA Holliday junctions and perform double strand exchange at specific sites in genomes. These proteins are of great interest due to their potential practical application in medicine and biotechnology, where site-specific editing of genomes is critical for the development of technologies in gene therapy and cell engineering [8-10].

Evidence from baculoviruses suggests that a highly conserved catalytic tyrosine in Vlf-1 is involved in processing amplified viral DNA, as well as being a critical nucleocapsid component [11, 12]. This catalytic residue belongs to a highly conserved motif identified in other integrases [6, 7]**.** Sequencing has identified five homologs of *vlf-1* in the BV genome, namely *vlf-1a*, *vlf-1b-1*, *vlf-1b-2*, *int-1*, *int-2* [4]. As mentioned above, BVs amplified proviral DNAs are processed before packaging into virions. After RU amplification, segments are excised from RUs and circularized and packaged into nucleocapsids [5, 13]. Excision of individual segments happens at direct repeat junctions (DRJs), short sequences marking boundaries where segments are first excised and then integrated into host cell genomes upon infection [13]. The presence of integrase homologs suggests that BVs might rely on these genes for processing proviral DNA processing. Previously it was shown that knockdown of MdBV *vlf-1a* and *int-1* resulted in a reduction in copy number of mature, circularized segment B [14]. This observation first implicated MdBV integrase genes in the processing of amplified proviral DNA.

In this chapter I further investigate the role of integrases in processing MdBV proviral segments. Results from only two integrases and only one segment were reported

on previously. I expand on this by testing all MdBV integrases and a greater selection of segments. I hypothesize that the integrase family expanded in BVs because they might have roles in processing segments from different amplified proviral DNA intermediates. In addition, I investigate uncharacterized nudivirus-like genes, *k425_451*, *k425_468*, *k425_475* and *HzNVorf93-like*, which are potentially involved in the amplification of proviral DNA. These viral genes are expressed in wasp ovaries during MdBV virion replication and none of their gene products have been found in virions in a recent proteomics study [4, 14]. These facts suggest that their roles in BV biology are limited to virion replication in wasp ovaries, which makes these genes strong candidates for being involved in DNA amplification relative to other unknown genes.

In this study I looked at how knockdown of each of the selected genes affected the copy number of amplified replication units (pre-processed segments) and processed viral DNA (circularized segments and rejoined empty RUs). To ensure a representative sample of the 25 proviral segments present in the MdBV genome, I selected segments that are amplified as part of different RUs. I selected segment P and segment L, both of which share the same locus (locus 1) along with many other segments (K, Q D, B, A, F, I, M, G, O) and are amplified in head-to-head/tail-to-tail orientation [5]. I also selected segments J and S, both of which are singly encoded on separate loci (locus 3 and 6, respectively) and amplified head-to-tail. Finally, I selected segment R and V, both of which are amplified head-to-head/tail-to-tail, though segment R is singly encoded on locus 5, whereas segment V resides on locus 2 with four other segments (W, E, C, X) [5]. I found that most MdBV integrases are required for successful processing of proviral DNA, but no pattern of specialization was observed when looking at differently amplified segments. In addition,

I characterized two of the nudivirus-like genes (*HzNVorf93-like* and *k425_475*) as also being involved in DNA processing.

## 4.2 Results

### 4.2.1 Sequence analysis

Lambda integrases are a class of enzymes involved in recombination of double stranded DNA. Bracovirus relatives have either 1 (baculoviruses) or 2 (nudiviruses) integrase genes. Large scale sequence analysis of lambda integrases has identified key features and characteristics [15, 16]. Mainly, integrases maintain a key catalytic site with a tyrosine residue. The MdBV genome contains 5 integrase genes, *vlf-1a*, *vlf-1b-1*, *vlf-1b-2*, *int-1*, and *int-2*, which were previously identified during transcriptomic analysis of *M. demolitor* ovaries [4]. Identities of the integrase duplicate gene products from MdBV with corresponding predicted proteins (Int and Vlf-1) from the closest known nudivirus-relative, *Heliothis zea* nudivirus-1 (HzNV-1), were: *vlf-1a* (27%), *vlf-1b-1* (26%), *vlf-1b-2* (22%), *int-1* (30%), and *int-2* (23%). Previous sequence analysis of Vlf-1a, Vlf-1b-2, and Int-1 showed that Vlf-1b-2 lacked the conserved tyrosine [14]. I performed a more detailed analysis of all previously identified MdBV integrases using whole protein sequences (Fig. 4.1). I found that Int-1, Vlf-1a and Vlf-1b-2 retain known integrase domains, including the complete R-X-R-Y motif characteristic to integrase [15]. While Vlf-1b-1 and Int-2 both aligned well to characteristic integrase regions (Box I and Box II), their protein sequences both show either partial or total absence of the R-X-R-Y motif. Vlf-1b-1 shows a substitution of the second arginine (R) residue for a different but still positively charged lysine (K) and an absence of the Y residue due to truncation. The Int-2 peptide sequence

completely lacks the integrase motif. Sequence analysis identified no integrase-like domains in *k425_451*, *k425_468, HzNVorf93-like* or *k425_475.* Phylogenetic analysis and bootstrapping using whole peptide sequences show that MdBV integrase family members follow an expected pattern of divergence based on the relationship between nudiviruses and baculoviruses (Fig. 4.2). Clearly separated into two main branches are Vlf-1 and Int-1, reflecting the duplication of Vlf-1 in nudiviruses. The MdBV integrase protein sequences Vlf-1, Vlf-1b-1, Vlf-1b-2, are nested in the Vlf-1 branch, sister to the betanudivirus protein sequences. Similarly, MdBV Int-1 and Int-2 are sister to the betanudiviruses in the Int-1 branch.

### 4.2.2 MdBV Integrase proteins localize to the MdBV nucleocapsid

Prior proteomic analysis detected all MdBV integrases in MdBV virions, save for Int-2 [14]. In chapter two I report that integrase genes exclusively localized to the capsid fraction, except for Int-2 which I did not detect in any of the fractions.

### 4.2.3 Knockdown efficiency

I first generated primer sets to all genes (Table 4.1). Using dsRNA specific to each integrase I was able to separately knock down their expression. For targeted gene knockdowns I injected wasp larvae with dsRNA after they had emerged from caterpillar hosts and spun their cocoon. After they emerged, I extracted total RNA from one half of the reproductive tract of adult female wasps. Results indicated that dsRNA injection reduced transcript abundance for *vlf-1a* (88%), *vlf-1b-1* (80%), *vlf-1b-2* (80%), *int-1* (56%), and *int-2* (88%) (Fig. 4.3). In addition, I found that injection of gene specific dsRNA did

not have off target effects on other integrases (Fig. 4.4). I was able to significantly knock down transcript abundance of *k425_451*, *k425_475* and *HzNVorf93-like*, but failed to knock down *k425_468* (Fig. 4.5). I picked these genes because they are viral genes expressed during virion replication and their gene products are not found in virions, increasing their chance of being involved in proviral DNA amplification [1, 11].

### 4.2.4 Integrase knockdown affects proviral DNA segment abundance

To further investigate the possibility of MdBV integrases being involved in proviral segment processing I generated primer sets to distinguish between the three types of proviral DNA mentioned earlier, namely the pre-processed segment integrated into the replication unit, the circularized mature segment that is packaged into virions, and the rejoined replication unit from which the circularized segment is excised. I designed primer sets for 5 proviral DNA segments (L, J, S, V, R) that distinguish particular products related to copy number before processing and copy number of products after processing. Segment primers specific to the proviral segment integrated into the replication unit were used to amplify pre-processed proviral DNA (Table 4.2, Table 4.3, Fig. 4.6). Segment primers flanking the point of circularization in the viral segment were used to amplify circularized viral DNA. Segment primers specific for the empty locus were used to quantify excision of viral segments. I was unable to produce primers for segment P rejoined empty locus. In addition, I generated qPCR primers to detect absolute copy number of segments S and R (Segments both still integrated into the replication unit and circularized segments), as well as primers to detect copy number of the nudivirus cluster, which is a region of proviral DNA that is amplified in calyx cells during virion replication but not

packaged into virions. Primer sequences and combinations are listed in Table 4.2 and Table 4.3 respectively, primer relative positions are illustrated in Figure 4.6.

To measure the effects of MdBV integrase knockdown on proviral segment processing, I injected wasp larvae with double stranded RNA corresponding to individual integrases. After emergence, total DNA was extracted from one half of the female reproductive tract and used as a template for qPCR. My results indicate that the individual knockdown of each of the previously identified MdBV integrases results in an accumulation of pre-processed proviral segments and a reduction in the number of mature, circularized segments and rejoined empty loci (Fig. 4.7). Figure 4.7 shows the relative change of mean DNA copy number (pre-processed segments or circularized segments) in the treatment group relative to the control group of each gene knockdown. Figure 4.8 is companion to Figure 4.7 provides supplemental data for rejoined segment DNA type. The data are transformed on a base ten log scale. Statistical significance (ANOVA) of results was calculated by comparing raw scores from the treatment to the control group for each individual knockdown. Almost every integrase knockdown resulted in higher copies of pre-processed DNA and lower copies of mature (circularized) DNA for every segment, indicating that integrase knockdowns interrupted the processing of amplified segments into circularized segments and rejoined RUs. Of all the integrases, the effects caused by *int-2* knockdown consistently were the lowest in magnitude and least significant across DNA types for all segments.

When looking at absolute amplification, my results indicated that some integrase knockdowns have an effect on total abundance of segments R, S, and the nudivirus cluster, though the effects on the treatment groups are far smaller and less statistically

significant relative to their control groups, and relative change is in different directions across all three measured DNAs (Fig. 4.9).

### 4.2.5 Two uncharacterized genes with integrase-like knockdown phenotype

As stated previously, the absence of a viral DNA polymerase in the MdBV genome suggests that the task of amplifying proviral DNA is now done by wasp genes. However, there are several MdBV genes of unknown function that are known only to exist in other BVs or are homologs of nudivirus genes. These genes also share no domain features with other genes in public databases. I thus asked if knockdown of any of these genes (*k425_451*, *k425_468*, *k425_475* and *HzNVorf93-like*) affected viral DNA amplification. Knockdown of k*425_451* showed no effect on abundance of segments S and R, and no change in abundance of nudivirus cluster (Fig. 4.10). In contrast, knockdown of *HzNVorf93-like* and *k425_475* resulted reduced the abundance of processed proviral segments while increasing the abundance of pre-processed DNA (Fig. 4.7). Thus, the phenotypes of these gene knockdowns were very similar to the integrase gene knockdowns, despite neither gene having any integrase-like domains.

## 4.3 Discussion

The fragmented integration of BV proviral genomes in the genomes of microgastroids differs greatly from how nudiviruses and baculoviruses organize their genomes [4, 17]. Their relatively complex genomic organization suggests that BVs rely on different molecular mechanisms for DNA amplification and processing. Roughly half of the MdBV genes with predicted functions in replication and virion formation are

baculovirus/nudivirus homologs, however none of these homologs have known roles in DNA amplification. This study investigated uncharacterized nudivirus-like genes for their potential role in BV DNA amplification as well as predicted tyrosine recombinase family members for their role in DNA processing [4, 14].

In the first part of this study (Chapter 2), I built upon previous proteomic results by separating MdBV virions into envelope and nucleocapsid fractions to: 1) assess whether the baculovirus-like structural core gene products localize to the same fractions as reported for occlusion-derived baculoviruses [18], and 2) localize unknown nudivirus-like BV genes to the capsid or envelope fractions of MdBV virions. My data indicate that gene products of *k425_475* are absent form MdBV virions, however I found *HzNVorf93-like* to localize to the viral nucleocapsid. Moreover, I found gene products of *vlf-1a*, *vlf-1b-1*, *vlf-1b-2*, and *int-1* in MdBV virions. These results are consistent with previous proteomics work done on MdBV [14]. The integrase gene products were found exclusively in the nucleocapsid fraction of MdBV. These data are consistent with functional evidence from MdBV and baculoviruses showing that VLF-1 is a critical structural component of nucleocapsids [11, 14, 18]. Furthermore, presence of integrases in viral nucleocapsids suggests they might have roles in processes that occur in the hosts wasps parasitize. Notably, BV proviral segments have been shown to stably integrate into host cells, though it is unknown if this relies on MdBV tyrosine recombinases [19]. A more thorough sequence analysis and comparison to integrases from other viruses showed us that MdBV integrases have mostly retained low level sequence similarity, most notably including the R-X-R-Y motif. Despite sequences being structurally similar to other integrases, MdBV Vlf-1b-1 and Int-2 both have incomplete motifs and are missing the

catalytic tyrosine residue. Contrary to previous analysis, I found that the peptide sequence from Vlf-1b-2 does indeed have a tyrosine residue that matches typical integrase alignment [14, 15].

Work on *vlf-1* in baculoviruses has shown that gene deletion does not affect viral DNA amplification, however baculovirus genomes are not amplified from the host genome but as episomes [1, 20]**.** Prior to more recent work, studies on BVs suggested that proviral DNA segments are first excised from wasp genomes before amplification [13, 21, 22]. In this scenario, integrases would be a prime candidate for this function. However, as discussed above, more recent work supports the hypothesis that excision of segments only happens after amplification [5]. My data show that there is small to negligible knockdown effect on DNA amplification across three types of proviral DNA amplified, further offering evidence against the possibility that integrase genes might function upstream of DNA amplification.

Evidence in baculoviruses points to the possibility that *vlf-1* acts as a resolvase to cleave circular viral genomes from amplified baculovirus DNA, a process in which the catalytic tyrosine residue is known to play an essential role [11, 12, 23]. Recombinant baculoviruses with a single mutation in the conserved tyrosine recombinase residue produce virus particles that fail to infect cells, but which otherwise have normal phenotype [11, 12]. Furthermore, *vlf-1* has been shown to bind to cruciform DNA that mimics recombination intermediates [23]. Previous work on MdBV suggested that *vlf-1* homologs are involved in processing of proviral segments [14]. My results show that knockdown of each MdBV integrase*,* as well as *HzNVorf93-like* and *k425_475*, affects processing of amplified proviral DNA. Some to a greater degree than others, with *int-2* knockdowns

generally having the least effect on changes in DNA copy number relative to the control. These data are surprising for the reason that vlf-1 is a single copy gene in baculoviruses [1]. To explain the expansion of *vlf-1* into a multi-member gene family in BVs, I hypothesized that they might have distinct roles in processing segments from proviral domains that produce different intermediates. My selection of proviral segments is representative of the population of MdBV segments and includes segments amplified head-to-tail or head-to-head, as well as segments singly encoded or encoded in tandem with others [5]. While my data show slight variability in gene knockdown effects, most notably for int-2 knockdown which produced the smallest disruptive effect, my results do not indicate that specialization has occurred among MdBV integrases. Notably, DNA processing is affected even in the knockdown of integrases that are missing the catalytic tyrosine residue or other motif elements (*vlf-1b-1*, *int-2*). These data are surprising because conserved residues in the integrase family are implicated in proper integrase functioning, including baculovirus *vlf-1* [11, 15, 16]. In this same vein, DNA processing is affected in the knockdown of *HzNVorf93-like* and *k425_475*, two genes that lack any identifiable features associated with recombinases.

Disruption of DNA processing affects all measured segments, despite the fact that amplified proviral DNA segments exist in different concatemeric conformations [5]. These data suggest that the differently amplified MdBV proviral DNA segments appear to be processed through a related mechanism. It seems possible that integrases and novel genes I investigated might not be directly involved in processing of proviral DNA, but rather in some process upstream of that. In baculoviruses, *vlf-1* is known to influence hyperexpression of late genes by binding near gene regulatory regions, and might do so

still in BVs, potentially affecting my results [24, 25]. Another possible interpretation is that integrases form a larger complex to achieve DNA processing in MdBV. Lambda integrases form tetramers that bind to DNA and facilitate double strand exchange [26]. Baculovirus VLF-1 has been shown to bind to cruciform DNA, a structure that likely mimics recombination DNA intermediates [23]. There are currently no data on whether this might be true for BV integrases. Future work should be done to determine if MdBV integrases interact in tetrameric fashion or form some sort of complex.

## 4.4 Methods

### 4.4.1 Insect rearing and staging

*M. demolitor* parasitizes certain species of Lepidoptera in their larval stages, including *Chrysodeixis includens* [27]. Both host and their parasitoids were reared at 27 ± 1°C with a 16 h light: 8 h dark photoperiodic schedule [28]. *M. demolitor* takes 11 days to develop from egg into adult. After parasitism, *M. demolitor* hatches and feeds for 6 days, after which the last larval instar emerges from the host to spin a silk cocoon [27]. Spinning a cocoon takes several hours, after which the wasps spend an additional nine-12 hours as larvae, before starting their pupation [14]. Adult wasps were maintained in constant dark at 18°C. Rearing and staging of *C. includens* for parasitism was done as previously described [29].

### 4.4.2 RNAi knockdowns and quantification of target gene expression

To knock down MdBV integrases, I designed gene-specific primers with added T7 promoter adaptors to generate 300-400 bp templates for double stranded RNA (dsRNA)

synthesis (Table 4.1). Previous work describes designing dsRNA Primers for *e*GFP [14]. I generated PCR products using as a template cDNA from adult wasp ovaries and used the PCR products as templates in the MegaScript RNAi Kit (Ambion). Larval stage wasp cocoons were selected and injected as previously described [14]. In short, individual wasp larvae were injected into the abdomen with 0.5-1 µl of 400-500 ng/µl dsRNA. Control wasps were injected a non-specific dsRNA probe (bacterial eGFP). After emerging as adults, wasp half ovary was extracted for each wasp to check the knockdown efficiency for the target gene. For RNAi phenotype assays, females were allowed to spend 2 h parasitizing 2$^{nd}$ instar *C. inlcudens* larvae each day for 5 days before being extracted. To check the knockdown efficiency of MdBV integrases, ovaries from each wasp used in the assays were extracted and separated. Half ovaries were stored at -80°C before RNA extraction. Total RNA from wasp ovaries was extracted using the Qiagen RNAeasy kit protocol. I synthesized cDNA from total RNA using RNA concentrations to normalize across samples. I used quantitative PCR (qPCR) to measure differences in gene expression across samples and treatment groups. I generated the qPCR primers corresponding to 180-220 bp regions of MdBV integrase genes (Table 4.1). I cloned the PCR product of this primer set into pSC-A-amp/kan, isolated and sequenced the plasmid, and generated an absolute standard curve by determining copy numbers from serially diluted amounts of plasmid ($10^2$ to $10^7$ copies). I used a Rotor-Gene Q with the Rotor-Gene SYBR Green PCR kit in conjunction with the qPCR primers.

### 4.4.3 Proteomic analysis of virions

Proteomic analysis of virions was performed as described in chapter two.

### 4.4.4 qPCR Segment Primer design

I designed qPCR primers to specifically target amplified and processed forms of MdBV proviral segments as described above(Fig. 4.6). Complementary qPCR primer sets were designed around excision junctions in replication units (Table 4.2). I generated standard curves to be able to quantify pre-processed, episomal, and rejoined forms of segment S, R, P, J, L, V.

### 4.4.5 Computer and statistical analysis

In the analysis of qPCR data I averaged the number of copies of gene or DNA product for all technical replicates within a biological sample. For functional assays, I calculated means from experimental values from biological replicates. Each biological replicate represents and individual wasp. I used JMP v14 for statistical analyses. Differences between means of biological replicates were tested using a *t*-test assuming equal variances or ANOVA. I used RAxML for the maximum-likelihood based phylogenetic inference of each MdBV integrase peptide sequence [30].

## 4.5 References


1. Rohrmann, G.F., *Baculovirus Molecular Biology*. 4th ed. 2019, Bethesda (MD): National Center for Biotechnology Information (US).
2. Oppenheimer, D.I. and L.E. Volkman, *Evidence for rolling circle replication of Autographa californica M nucleopolyhedrovirus genomic DNA.* Arch Virol, 1997. **142**(10): p. 2107-13.
3. Okano, K., A.L. Vanarsdall, and G.F. Rohrmann, *A baculovirus alkaline nuclease knockout construct produces fragmented DNA and aberrant capsids.* Virology, 2007. **359**(1): p. 46-54.

4. Burke, G.R. and M.R. Strand, *Deep sequencing identifies viral and wasp genes with potential roles in replication of Microplitis demolitor Bracovirus.* J Virol, 2012. **86**(6): p. 3293-306.

5. Burke, G.R., et al., *Microplitis demolitor Bracovirus Proviral Loci and Clustered Replication Genes Exhibit Distinct DNA Amplification Patterns during Replication.* J Virol, 2015. **89**(18): p. 9511-23.

6. Grindley, N.D., K.L. Whiteson, and P.A. Rice, *Mechanisms of site-specific recombination.* Annu Rev Biochem, 2006. **75**: p. 567-605.

7. Van Duyne, G.D., *A structural view of Cre-loxP site-specific recombination.* Ann Rev of Biophys Biomol Struct, 2001. **30**: p. 87-104.

8. Kohn, D.B. and C.Y. Kuo, *New frontiers in the therapy of primary immunodeficiency: From gene addition to gene editing.* J Allergy Clin Immunol, 2017. **139**(3): p. 726-732.

9. Fogg, P.C.M., et al., *New applications for phage integrases.* J Mol Biol, 2014. **426**(15): p. 2703-2716.

10. Hollis, R.P., et al., *Phage integrases for the construction and manipulation of transgenic mammals.* Reprod Biol Endocrinol, 2003. **1**: p. 79-79.

11. Vanarsdall, A.L., K. Okano, and G.F. Rohrmann, *Characterization of the role of very late expression factor 1 in baculovirus capsid structure and DNA processing.* J Virol, 2006. **80**(4): p. 1724-33.

12. Yang, S. and L.K. Miller, *Expression and mutational analysis of the baculovirus very late factor 1 (vlf-1) gene.* Virology, 1998. **245**(1): p. 99-109.

13. Savary, S., et al., *Excision of the polydnavirus chromosomal integrated EP1 sequence of the parasitoid wasp Cotesia congregata (Braconidae, Microgastinae) at potential recombinase binding sites.* J Gen Virol, 1997. **78 ( Pt 12)**: p. 3125-34.

14. Burke, G.R., et al., *Mutualistic polydnaviruses share essential replication gene functions with pathogenic ancestors.* PLoS Pathog, 2013. **9**(5): p. e1003348.

15. Esposito, D. and J.J. Scocca, *The integrase family of tyrosine recombinases: evolution of a conserved active site domain.* Nucleic Acids Res, 1997. **25**(18): p. 3605-3614.

16. Nunes-Düby, S.E., et al., *Similarities and differences among 105 members of the Int family of site-specific recombinases.* Nucleic Acids Res, 1998. **26**(2): p. 391-406.

17. Wang, Y. and J.A. Jehle, *Nudiviruses and other large, double-stranded circular DNA viruses of invertebrates: new insights on an old topic.* J Invertebr Pathol, 2009. **101**(3): p. 187-93.

18. Hou, D., et al., *Comparative Proteomics Reveal Fundamental Structural and Functional Differences between the Two Progeny Phenotypes of a Baculovirus.* J Virol, 2013. **87**(2): p. 829-839.

19. Beck, M.H., et al., *The encapsidated genome of Microplitis demolitor bracovirus integrates into the host Pseudoplusia includens.* J Virol, 2011. **85**(22): p. 11685-96.

20. Vanarsdall, A.L., K. Okano, and G.F. Rohrmann, *Characterization of a baculovirus with a deletion of vlf-1.* Virology, 2004. **326**(1): p. 191-201.

21. Gruber, A., et al., *Polydnavirus DNA of the braconid wasp Chelonus inanitus is integrated in the wasp's genome and excised only in later pupal and adult stages of the female.* J Gen Virol, 1996. **77**(11): p. 2873-2879.

22. Pasquier-Barre, F., et al., *Polydnavirus replication: the EP1 segment of the parasitoid wasp Cotesia congregata is amplified within a larger precursor molecule.* J Gen Virol, 2002. **83**(Pt 8): p. 2035-2045.

23. Mikhailov, V.S. and G.F. Rohrmann, *Binding of the baculovirus very late expression factor 1 (VLF-1) to different DNA structures.* BMC Mol Bio, 2002. **3**: p. 14-14.

24. McLachlin, J.R. and L.K. Miller, *Identification and characterization of vlf-1, a baculovirus gene involved in very late gene expression.* J Virol, 1994. **68**(12): p. 7746-7756.

25. Yang, S. and L.K. Miller, *Activation of Baculovirus Very Late Promoters by Interaction with Very Late Factor 1.* J Virol, 1999. **73**(4): p. 3404-3409.

26. Van Duyne, G.D., *Lambda Integrase: Armed for Recombination.* Curr Biol, 2005. **15**(17): p. R658-R660.

27. Strand, M.R., J.A. Johnson, and J.D. Culin, *Developmental interactions between the parasitoid Microplitis demolitor (Hymenoptera: Braconidae) and its host Heliothis virescens (Lepidoptera: Noctuidae).* Ann Entomol Soc Am, 1988. **81**(5): p. 822-830.

28. Strand, M.R. and T. Noda, *Alterations in the hemocytes of Pseudoplusia includens after parasitism by Microplitis demolitor.* J Insect Physiol, 1991. **37**(11): p. 839-850.

29. Strand, M.R., *Characterization of Larval Development in Pseudoplusia includens (Lepidoptera: Noctuidae).* Ann Entomol Soc Am, 1990. **83**(3): p. 538-544.

30. Stamatakis, A., *RAxML version 8: a tool for phylogenetic analysis and post-analysis of large phylogenies.* Bioinformatics, 2014. **30**(9): p. 1312-1313.

## 4.6 Figures and Tables

### Table 4.1: PCR and dsRNA primer sets for MdBV Integrases.

| Primer Name | Orientation | Primer Sequence |
|---|---|---|
| *vlf-1a* RNAi | Forward | 5'-TAATACGACTCACTATAGGGTCGATACTAAAATCGCAATCG-3' |
| | Reverse | 5'-TAATACGACTCACTATAGGGTTTTAAGCCCAAAGCCACAG-3' |
| *vlf-1a* qPCR | Forward | 5'-AACATTGAAAACGCACAACG-3' |
| | Reverse | 5'-TTGTCAAAGACGGTTGGATG-3' |
| *vlf-1b-1* RNAi | Forward | 5'-TAATACGACTCACTATAGGGCCCGTGCTACCGTTGATACT-3' |
| | Reverse | 5'-TAATACGACTCACTATAGGGGATCGTAGGTTTTCTTTCGTGTG-3' |
| *vlf-1b-1* qPCR | Forward | 5'-TGACAATGGTGTGAAAATTCG-3' |
| | Reverse | 5'-CGTTATTGCACTTCCACGAG-3' |
| *vlf-1b-2* RNAi | Forward | 5'-TAATACGACTCACTATAGGGTTGACGAATCTACGTACAACTGAA-3' |
| | Reverse | 5'-TAATACGACTCACTATAGGGCGTGAACCGTCAATGTGTTG-3' |
| *vlf-1b-2* qPCR | Forward | 5'-ATCCCTCACGAAAACTGCAA-3' |
| | Reverse | 5'-GTATCGATTTTGCGTCGTGA-3' |
| *int-1* RNAi | Forward | 5'-TAATACGACTCACTATAGGGGATAATGACGAACGCGCTAA-3' |
| | Reverse | 5'-TAATACGACTCACTATAGGGTCTTCCAACACACGATTCCA-3' |
| *int-1* qPCR | Forward | 5'-AAAATATCGACGCACGGGTA-3' |
| | Reverse | 5'-GCGCAGCAGCTAAGTCATTT-3' |
| *int-2* RNAi | Forward | 5'-TAATACGACTCACTATAGGGTGTCACCTTCGGTACAGCAC-3' |
| | Reverse | 5'-TAATACGACTCACTATAGGGCAATGACGTAAGTGACGCTGT-3' |
| *int-2* qPCR | Forward | 5'-TGGGAAGCCCCATATTATCA-3' |
| | Reverse | 5'-TCCGATTGGTGGTATTTTGC-3' |
| *HzNVorf93-like* RNAi | Forward | 5'-TAATACGACTCACTATAGGGAGAATCAGAAGAACGCAAGTTGT-3' |
| | Reverse | 5'-TAATACGACTCACTATAGGGCAAAAGCTTGTTGAATCGGAAT-3' |
| *HzNVorf93-like* qPCR | Forward | 5'-CCTTATCAGATACCTCAAAAACGTG-3' |
| | Reverse | 5'-TTTTCGAAACTGAGGGAACC-3' |
| *k425_475* RNAi | Forward | 5'-TAATACGACTCACTATAGGGTGATGACACGGATCATGGTT-3' |
| | Reverse | 5'-TAATACGACTCACTATAGGGCAAAGTGCTTCGTCGATTACG-3' |
| *k425_475* qPCR | Forward | 5'-TCATCTTGATGAATTCCCACT-3' |
| | Reverse | 5'-TCAAAGTTGCGGTAGATTCG-3' |

**Table 4.2: qPCR Segment Primers.**

| Segment | Primer Name | Primer Sequence |
|---|---|---|
| Segment S | ES2RF | 5'-CATCGAGAAACCAAGAAATCG-3' |
| | ES2RR | 5'-TATGGCTTACGTGGCTGCTT-3' |
| | ES2LR | 5'-TGCCGGCTTAATTACCATTC-3' |
| | ES2LF | 5'-TGCATAAGCATACCGATTTGA-3' |
| | Inside_F | 5'-TTGGTCAATTCTTGCGACTG-3' |
| | Inside_R | 5'-TACGGGTGGCTAAAATGGAG-3' |
| Segment R | ES2LR | 5'-TAAAGAATGGCTTGCTGGTT-3' |
| | ES2LF | 5'-GATTCAAAGACGACTTCAAAACTT-3' |
| | ES2LRstar | 5'-GAACGAAAAACGTACCATGC-3' |
| | ES2RF | 5'-TAAAGAATGGCTTGCTGGTT-3' |
| | ES2RR | 5'-TTCGCTATGTAGACCACGCTTA-3' |
| | Inside_F | 5'-CACACCCACACATTCGGATA-3' |
| | Inside_R | 5'-CCGTGCATTTTCTGTTCTGA-3' |
| Segment J | ES2LF | 5'-AGCCAAGACCAAGAAATTTGA-3' |
| | ES2LRa | 5'-TCGAACATATGGGATACGACA-3' |
| | ES2RF | 5'-AAGTTTGGTTGTGTATCTGGTGT-3' |
| | ES2RR | 5'-GGAAATCCCTAGATCGATTGAA-3' |
| | ES2LRb | 5'-GACATAATTCCCGGTGTGCT-3' |
| Segment P | ES2LF | 5'-ATCGTGAATCGCCACCTTTA-3' |
| | ES2LR | 5'-CGCCTAAACAAATCATAAACAA-3' |
| | ES2RF | 5'-CGCACTAGGTATGATTGTCAGC-3' |
| Segment L | ES2LF | 5'-TTCAATTTCAGCTCCCGAGT-3' |
| | ES2LR | 5'-TCTGGTCTAGGAGTCTCAGATCATT-3' |
| | ES2RF | 5'-TTTTTAGTGGATGACGCCATAA-3' |
| | ES2RR | 5'-CAATATTGCTTAGGGACTCCAA-3' |
| | Circ_R | 5'-TCTCTGGTCTAGGAGTCTCAGA-3' |
| | Circ_F | 5'-TGCATCTGGAAACTTAGTTCAGT-3' |
| Segment V | ES2LF | 5'-CCATCATCGAGAATTTGAACG-3' |
| | ES2LR | 5'-TGAATTTGAATAATGACCTAATTGTGA-3' |
| | ES2RF | 5'-TGTTTATTTGTTTACCCAGCTTCA-3' |
| | ES2RR | 5'-TTCATAATTTTTATAGAATCACGTCTG-3' |
| NV Cluster | VP39 F | 5'-CGCTACACGCTATCGATTTG-3' |
| | VP39 R | 5'-CACTGACTGTGCACAAAATTCA-3' |

**Table 4.3: Segment Primer combinations and amplified products.**

| Segment | DNA Type Amplified | Primer Combination |
|---|---|---|
| Segment S | Pre-Processed | ES2RF - ES2RR |
| | Ciruclarized/Episomal | ES2LR - ES2RF |
| | Rejoined | ES2LF - ES2RR |
| | Pre-processed and circularized | Inside_F - Inside_R |
| Segment R | Pre-Processed | ES2LR - ES2LF |
| | Ciruclarized/Episomal | ES2LRStar - ES2RF |
| | Rejoined | ES2LF - ES2RR |
| | Pre-processed and circularized | Inside_F - Inside_R |
| Segment J | Pre-Processed | ES2LF - ES2LRa |
| | Ciruclarized/Episomal | ES2LRb - ES2RF |
| | Rejoined | ES2LF -ES2RR |
| Segment P | Pre-Processed | ES2LF - ES2LR |
| | Ciruclarized/Episomal | ES2LR  ES2RF |
| Segment L | Pre-Processed | ES2LF - ES2LR |
| | Ciruclarized/Episomal | Circ_F - Circ_R |
| | Rejoined | ES2LF - ES2RR |
| Segment V | Pre-Processed | ES2LF - ES2LR |
| | Ciruclarized/Episomal | ES2LR - ES2RF |
| | Rejoined | ES2LF - ES2RR |
| NV Cluster | NV Cluster | VP39 F - VP39 R |

**Figure 4.1: Alignment of MdBV integrases show conserved domains and residues.** Alignment of MdBV Vlf-1a, Vlf-1b-1, Vlf-1b-2, Int-1, and Int-2 to integrases from select nudiviruses and baculoviruses. Alignment shows two conserved domains (Box I and Box II) that are indicative of Int family recombinases. Arrows indicate highly conserved Int family signature residues, R-X-R-Y. Conserved residues are highlighted with background colors. MdBV pif sequence files are available at AgDataCommons (http://dx.doi.org/10.15482/USDA.ADC/1432667). Accession numbers; Vlf-1a, MDEMTmpGB000094-RA; Vlf-1b-1, MDEMTmpGB000109-RA; Vlf-1b-2, MDEMTmpGB000162-RA; Int-1, MDEMTmpGB000071-RA; Int-2, MDEMTmpGB000021-RA. Other viral peptide sequences are available through the NCBI RefSeq via accession numbers in parentheses. Red sequence name corresponds to MdBV, grey corresponds to β nudiviruses, green to α nudiviruses, and blue to baculoviruses.

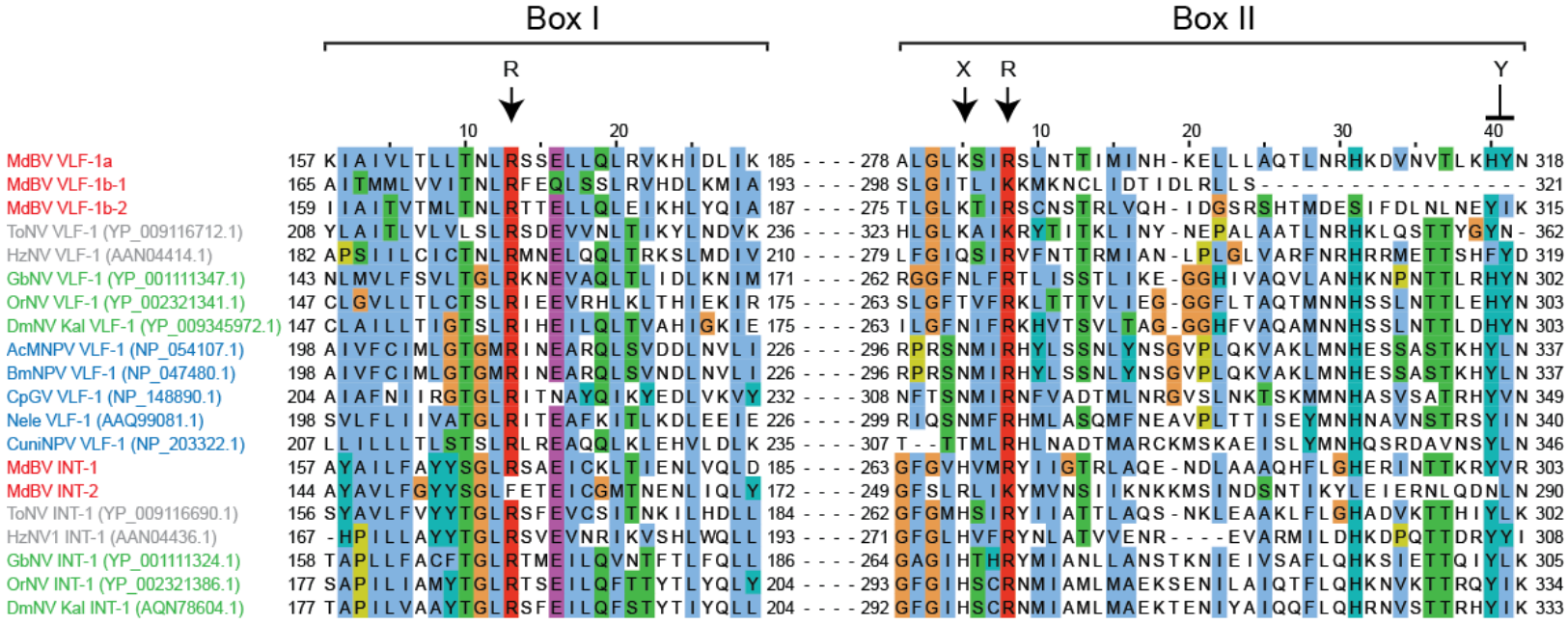
Box I
Box II
R
X
R
Y
10
20
10
20
30
40
MdBV VLF-1a 157 KIAIVLTLLTNLRSSELLQLRVKHIDLIK 185 ---- 278 ALGLKSIRSLNTTIMINH-KELLLAQTLNRHKDVNVTLKHYN 318
MdBV VLF-1b-1 165 AITMMLVVITNLRFEQLSSLRVHDLKMIA 193 ---- 298 SLGITLIKKMKNCLIDTIDLRLLS------------------ 321
MdBV VLF-1b-2 159 IIAITVTMLTNLRTTELLQLEIKHLYQIA 187 ---- 275 TLGLKTIRSCNSTRLVQH-IDGSRSHTMDESIFDLNLNEYIK 315
ToNV VLF-1 (YP_009116712.1) 208 YLAITLVLVLSLRSDEVVNLTIKYLNDVK 236 ---- 323 HLGLKAIKRYTITKLINY-NEPALAATLNRHKLQSTTYGYN- 362
HzNV VLF-1 (AAN04414.1) 182 APSIILCICTNLRMNELQQLTRKSLMDIV 210 ---- 279 LFGIQSIRVFNTTRMIAN-LPLGLVARFNRHRRMETTSHFYD 319
GbNV VLF-1 (YP_001111347.1) 143 NLMVLFSVLTGLRKNEVAQLTLIDLKNIM 171 ---- 262 RGGFNLFRTLISSTLIKE-GGHIVAQVLANHKNPNTTLRHYN 302
OrNV VLF-1 (YP_002321341.1) 147 CLGVLLTLCTSLRIEEVRHLKLTHIEKIR 175 ---- 263 SLGFTVFRKLTTTVLIEG-GGFLTAQTMNNHSSLNTTLEHYN 303
DmNV Kal VLF-1 (YP_009345972.1) 147 CLAILLTIGTSLRIHEILQLTVAHIGKIE 175 ---- 263 ILGFNIFRKHVTSVLTAG-GGHFVAQAMNNHSSLNTTLDHYN 303
AcMNPV VLF-1 (NP_054107.1) 198 AIVFCIMLGTGMRINEARQLSVDDLNVLI 226 ---- 296 RPRSNMIRHYLSSNLYNSGVPLQKVAKLMNHESSASTKHYLN 337
BmNPV VLF-1 (NP_047480.1) 198 AIVFCIMLGTGMRINEARQLSVNDLNVLI 226 ---- 296 RPRSNMIRHYLSSNLYNSGVPLQKVAKLMNHESSASTKHYLN 337
CpGV VLF-1 (NP_148890.1) 204 AIAFNIIRGTGLRITNAYQIKYEDLVKVY 232 ---- 308 NFTSNMIRNFVADTMLNRGVSLNKTSKMMNHASVSATRHYVN 349
Nele VLF-1 (AAQ99081.1) 198 SVLFLIIVATGLRITEAFKITLKDLEEIE 226 ---- 299 RIQSNMFRHMLASQMFNEAVPLTTISEYMNHNAVNSTRSYIN 340
CuniNPV VLF-1 (NP_203322.1) 207 LLILLLTLSTSLRLREAQQLKLEHVLDLK 235 ---- 307 T--TTMLRHLNADTMARCKMSKAEISLYMNHQSRDAVNSYLN 346
MdBV INT-1 157 AYAILFAYYSGLRSAEICKLTIENLVQLD 185 ---- 263 GFGVHVMRYIIGTRLAQE-NDLAAAQHFLGHERINTTKRYVR 303
MdBV INT-2 144 AYAVLFGYYSGLFETEICGMTNENLIQLY 172 ---- 249 GFSLRLIKYMVNSIIKNKKMSINDSNTIKYLEIERNLQDNLN 290
ToNV INT-1 (YP_009116690.1) 156 SYAVLFVYYTGLRSFEVCSITNKILHDLL 184 ---- 262 GFGMHSIRYIIATTLAQS-NKLEAAKLFLGHADVKTTHIYLK 302
HzNV1 INT-1 (AAN04436.1) 167 -HPILLAYYTGLRSVEVNRIKVSHLWQLL 193 ---- 271 GFGLHVFRYNLATVVENR----EVARMILDHKDPQTTDRYYI 308
GbNV INT-1 (YP_001111324.1) 158 TAPLLFACFTGLRTMEILQVNTFTLFQLL 186 ---- 264 GAGIHTHRYMIANLLANSTKNIEIVSAFLQHKSIETTQIYLK 305
OrNV INT-1 (YP_002321386.1) 177 SAPILIAMYTGLRTSEILQFTTYTLYQLY 204 ---- 293 GFGIHSCRNMIAMLMAEKSENILAIQTFLQHKNVKTTRQYIK 334
DmNV Kal INT-1 (AQN78604.1) 177 TAPILVAAYTGLRSFEILQFSTYTIYQLL 204 ---- 292 GFGIHSCRNMIAMLMAEKTENIYAIQQFLQHRNVSTTRHYIK 333

**Figure 4.2: Phylogenetic relationship of MdBV integrases with homologs from free-living virus relatives.** The maximum-likelihood (ML) phylogram was generated with RAxML using ML inference analysis of available integrase protein sequences from baculoviruses and nudiviruses (Table 4.2)(Stamatakis, RAxML). Numbers on nodes indicate ML bootstrap support (100 replicates). Red sequence name corresponds to MdBV, grey corresponds to β nudiviruses, green to α nudiviruses, and blue to baculoviruses. Inset tree shows cladogram of current phylogenetic constructions of viruses related to Bracoviruses [See chapter 2 references [2, 34, 35].

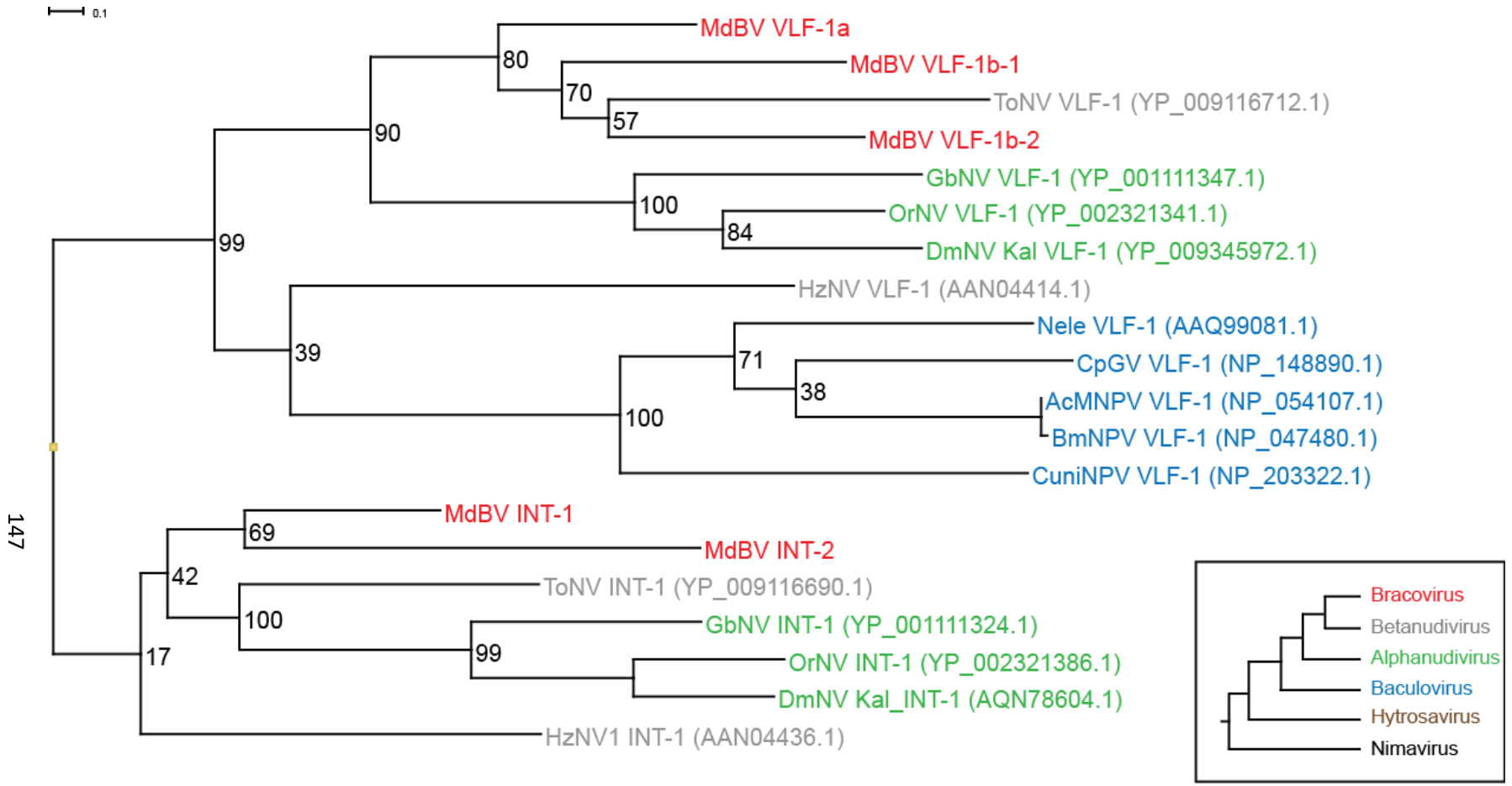
0.1
MdBV VLF-1a
MdBV VLF-1b-1
ToNV VLF-1 (YP_009116712.1)
MdBV VLF-1b-2
GbNV VLF-1 (YP_001111347.1)
OrNV VLF-1 (YP_002321341.1)
DmNV Kal VLF-1 (YP_009345972.1)
HzNV VLF-1 (AAN04414.1)
Nele VLF-1 (AAQ99081.1)
CpGV VLF-1 (NP_148890.1)
AcMNPV VLF-1 (NP_054107.1)
BmNPV VLF-1 (NP_047480.1)
CuniNPV VLF-1 (NP_203322.1)
MdBV INT-1
MdBV INT-2
ToNV INT-1 (YP_009116690.1)
GbNV INT-1 (YP_001111324.1)
OrNV INT-1 (YP_002321386.1)
DmNV Kal_INT-1 (AQN78604.1)
HzNV1 INT-1 (AAN04436.1)
80
70
57
90
100
84
99
39
71
38
100
69
42
100
99
17
Bracovirus
Betanudivirus
Alphanudivirus
Baculovirus
Hytrosavirus
Nimavirus

**Figure 4.3: Knockdown of *vlf-1a*, *vlf-1b-1*, *vlf-1b-2*, *int-1*, *int-2*, *HzNVorf93-like*, and *k425_475* in MdBV using RNAi.** *M. demolitor* larvae were injected with double stranded RNA (dsRNA) specific to (A) *vlf-1a*, (B) *vlf-1b-1*, (C) *vlf-1b-2*, (D) *int-1* or (E) *int-2*. Control larvae were injected with ds-eGFP. Wasps were allowed to emerge, after which ovaries were dissected and total RNA was isolated from one half ovary. I used qPCR to measure transcript copy number. Error bars represent one standard error from the mean. The number of individuals examined for each treatment is indicated by the N value at the bottom of each bar. Statistical significance is indicated by asterisks: *,p≤0.05; **, p≤0.01; ***, p≥0.001; ****, p≥0.0001; N. S., not significant.

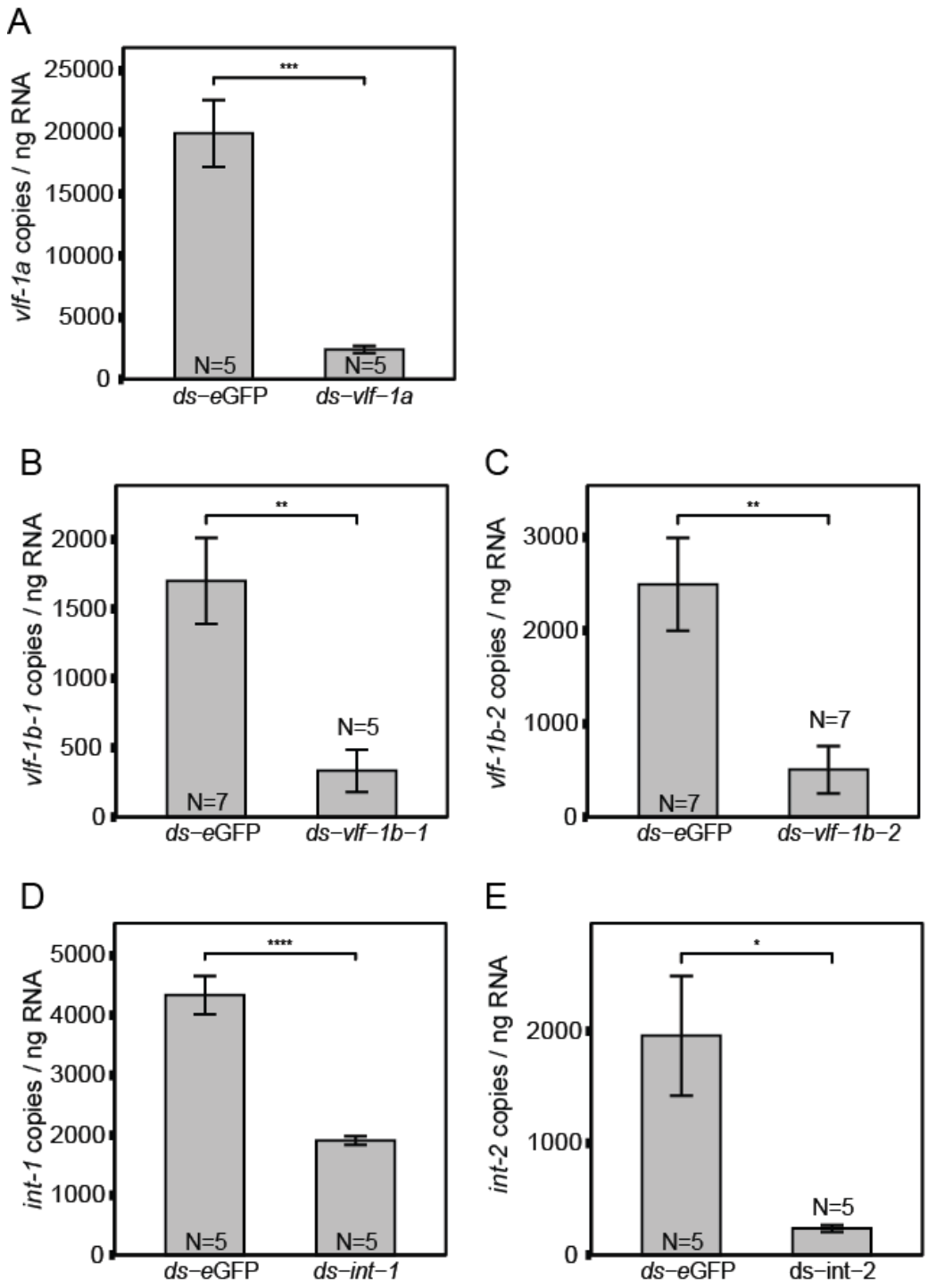
A
vlf-1a copies / ng RNA
25000
20000
15000
10000
5000
0
***
N=5
N=5
ds−eGFP
ds−vlf−1a
B
vlf-1b-1 copies / ng RNA
2000
1500
1000
500
0
**
N=7
N=5
ds−eGFP
ds−vlf−1b−1
C
vlf-1b-2 copies / ng RNA
3000
2000
1000
0
**
N=7
N=7
ds−eGFP
ds−vlf−1b−2
D
int-1 copies / ng RNA
5000
4000
3000
2000
1000
0
****
N=5
N=5
ds−eGFP
ds−int−1
E
int-2 copies / ng RNA
2000
1000
0
*
N=5
N=5
ds−eGFP
ds−int−2

**Figure 4.4: Knockdown of MdBV integrases shows no off-target effects.** *M. demolitor* larvae were injected with double stranded RNA (dsRNA) specific to *vlf-1b-2*, *int-1*, or *int-2*. Knockdown of individual integrases has no off-target knockdown effect. Control larvae were injected with *ds-e*GFP. Wasps were allowed to emerge, after which ovaries were dissected and total RNA was isolated from one half ovary. I used qPCR to measure transcript copy number. Error bars represent one standard error from the mean. The number of individuals examined for each treatment is indicated by the N value at the bottom of each bar. Statistical significance is indicated by asterisks: *,p≤0.05; **, p≤0.01; ***, p≥0.001; ****, p≥0.0001; N. S., not significant.

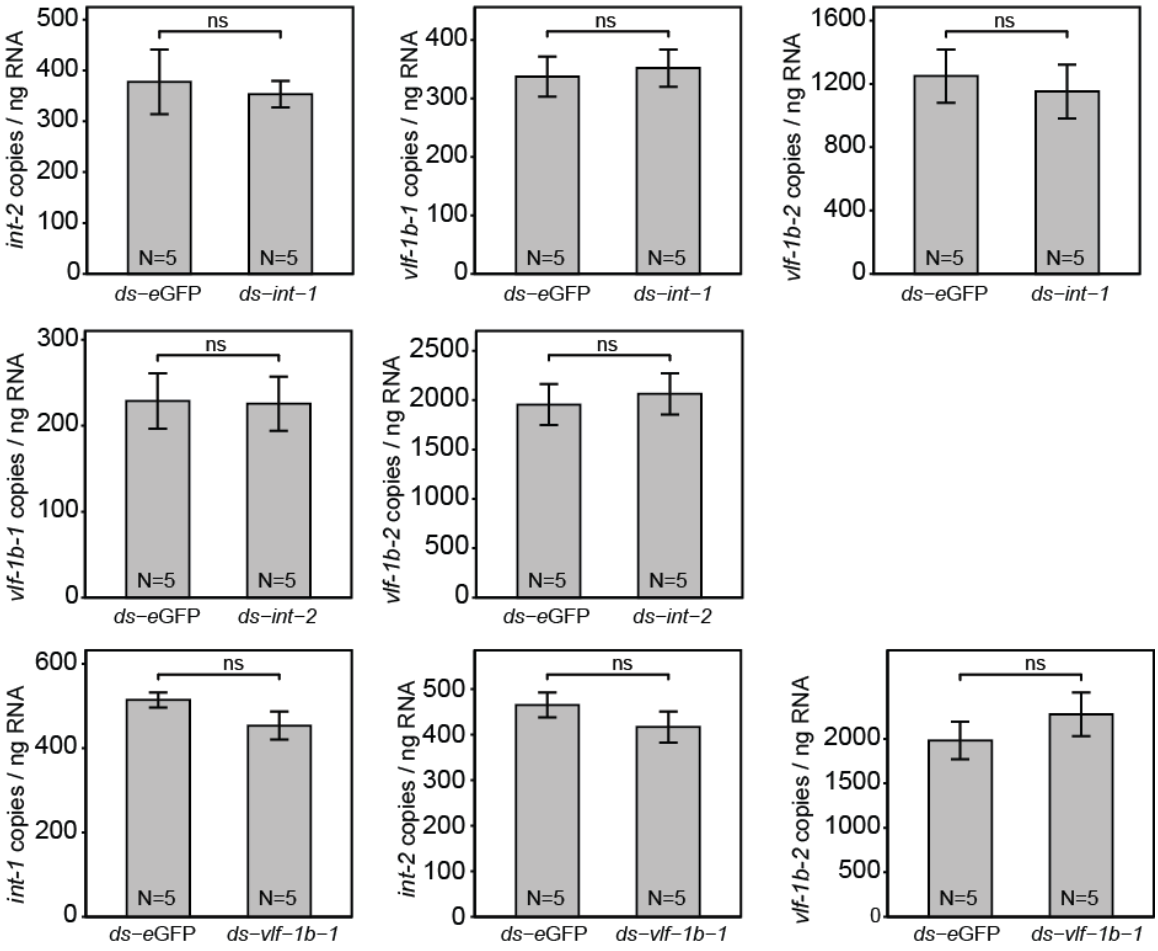
int-2 copies / ng RNA
vlf-1b-1 copies / ng RNA
vlf-1b-2 copies / ng RNA
vlf-1b-1 copies / ng RNA
vlf-1b-2 copies / ng RNA
int-1 copies / ng RNA
int-2 copies / ng RNA
vlf-1b-2 copies / ng RNA
ns
N=5
ds–eGFP
ds–int–1
ds–int–2
ds–vlf–1b–1

**Figure 4.5: Treatment of wasps using dsRNA of *HzNVorf93-like*, *k425_451*, *k425_468*, *k425_475*.** *M. demolitor* larvae were injected with double stranded RNA (dsRNA) specific to (A) *HzNVorf93-like*, (B) *k425_451*, (C) *k425_468*, (D) *k425_475*. Control larvae were injected with *ds-e*GFP. Wasps were allowed to emerge, after which ovaries were dissected and total RNA was isolated from one half ovary. I used qPCR to measure transcript copy number. Error bars represent one standard error from the mean. The number of individuals examined for each treatment is indicated by the N value at the bottom of each bar. Statistical significance is indicated by asterisks: *, p≤0.05; **, p≤0.01; ***, p≥0.001; ****, p≥0.0001; N. S., not significant.

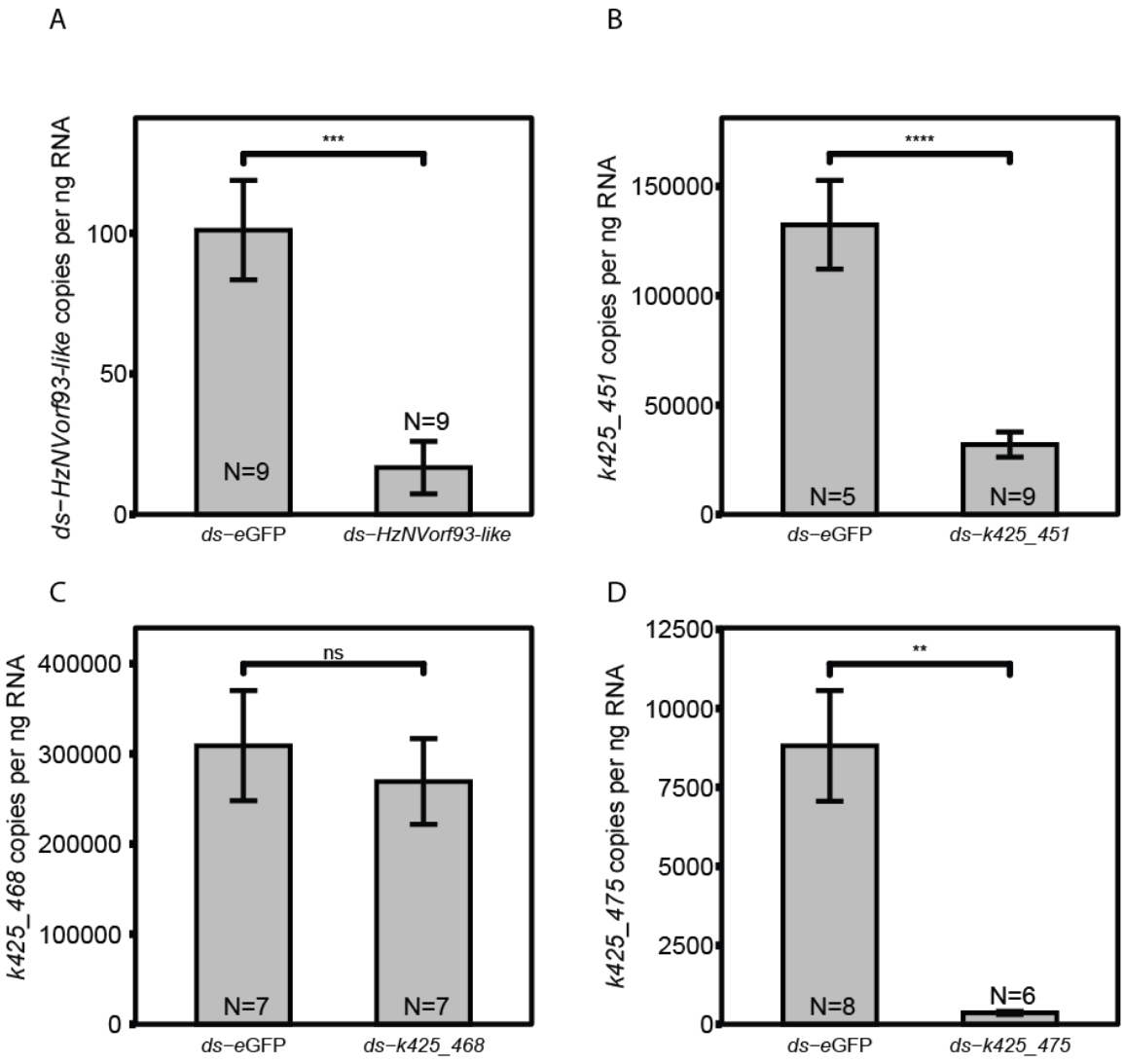
A
B
C
D
ds-HzNVorf93-like copies per ng RNA
k425_451 copies per ng RNA
k425_468 copies per ng RNA
k425_475 copies per ng RNA
***
****
ns
**
N=9
N=9
N=5
N=9
N=7
N=7
N=8
N=6
ds-eGFP
ds-HzNVorf93-like
ds-k425_451
ds-k425_468
ds-k425_475

**Figure 4.6: Six panels show segment primers and their relative positions.** Each proviral segment is part of replication unit after initial amplification (Pre-Processed). Replication units indicated at the top of each panel, shown with proviral segment still integrated. The proviral segment is excised from the replication unit resulting in a mature, circularized segment (Episomal). Circularized segments shown bottom left in each panel as grey circle. The flanking regions of DNA are rejoined during processing (Rejoined). Rejoined segments shown bottom right in each panel. Primers locations and orientations (5’ to 3’) are indicated with arrowheads.

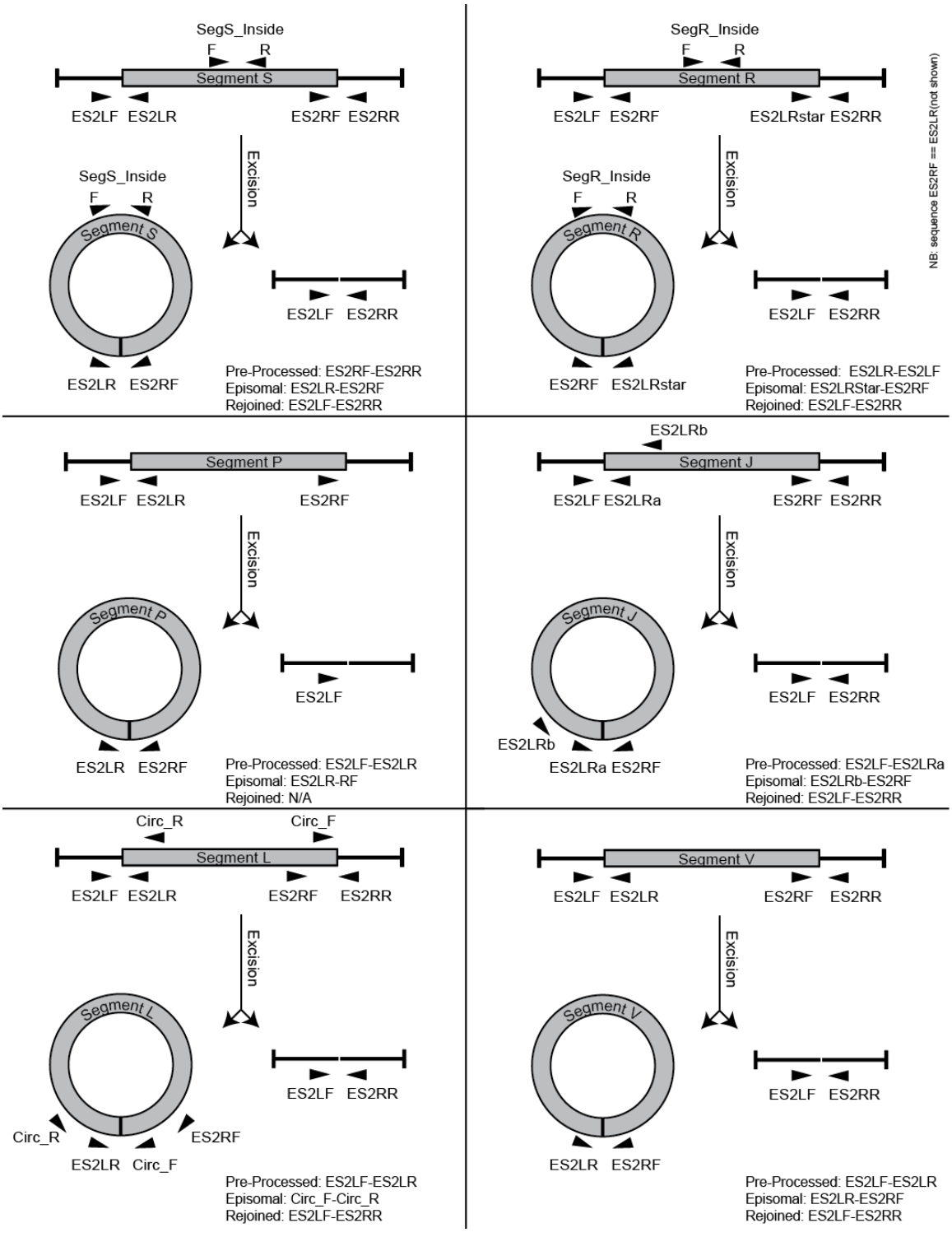
SegS_Inside
F
R
Segment S
ES2LF ES2LR
ES2RF ES2RR
Excision
SegS_Inside
F
R
Segment S
ES2LF ES2RR
ES2LR ES2RF
Pre-Processed: ES2RF-ES2RR
Episomal: ES2LR-ES2RF
Rejoined: ES2LF-ES2RR
SegR_Inside
F
R
Segment R
ES2LF ES2RF
ES2LRstar ES2RR
Excision
SegR_Inside
F
R
Segment R
ES2LF ES2RR
ES2RF ES2LRstar
Pre-Processed: ES2LR-ES2LF
Episomal: ES2LRStar-ES2RF
Rejoined: ES2LF-ES2RR
NB: sequence ES2RF == ES2LR(not shown)
Segment P
ES2LF ES2LR
ES2RF
Excision
Segment P
ES2LF
ES2LR ES2RF
Pre-Processed: ES2LF-ES2LR
Episomal: ES2LR-RF
Rejoined: N/A
ES2LRb
Segment J
ES2LF ES2LRa
ES2RF ES2RR
Excision
Segment J
ES2LF ES2RR
ES2LRb
ES2LRa ES2RF
Pre-Processed: ES2LF-ES2LRa
Episomal: ES2LRb-ES2RF
Rejoined: ES2LF-ES2RR
Circ_R
Circ_F
Segment L
ES2LF ES2LR
ES2RF ES2RR
Excision
Segment L
ES2LF ES2RR
Circ_R
ES2RF
ES2LR Circ_F
Pre-Processed: ES2LF-ES2LR
Episomal: Circ_F-Circ_R
Rejoined: ES2LF-ES2RR
Segment V
ES2LF ES2LR
ES2RF ES2RR
Excision
Segment V
ES2LF ES2RR
ES2LR ES2RF
Pre-Processed: ES2LF-ES2LR
Episomal: ES2LR-ES2RF
Rejoined: ES2LF-ES2RR

**Figure 4.7: Graphs showing copy number of Pre-Processed, Episomal, and Rejoined DNA types for various segments.** Data for each segment shows an increase in amplified Pre-Processed DNA and a decrease in both Episomal DNA. (A) Segment P, (B) Segment L, (C) Segment V, (D) Segment R, (E) Segment J, and (F) Segment S. The y axis indicates base 10 log of the fold change of treatment group relative to the control group. Both treatment and control group consist of 5-10 individual wasps. Error bars indicate standard error, asterisks indicate statistical significance of data.

# Head to Head/Tail to Tail Amplficiation

## Locus 5

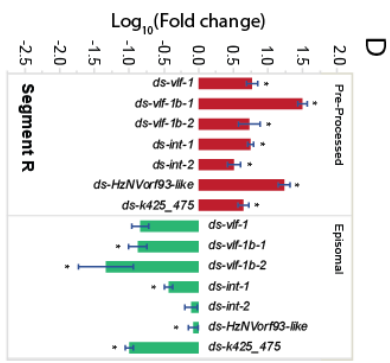


## Locus 2

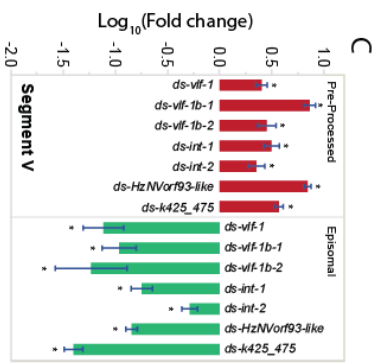


## Locus 1

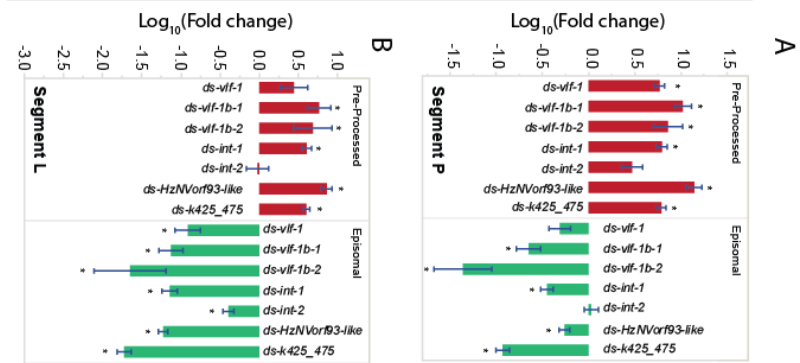


# Head to Tail Amplficiation

## Locus 6

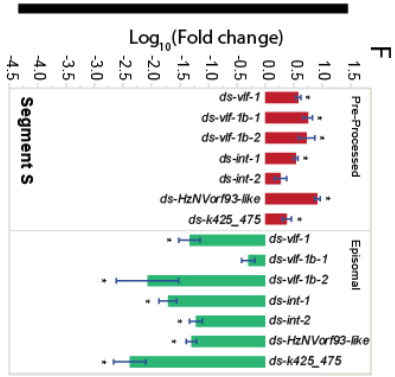


## Locus 3

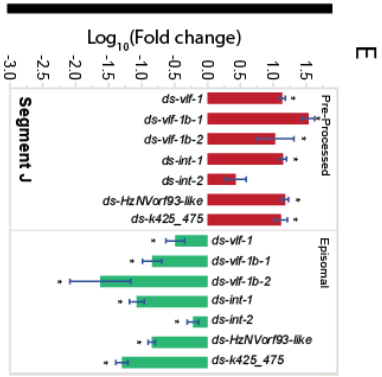

**Figure 4.8: Graphs showing copy number of Rejoined DNA types for various segments.** These data supplement Figure 4.7 and show rejoined segment types. (A) Segment L, (B) Segment V, (C) Segment R, (D) Segment J, and (E) Segment S. The y axis indicates base 10 log of the fold change of treatment group relative to the control group. Both treatment and control group consist of 5-10 individual wasps. Error bars indicate standard error, asterisks indicate statistical significance of data. Statistical significance (ANOVA) of results was calculated by comparing raw scores from the treatment to the control group for each individual knockdown.

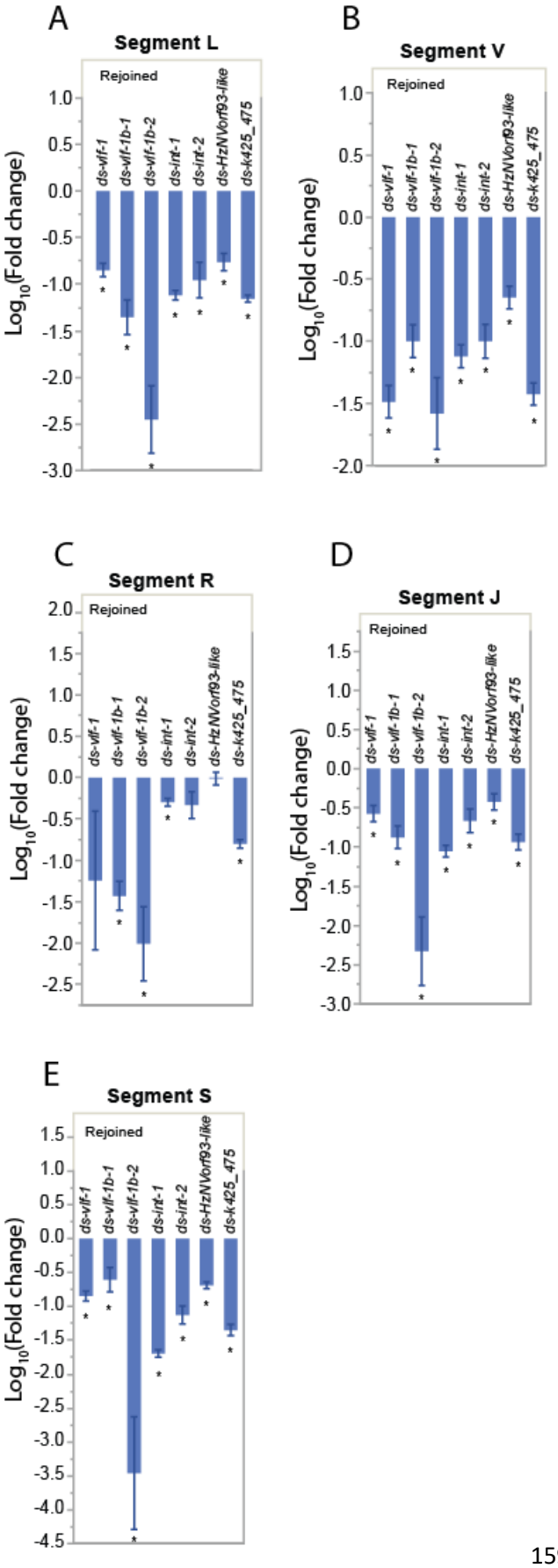
A
Segment L
Rejoined
ds-vlf-1
ds-vlf-1b-1
ds-vlf-1b-2
ds-int-1
ds-int-2
ds-HzNVorf93-like
ds-k425_475
Log10(Fold change)
B
Segment V
C
Segment R
D
Segment J
E
Segment S

**Figure 4.9: Graphs showing DNA amplification for segment R, S, and the nudivirus cluster.** The y axis indicates base 10 log of the fold change of treatment group relative to the control group. Both treatment and control group consist of 5-10 individual wasps. Error bars indicate standard error, asterisks indicate statistical significance of data. Statistical significance (ANOVA) of results was calculated by comparing raw scores from the treatment to the control group for each individual knockdown.

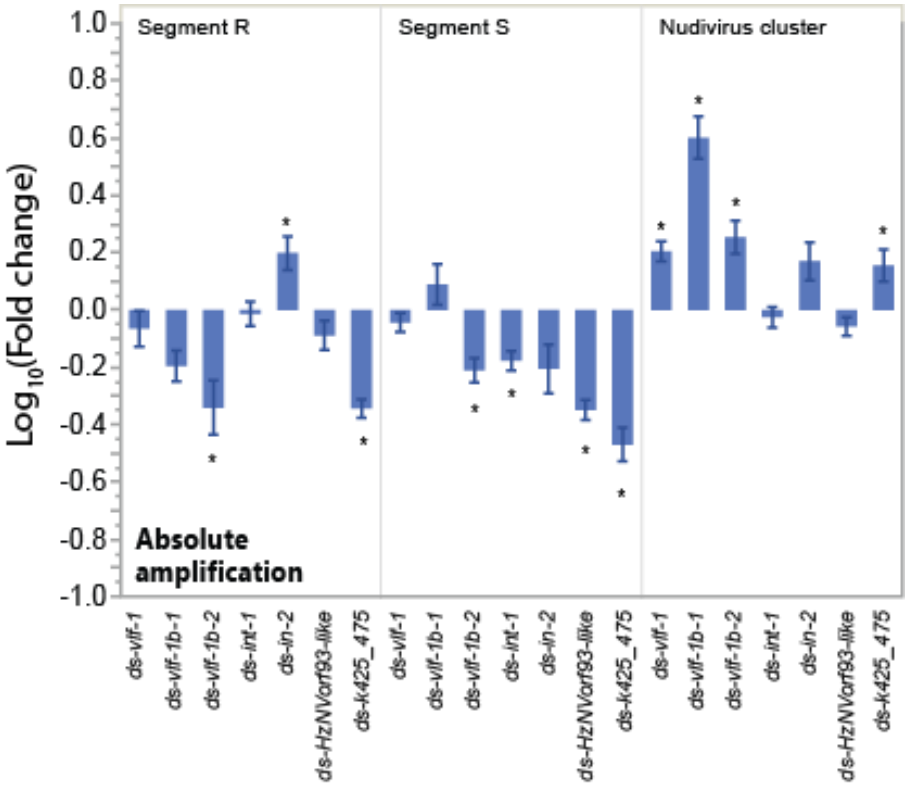
Segment R
Segment S
Nudivirus cluster
Absolute amplification
Log10(Fold change)
1.0
0.8
0.6
0.4
0.2
0.0
-0.2
-0.4
-0.6
-0.8
-1.0
ds-vlf-1
ds-vlf-1b-1
ds-vlf-1b-2
ds-int-1
ds-in-2
ds-HzNVorf93-like
ds-k425_475
ds-vlf-1
ds-vlf-1b-1
ds-vlf-1b-2
ds-int-1
ds-in-2
ds-HzNVorf93-like
ds-k425_475
ds-vlf-1
ds-vlf-1b-1
ds-vlf-1b-2
ds-int-1
ds-in-2
ds-HzNVorf93-like
ds-k425_475

**Figure 4.10: Knockdown of *k425_451* has no effect on proviral DNA Pre-Processed segment abundance or DNA amplification.** (A) shows segment R Pre-Processed DNA copies, (B) shows segment S Pre-Processed DNA copies, (C) shows nudivirus cluster DNA copies. Nudivirus cluster amplification is measured using primers to *vp39*, a gene found in that cluster of genes whose genomic region is amplified. Error bars represent one standard error from the mean. The number of individuals examined for each treatment is indicated by the N value at the bottom of each bar. Statistical significance is indicated by asterisks: *,p≤0.05; **, p≤0.01; ***, p≥0.001; ****, p≥0.0001; N. S., not significant.

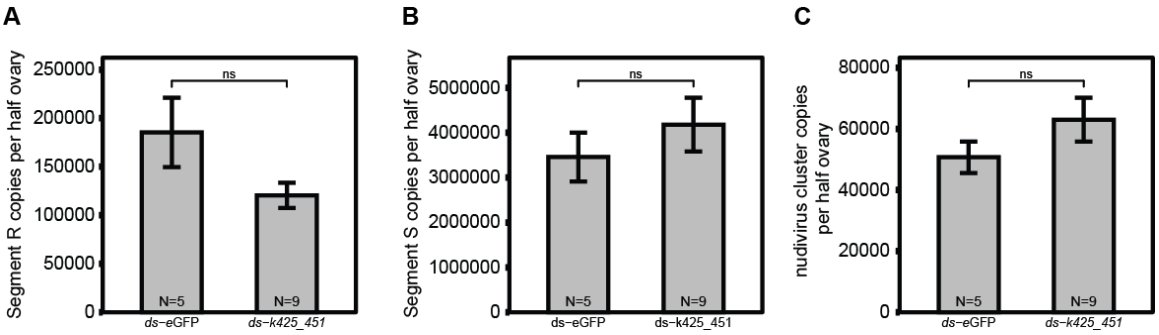
A
Segment R copies per half ovary
250000
200000
150000
100000
50000
0
ns
N=5
N=9
ds-eGFP
ds-k425_451
B
Segment S copies per half ovary
5000000
4000000
3000000
2000000
1000000
0
ns
N=5
N=9
ds-eGFP
ds-k425_451
C
nudivirus cluster copies per half ovary
80000
60000
40000
20000
0
ns
N=5
N=9
ds-eGFP
ds-k425_451

# 5. GENERAL DISCUSSION AND CONCLUSIONS

## 5.1 Research objectives and subsequent findings

In this dissertation I report the findings of my investigation into the molecular biology of *Microplitis demolitor* bracovirus (MdBV). As mentioned in the introduction, the aims of this study were to: 1) characterize unknown nudivirus-like BV genes 2) characterize the function of genes with hypothesized roles in MdBV infection; 3) investigate candidate genes with functions in viral DNA amplification and processing. This chapter summarizes the conclusions from the work described in the previous chapters and places it in the context of the current literature, as well as offering recommendations for future work.

Previous work has shown that BVs have retained many members of a conserved baculovirus core gene set [1, 2]. Many of these genes are actively transcribed during virion replication and some have previously been shown to be required for normal morphogenesis [1, 3]. Previous proteomic analysis found many baculovirus-like and nudivirus-like gene products in BV virions [3, 4]. In chapter 2 I described the results of my proteomics analysis of MdBV virion envelopes and nucleocapsids. I found that most MdBV baculovirus-like core gene products assign to the same fractions that homologs were assigned to for occlusion-derived baculovirus virions [5]. These data support previous work showing that baculovirus core gene homologs have retained conserved functions in BVs and in addition suggest that BV genes with no known homologs can be correctly assigned envelope or capsid components based on these data [3]

Nudiviruses have not been functionally studied to the degree that baculoviruses have. Many of the nudivirus-like genes found in BV genomes therefore have no known or hypothesized function. I selected *HzNVorf64-like* (*MdBVe46*), a nudivirus-like gene highly expressed during virion replication, whose gene products were found primarily in the envelope fraction of MdBV virions [1]. So far homologs of *MdBVe46* have only been found in the few betanudiviruses that have been sequenced [6, 7]. In my investigations I found *MdBVe46* to be critical for viral envelope formation and the enveloping of MdBV nucleocapsids, drastically reducing the amount of mature virions in calyx fluid. Furthermore, knockdown of *MdBVe46* greatly reduced wasp offspring survival in natural parasitism, supporting a key role for MdBV in successful parasitism of *C. includens*. However, the fact that most *C. includens* hosts parasitized by *MdBVe46* knockdown wasps failed to pupate suggests that other factors besides MdBV cause developmental alterations [8]. Lastly, my findings agree with earlier work showing MdBV encodes virulence genes with immunosuppressive functions which prevent host immune systems from killing wasp offspring [9].

The different stages in baculovirus infection of host cells and accompanying molecular mechanics have been well documented [10]. The role of PIFs in oral infection stage in baculoviruses has also been well studied, including their interactions as a cell entry complex embedded in the viral envelope [11, 12]. The presence of PIFs in BV genomes suggests that BVs require them for successful infection of host cells [1, 4]. However, BV infection differs greatly from the oral infection stage in baculoviruses where PIFs are required to mediate cell entry. Recent evidence showed that some MdBV PIFs are involved in viral gene expression of infected cells [3]. Based on proteomics work in

chapter 2, MdBV PIFs are primarily envelope proteins, mirroring their homologs in baculoviruses. Sequence analysis showed that MdBV PIFs have retained features critical for proper functioning in their baculovirus homologs, including transmembrane domains required for shuttling proteins to inner nuclear membranes during virion formation [13, 14]. Building on previous work, results from the PIF knockdown assays (*pif-2*, *pif-5-1*, *pif-5-2*, *pif-5-3*, *pif-8*) show that they are not critical for MdBV infection of host cells, though might still relate to BV infection by indirect means, such as translocating viral DNA to host cell nuclei. Combined with data from electron microscopy images, DNase treatment assays indicated that PIFs are unlikely to play a structural role in MdBV nucleocapsids. However, my evidence suggests that *pif-5-2*, *pif-5-3* and *pif-8* could be involved in virion morphogenesis.

Baculovirus genome amplification happens through a process involving rolling circle amplification, resulting in concatemeric intermediates that must be excised and circularized before being packaged into virions [10]. Maturation of baculovirus genomes is likely mediated by *vlf-1a,* a tyrosine recombinase from the λ integrase gene family [15, 16]. Proviral DNA amplification and processing in MdBV is subject to different constraints than in baculoviruses, namely that proviral segments must be amplified off of the wasp genome and then excised from amplified DNA. My investigations into the five member gene family of MdBV integrase homologs (*vlf-1a*, *vlf-1b-1*, *vlf-1b-2*, *int-1*, and *int-2*) as well as candidate nudivirus-like genes (*k425_451*, *k425_468*, *k425_475* and *HzNVorf93-like*) revealed that many of these genes are involved in processing proviral DNA. qPCR assays revealed that proviral DNA processing is hampered by the knockdown of each individual integrase, though *int-2* to a lesser degree, as well as two of the uncharacterized

nudivirus-like genes (*k425_475* and *HzNVorf93-like*). Most MdBV integrases have retained critical integrase features, namely the R-X-R-Y motif [17]. In line with expectations, complete absence of this motif in *int-2* coincided with the knockdown not disrupting DNA processing as much as with other integrases. In contrast, while *k425_475* and *HzNVorf93-like* do not have any recognizable recombinase motifs, their knockdowns produce phenotypic effects similar to the knockdown of other integrases. My data suggest a strong interdependence of processing-related viral genes, which could involve complex formation, a chain of interactions, or transcriptional regulation. Furthermore the data suggest that MdBV proviral DNA segments are processed through the same mechanism. None of the genes investigated show any involvement in amplification of proviral DNA.

### 5.2 Recommendations for further research

The follow up to the data presented in this dissertation could go in different directions. Due to the complex and integrated nature of BVs, one of the biggest challenges to characterizing BV genes is producing knockdown wasps. dsRNA mediated RNAi did not work for every gene I investigated, and even good knockdowns don't completely eliminate gene expression. Developing better techniques for gene knockdown would increase confidence in the knockdown effects as there would be less chance of residual gene products producing normal phenotype. Most MdBV genes are still uncharacterized, many of those are nudivirus-like genes. It is likely that more of these genes play a critical role in BV function and that these functions are conserved from nudiviruses, a mostly unstudied virus family. Therefore, discovering their function in BVs would be a significant contribution to the understanding of the closest known relatives of BVs.

Not all MdBV PIF genes were investigated in this dissertation and some have yet to be characterized at all (*pif-3*, *pif-6*). Future work should involve knocking down the leftover PIFs in MdBV. It is possible that MdBV PIFs form some sort of complex as in baculoviruses. Individually MdBV PIFs might be redundant from the perspective of forming a potential complex, knocking down multiple PIFs might produce clearer phenotypes. Furthermore, development of antibodies could help us find out if MdBV PIFs function as a complex as they do in baculoviruses.

The non-redundancy of integrase involvement in MdBV DNA processing suggests some interaction between these genes, either through physical interaction or transcriptional regulation. Future research could eliminate some of these possibilities by using antibodies to target and localize individual integrase gene products to possible protein-DNA complexes.

### 5.3 References


1. Burke, G.R. and M.R. Strand, *Deep sequencing identifies viral and wasp genes with potential roles in replication of Microplitis demolitor Bracovirus.* J Virol, 2012. **86**(6): p. 3293-306.

2. Bezier, A., et al., *Polydnaviruses of braconid wasps derive from an ancestral nudivirus.* Science, 2009. **323**(5916): p. 926-30.

3. Burke, G.R., et al., *Mutualistic polydnaviruses share essential replication gene functions with pathogenic ancestors.* PLoS Pathog, 2013. **9**(5): p. e1003348.

4. Wetterwald, C., et al., *Identification of bracovirus particle proteins and analysis of their transcript levels at the stage of virion formation.* J Gen Virol, 2010. **91**(Pt 10): p. 2610-9.

5. Hou, D., et al., *Comparative Proteomics Reveal Fundamental Structural and Functional Differences between the Two Progeny Phenotypes of a Baculovirus.* J Virol, 2013. **87**(2): p. 829-839.

6. Cheng, C.H., et al., *Analysis of the Complete Genome Sequence of the Hz-1 Virus Suggests that It Is Related to Members of the Baculoviridae.* J Virol, 2002. **76**(18): p. 9024-9034.

7. Bezier, A., et al., *The genome of the nucleopolyhedrosis-causing virus from Tipula oleracea sheds new light on the Nudiviridae family.* J Virol, 2015. **89**(6): p. 3008-25.

8. Burke, G.R. and M.R. Strand, *Systematic analysis of a wasp parasitism arsenal.* Mol Ecol, 2014. **23**(4): p. 890-901.

9. Strand, M.R. and T. Noda, *Alterations in the hemocytes of Pseudoplusia includens after parasitism by Microplitis demolitor.* J Insect Physiol, 1991. **37**(11): p. 839-850.

10. Rohrmann, G.F., *Baculovirus Molecular Biology*. 2013, National Center for Biotechnology Information (US): Bethesda (MD), USA.

11. Boogaard, B., M.M. van Oers, and J.W.M. van Lent, *An Advanced View on Baculovirus per Os Infectivity Factors.* Insects, 2018. **9**(3).

12. Wang, X., et al., *Per os infectivity factors: a complicated and evolutionarily conserved entry machinery of baculovirus.* Sci China Life Sci, 2017. **60**(8): p. 806-815.

13. Li, X., et al., *The N-terminal hydrophobic sequence of Autographa californica nucleopolyhedrovirus PIF-3 is essential for oral infection.* Arch Virol, 2007. **152**(10): p. 1851-1858.

14. Zhu, S., et al., *The Baculovirus Core Gene ac83 Is Required for Nucleocapsid Assembly and Per Os Infectivity of Autographa californica Nucleopolyhedrovirus.* J Virol, 2013. **87**(19): p. 10573-10586.

15. Yang, S. and L.K. Miller, *Expression and mutational analysis of the baculovirus very late factor 1 (vlf-1) gene.* Virology, 1998. **245**(1): p. 99-109.

16. Vanarsdall, A.L., K. Okano, and G.F. Rohrmann, *Characterization of the role of very late expression factor 1 in baculovirus capsid structure and DNA processing.* J Virol, 2006. **80**(4): p. 1724-33.

17. Esposito, D. and J.J. Scocca, *The integrase family of tyrosine recombinases: evolution of a conserved active site domain.* Nucleic Acids Res, 1997. **25**(18): p. 3605-3614.